

Groundwater Storage Potential in the Yakima River Basin: A Spatial Assessment
of Shallow Aquifer Recharge and Aquifer Storage and Recovery

Maria T. Gibson and Michael E. Campana

Groundwater Storage Potential in the Yakima River Basin: A Spatial Assessment of Shallow Aquifer Recharge and Aquifer Storage and Recovery

Prepared for the Washington State Department of Ecology: Office of Columbia River
October 2018

Maria T. Gibson and Michael E. Campana
College of Earth, Ocean and Atmospheric Sciences
Oregon State University
Corvallis, OR 97331



Table of Contents

Introduction.....	1
Previous Research	2
Setting	4
Geology.....	4
Hydrogeology	4
Groundwater Withdrawals.....	5
1. Aquifer Recharge Potential	6
Weighted Overlay Method	7
Multi-Criteria Decision Analysis.....	8
Transmissivity.....	8
Land use	8
Lithology.....	8
Slope	10
Depth to Static Water Level.....	10
Analytical Hierarchy Process	12
Sensitivity Analyses.....	14
Groundwater Storage Recharge Rates: Analytical Methods	14
Shallow Aquifer Recharge.....	15
Aquifer Storage and Recovery	17
Results.....	18
Analytical Hierarchy Results.....	18
Sensitivity Analysis Results	26
Analytical Results	27
Shallow Aquifer Recharge	27
Combined Section Results.....	34
Infiltration Potential by Select Geological Units.....	34
ASR Results.....	41
2. System Dynamics Modelling: YAK-SDM	43
System Dynamics Modelling	44
Model Construct.....	Error! Bookmark not defined.
YAK-SDM.....	47
Capture Potential Sector	52
Capture Potential Modules	54
Instream Flow Targets.....	57
Historical Streamflow Data.....	57
Groundwater Storage Potential Sector.....	57
Climate Change Sector	60
Model Validation	63
Additional Applications of YAK-SDM.....	64
Section Results and Discussion.....	65
Capture Days.....	66
Climate Change	68
Mutual Gains Approach to Groundwater Storage.....	70
3. Recommendations.....	72
Site-Specific Carry over Storage and Climate Change Scenarios	73
Roslyn Basin	75
Kittitas Basin	77

Selah Basin.....	81
Lower Yakima Basin.....	83
Toppenish Basin	85
Benton Basin.....	87
ASR Results	89
References.....	90
Appendices.....	98
Appendix A: Sensitivity Results.....	99
Appendix B: Raster Datasets Reclassified	112
Appendix C: Mean and Median Infiltration Rates of Select Geologic and Lithologic Units.....	119
Appendix D: Stream Depletion Factor Maps.....	123

Figures

Figure 1. Shallow Aquifer Recharge and Aquifer Storage and Recovery.....	1
Figure 2. Location of six structural basins partly separated by anticlinal folds of the Yakima fold-and-thrust belt.....	5
Figure 3. The method used to obtain the site suitability maps, hydraulic load estimates and overall potential for enhanced groundwater recharge within each structural basin.....	9
Figure 4. Raster datasets of the Selah basin.	11
Figure 5. Location of wells surveyed, and subject wells used in this study.....	18
Figure 6. Results of the AHP Analysis	20
(a) Roslyn Basin	20
(b) Kittitas Basin.....	21
(c) Selah Basin.....	22
(d) Lower Yakima Basin.....	23
(e) Toppenish Basin	24
(f) Benton Basin	25
Figure 7. Simulation results of the sensitivity	27
Figure 8. Spatial representation of potential recharge capacity of each structural basin within the Yakima River Basin.....	28
(a) Roslyn Basin.....	28
(b) Kittitas Basin	29
(c) Selah Basin	30
(d) Lower Yakima Basin.....	31
(e) Toppenish Basin.....	32
(f) Benton Basin.....	33
Figure 9. Combined Results.....	35
(a) Roslyn Basin.....	35
(b) Kittitas Basin	36
(c) Selah Basin	37
(d) Lower Yakima Basin.....	38
(e) Toppenish Basin.....	39
(f) Benton Basin.....	40
Figure 10. Results of the ASR analysis targeting the confined Ellensburg Formation, with respective injection rates of each structural basin, with the exception of the Roslyn Basin, as no data were available in the basin to complete the analysis.....	42
Figure 11. Core components of system dynamics modelling within STELLA.	45
Figure 12. A simplified diagram of the YAK-SDM model with corresponding units and respective sectors and modules.....	47
Figure 13. YAK-SDM: Regional Watershed Unit	49
Figure 14. YAK-SDM: Regional Watershed Unit	50
Figure 15. Percent estimates MAR can meet precipitation deficits.....	51
Figure 16. Stream gauges within YAK-SDM.....	52
Figure 17. The capture potential sector in the YAK-SDM.....	53

Figure 18. The KEE module.....	55
Figure 19. The PARW module.....	56
Figure 20. (a) Daily flows from KEE sector associated instream flow targets. (b) Capture period for KEE during drought year 2005.....	57
Figure 21. The Groundwater Storage Potential Sector.	59
Figure 22. Historical, 2040, and 2080 predicted hydrograph for the PARW location.....	60
Figure 23. The 2080 Climate Sector.....	61
Figure 24. The sub-model of the Climate Sector.....	62
Figure 25. The departure from average precipitation conditions calculated by the YAK-SDM.	63
Figure 26. Predicted prorating for 2005 to 2017.	64
Figure 27. The hydrograph flip-flop of the Yakima River watershed for year 2006.....	64
Figure 28. Hydrograph of KEE in comparison to instream flow target goals.	65
Figure 29. Banked groundwater storage.....	66
Figure 30. Hydrographs at PARW with respect to historical conditions and climate change.....	68
Figure 31 . Cumulative historical capture potential compared against the following: natural flows, which are calculated based on pre-storage conditions; RCP 8.5 Flow, which is the more adverse climate scenario; and RCP 4.5 Flow, which is the less adverse climate scenario	69
Figure 32. Potential surface water capture for groundwater storage	70
Figure 33. Locations identified as well-suited or suitable for groundwater	74
Figure 34. Suitable locations for groundwater storage in the Roslyn Basin.....	76
Figure 35. Kittitas Basin: Standing water present January 2014.....	77
Figure 36. Kittitas Basin: Standing water present May 2014	78
Figure 37. Suitable locations for groundwater storage in the Kittitas Basin.....	80
Figure 38. Suitable locations for groundwater storage in the Selah Basin.	82
Figure 39. Suitable locations for groundwater storage in the Lower Yakima Basin.....	84
Figure 40. Suitable location for groundwater storage in the Toppenish Basin.....	86
Figure 41. Suitable locations for groundwater storage in the Benton Basin.	88
Figure 42. Locations for ASR expansion or development.....	89

Tables

Table 1. Subcategory scores used in the AHP matrix	12
Table 2. The AHP pairwise matrix, subsequent normalized values, and the consistency check scores used in this study	14
Table 3. Weighted overlay results by percent of basin area	19
Table 4. Results of sensitivity analysis with 50% reduction of criterion with equal distribution of weight to the criteria.....	26
Table 5. The table represents estimated annual recharge capacity constrained to locations considered suitable for SAR within each structural basin.....	34
Table 6. Values used and their source for specific converters in the YAK-SDM.....	46
Table 7. Number of potential capture days for each module for year 2005 to 2017.	67

Document Utility

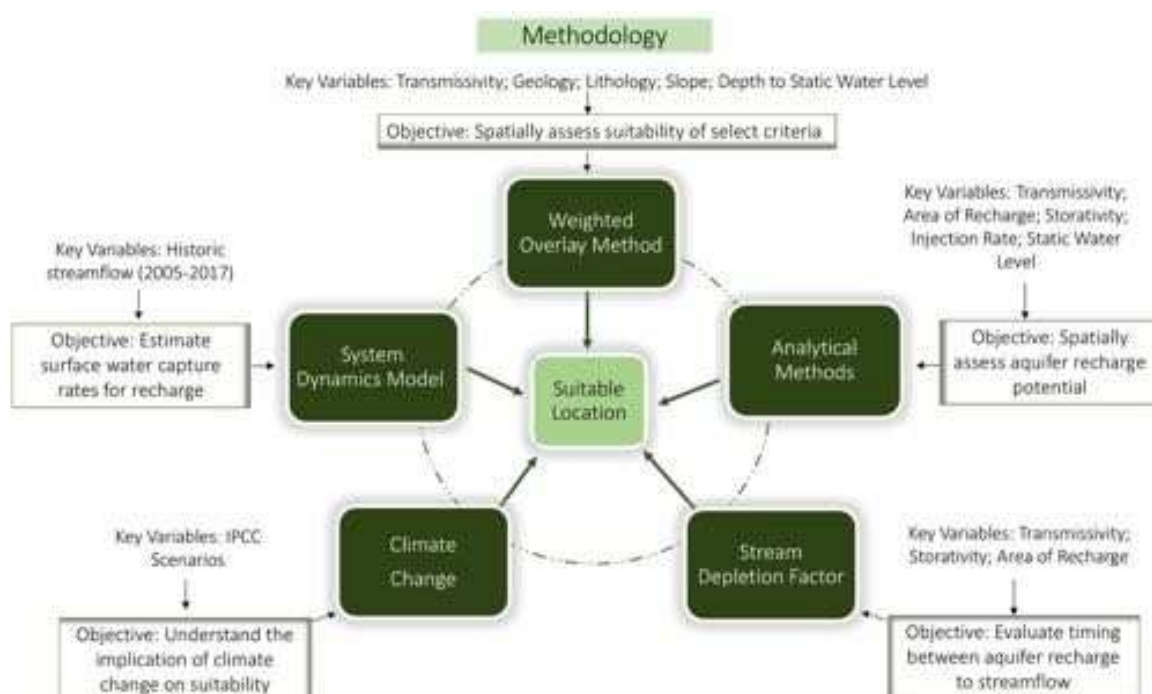
Multiple methods were utilized to spatially assess the suitability of Shallow Aquifer Recharge (SAR) and Aquifer Storage and Recovery (ASR). Detailed maps based on each assessment can be used as individual reference guides. Recommendations and maps of overall suitability are provided in section 3. The following sections include:

Section 1: Aquifer Recharge Potential. This section describes results obtained from a weighted overlay method that assessed suitable locations for SAR based on the following weighed criteria: land use, slope, lithology, geology, transmissivity, and depth to static water level. Two analytical methods were used to provide a spatial assessment of aquifer recharge potential for SAR and ASR.

Section 2: The System Dynamics Model. This section describes the development and model construct of YAK-SDM, which is an integrated model created to compare spatial recharge potential obtained in section 1 against available surface water available for groundwater storage. The capture component is centered on historical streamflow data for water year 2005 to 2017. Capture potential is estimated at 8 stream gauge locations, is generally limited to winter months, and is bounded by instream flow goals. The model was also used to understand the influence climate change may alter results.

Section 3. Recommendations. This section provides recommendations of suitable SAR and ASR locations. Carry over storage and relocation due to climate change were spatially evaluated within 6 sub-basins. Recommendations were also guided by a mutual gains approach to gage public perspective of future groundwater storage projects.

Methodology Overview:



Introduction

Influencing natural aquifer recharge by injection wells or passive infiltration basins are engineering tools used to develop aquifers as underground storage reservoirs. Global interest in this alternative water supply approach is on the rise (Sprenger et al., 2017; Dillon et al., 2018). However, the system requires 1) surface water for banking and 2) aquifer storage 'space' as defined by an aquifer's ability to add to the groundwater without negative consequences, including degradation of water quality or increase risk of groundwater flooding. The Yakima River Basin Integrated Water Resource Management Plan (IWRMP) (U.S. Bureau of Reclamation and Washington Department of Ecology, 2012) includes a groundwater storage component to enhance water supply. This research supports the IWRMP by spatially assessing groundwater storage potential throughout the Yakima River Basin, with respect to the Ellensburg Formation and throughout the watershed's 6 structural basins.

Two types of groundwater recharge methods were spatially surveyed in the Yakima Basin for suitability: Aquifer Storage and Recovery (ASR) and Shallow Aquifer Recharge (SAR). Aquifer storage and recovery uses wells targeted within confined aquifers to inject water, while SAR passively increases the water table in unconfined aquifers through ground-level infiltration (Figure 1). Since ASR uses injection wells, the potentiometric surface – the level the water would rise to if not under pressure – generally forms a cone shape, whereas mounding of the water table occurs beneath SAR zones (Figure 1).

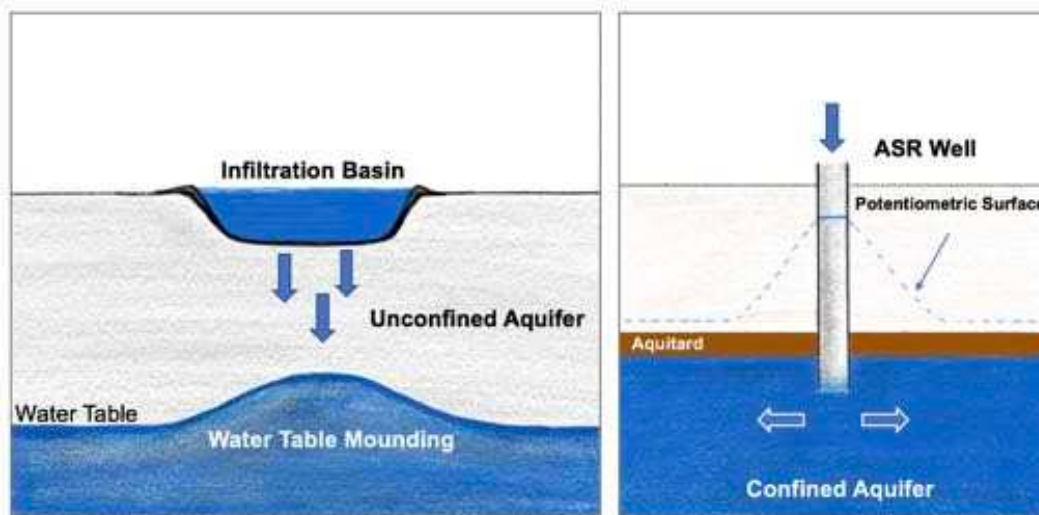


Figure 1. Shallow Aquifer Recharge and Aquifer Storage and Recovery. Shallow Aquifer Recharge (left) is a passive method that influences the water table through infiltration at ground surface, generally producing a mounding of the water table. Aquifer Storage and Recovery (right) uses injection wells to recharge confined aquifers. The potentiometric surface forms a cone shape within the vicinity of the water well.

Previous Research

The following summarizes previous studies of ASR and SAR in the Yakima Basin. In 2000, the City of Yakima conducted a feasibility assessment of ASR in the Ahtanum-Moxee sub-basin to store water in the lower section of the Upper Ellensburg Formation. A pilot test was completed in 2001, which included a recharge and recovery period of 25 and 55 days, respectively. Recharge occurred in the City's Kissel water well and results indicated the Ellensburg Formation maintained sufficient storage capacity suitable for ASR (Golder Associates, 2002). In 2002, a numerical groundwater model in MODFLOW was developed to simulate the residence time of stored water for a period of 10 years. Steady-state groundwater calibration was achieved but unresolved single-cell anomalies were observed during transient modeling. Overall, modelling results indicate the lower member of the Upper Ellensburg Formation was feasible for long-term water storage (Golder Associates, 2002).

In 2009, Anderson et al. conducted a groundwater storage assessment for the Yakima River Basin to understand the viability of using 1) surface recharge with passive recovery, 2) municipal aquifer storage and recovery, and 3) direct injection with passive recovery (Anderson, et al., 2009).

Using target flow profiles and estimates of excess surface storage, surface recharge with passive recovery was evaluated by analyzing volume and timing of diverted water to infiltration ponds, and the timing and volume of return flow. When excess surface storage exceeded 25,000 AF, it was assumed up to 20,000 AF could be diverted, with an annual volume of 33,000 AF during average years and 10,000 to 20,000 AF during drought years. Streamflow improvements were estimated using a Stream Depletion Factor (SDF) software with historic flows at the Umtanum gauge. The SDF software used aquifer transmissivity, storativity and distance between infiltration location and stream to generate a stream depletion function which showed peak return flow and decay over time. SDF values of 30, 40, 50, and 60 days were used. It was estimated that when excess flows were available, infiltration from 10,000 to 20,000 AF could yield up to 5.2 to 9.6 percent improvement in August, respectively. A distance buffer around the Yakima River and its main tributaries that would result in an SDF of 30, 40, 50, or 60 days was conducted to screen for potential areas based on surficial geology, land cover, and aquifer properties. It was estimated that total suitable land area ranged between 166 and 500 acres, with an expected value of 300 acres (Anderson, et al., 2009).

Municipal ASR and *injection with passive recovery* was also analyzed for suitability within the Yakima River Basin. Municipal ASR was defined as the intent of recovering stored water for potable uses, and *injected water with passive recovery* was considered when injected water naturally discharges to surface water sources. A groundwater flow model for the Ahtanum-Moxee sub-basin was used to estimate ASR potential as a groundwater management option. Three injection wells were modeled to estimate the quantity of recharge water that would return to the Yakima River, discharge to hydrologic sinks, and remain in the subsurface in the deeper portion of the Ellensburg Formation. A constant injection rate of 2,000 gpm at each well for 6 months, and up to nine cycles was conducted. Results were later extrapolated to include 4 wells with a total rate of 8,000 gpm

and an annual recharge volume of 6,400 AF. By replacing current municipal summer surface water diversion with ASR, it could add an additional 6,000 AF of streamflow from April to September, with augmentation of up to 1.2 cfs of seepage from injected water. Passive recovery could augment flows by 3,200 AF during irrigation season, and if used for water short years, approximately 38,000 AF with an estimated seepage rate of 5.3 cfs could be returned back to the Yakima River over 10 years, at a rate of 8,000 gpm during a 6-month recharge period (Anderson, et al., 2009).

In 2011, Golder and HDR appraised the potential for groundwater infiltration in the Kittitas Reclamation District (KRD) and the Wapato Irrigation Project (WIP). A groundwater mounding analyses to estimate the water table response below an infiltration pond was conducted. The research was performed in the AQTESOLV 4.03 software using Hantush (1967) solution. Six configurations of pond size and saturated thickness were evaluated based on a range of three hydraulic conductivity values for a 90-day period. Pond size ranged from 5 to 20 acres; saturated thickness ranged from 100 to 200 ft and hydraulic conductivity ranged from 20 to 100 ft per day. A recharge rate of 2.5 feet per day for 90 days was assumed. In WIP, it was estimated that winter and spring infiltration could return groundwater levels to normal trends. In KRD, long term infiltration potential exist as convergence of flow above Umtanum would likely increase baseflow. A hydrogeological analysis with respect to the groundwater system was conducted in RiverWare for year 1981 to 2005. Water used for infiltration were modeled based on pre-storage control flows and uncontrolled natural flows between November and March. The daily discharge rate of 0 to 595 cfs was applied for each area, with flows constrained by instream flow requirements. Available water diverted for infiltration was assumed to occur when river flows were above 1,000 cfs with a maximum volume of 54,000 AF per year for each location. A constant seepage function was used to simulate recovery of groundwater. It was assumed that the water was used in the same year as infiltration occurred, therefore a high rate of total return flow was used. Infiltrated water was modeled as a simple reservoir, and it was assumed to leak at a rate of 0.7 percent of daily stored volume with a maximum of 190 cfs. Due to the limitations of the model, groundwater stored beyond an annual basis was not possible, nor was evaluating higher daily or monthly recovery volumes for specific water users completed. Results suggest KRD could infiltrate 4,000 to 54,000 AF per year with an average of 32,719 AF annually over a 25-year period. Return flows to the river ranged from 8,000 to 55,000 AF annually. For WIP, inflows and return flows were estimated at 54,000 AF per year (Golder Associates & HDR Engineering, 2011).

Field investigation to evaluate the potential of shallow aquifer recharge was conducted in the eastern Kittitas Valley in 2013 (Golder Associates, 2013). Field investigation took place on November 7-8, 2012 along the KRD North Branch Canal. It was previously thought that the unsaturated zone was 20 to 80 feet below land surface but standing water was observed in many locations. Water in the canal was observed where perennial streams cross the canals. No sites with favorable conditions for surface infiltration were identified in the Dry Creek drainage in the northwest part of Kittitas Valley; however, glacial terminal moraine and outwash sediments between Thorp and Cle Elem were thought to be candidates for further investigation. A groundwater monitoring network in the Kittitas Valley was established in privately owned wells.

Pumping tests were performed on 3 wells - 9.9 to 42 feet below land surface - and transmissivities ranged from 4 ft²/d to 460 ft²/d. Three groundwater samples and one sample from the Yakima River were analyzed for compatibility. Groundwater and surface water were considered compatible for surface infiltration except for variation in pH. The groundwater sampled measured a pH between 6.31 to 6.60, while the Yakima River water measured an 8.6. Therefore, consideration of calcite formation due to high pH conditions was suggested.

Setting

Geology

The geology of the Yakima River basin is dominated by the Columbia River Basalt Group (CRBG). The CRBG are tholeiitic flood basalts formed between 17 to 6 million years ago, but mostly erupted before 14.5 MA. They are laterally extensive sheet flows, subdivided by variations in geologic signatures. From oldest to youngest, the CRBG are composed of the Imnaha, Grande Ronde, Picture Gorge, Wanapum, and Saddle Mountain basalts. Interbedded, and in some location overlying the CRBG, is the Ellensburg formation, which consists of epiclastic and volcanoclastic sedimentary rocks (Reidel et al., 2003).

The formation of the Yakima River watershed is largely due to the oblique subduction of the Juan de Fuca oceanic plate beneath the North America continental plate. It is further influenced by the distributed shear stress created by the Pacific plate moving northwest, relative to the North America plate (Atwater, 1970). Compression deformation yielded the Yakima fold-and-thrust belt, which includes deformed CRBG that folded into principally trending east-west and northwest-southeast anticlinal ridges and synclinal valleys (Newell and Bentley, 1981; Reidel et al., 2003; Blakely et al., 2011; Gomberg et al., 2012; McCaffrey et al., 2016). The meandering, yet entrenched and incised Yakima River suggests the river flowed prior to regional deformation (Waters, 1955).

Hydrogeology

Valley-fill deposits and the CRBG are the principal aquifers. The basalt of the CRBG reaches a thickness of 8000 ft. Most of the valley-fill deposits are the Ellensburg Formation, which formed from erosion of the Cascade Range during intermittent flows of the CRBG. The structural geology of the Yakima River Basin heavily influences groundwater movement and surface water flows. Anticlinal folds segment six basin-fill units (Figure 2) with groundwater movement generally occurring from the highlands to topographic lows along stream paths (Jones et al., 2006, Vaccaro et al., 2009). Groundwater movement within the CRBG is also compartmentalized but to a lesser extent than the basin fill units, and water table gradients of the CRBG follow the topography within 5 degrees (Vaccaro et al., 2009).

The unique topographic arrangement of the Yakima River watershed isolates six structural basins (Figure 2), yet all are spatially connected by the river system. Hydrogeologic units have been mapped within each basin based on regional lithology but units were determined according to local conditions (Jones et al., 2006). Since the spatial arrangement among the basins generally follow a stepdown pattern from higher to lower elevation, while remaining geologically isolated, groundwater and surface water tend to ‘funnel’ down from one basin to another before reaching the Columbia River. The rate in which this occurs depends on the thickness of each unit, runoff patterns, return flows, and reservoir influences.

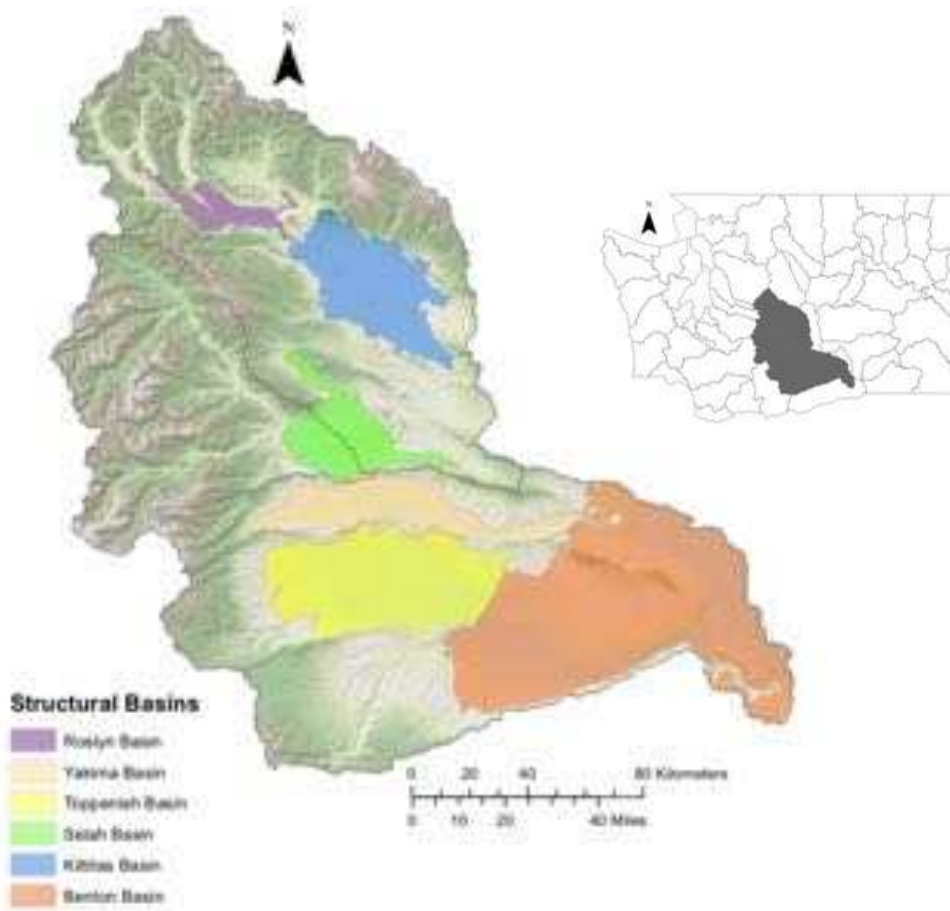


Figure 2. Location of six structural basins partly separated by anticlinal folds of the Yakima fold-and-thrust belt.

Groundwater Withdrawals

Although up to 80 percent of the population utilizes groundwater as their principal drinking water source, the greatest quantity of groundwater withdrawals is designated for irrigation use (Vaccaro and Sumioka, 2006)

1. Aquifer Recharge Potential

The recharge potential assessment included 1) identifying suitable locations for SAR and 2) estimating the groundwater storage recharge rates for SAR and ASR through analytical methods based on aquifer type. A weighted overlay method within a geographical information system (GIS) was developed to spatially assess suitable SAR locations within each structural basin. The use of GIS and remote sensing allows for efficient assessment of groundwater characteristics on regional and local scales (Saraf and Choudhury, 1998; Solomon and Quiel, 2006). The weighted overlay method included a Multi-Decision Criteria Analysis (MCDA) to productively organize the assessment, which generally involves a criteria selection process, incorporating some combination of technical, economic, environmental, and social factors. Following the MCDA, a weighting of criteria was performed. The most widely used approaches include a simple multi-attribute rating technique, consistence matrix analysis, a pairwise comparison, or the more vigorous version of a pairwise comparison, the Analytical Hierarchy Process (AHP) method (Wang et al., 2009), which was employed for this study, in addition to sensitivity analyses to estimate the robustness of this method.

To estimate groundwater storage rates for SAR, the Glover (1960) equation was used to calculate infiltration rates with respect to mounding of the water table within unconfined aquifers, and the Theis (1935) solution for confined aquifers was used to estimate injection rate capacities within the Ellensburg Formation of the CRBG.

The results obtained from the analytical solutions were imported into ArcMap and represented spatially within each basin. Locations with groundwater storage rates were merged with locations classified as suitable for SAR - estimated from the weighted overlay maps, which provided recharge potential within each structural basin. The methodology to obtain aquifer recharge potential is shown in Figure 3.

Identification of Suitable Locations

Weighted Overlay Method

An MCDA coupled with the AHP was used to estimate suitable locations for SAR. Criteria or parameters included in assessing SAR potential within a MCDA generally incorporate site-specific slope values, land cover, geology, and aquifer characteristics (Jamali et al., 2014; Kazakis, 2018). An MCDA was conducted within each structural basin using the following criteria: transmissivity, slope, land use, lithology, and depth to static water level, each of which is described in the following section. An AHP pairwise matrix was conducted on each criterion and within its respective subcategory. The thematic layers were assembled within ArcMap, converted to raster format, reclassified to a normalized scale, and subjected to a weighted overlay process using values obtained from the pairwise matrix. The weighted overlay in ArcMap uses a common scale of

measurement and weights each raster as a percentage of importance to produce a final map. A restrictive model was applied to each overlay raster to remove impervious surfaces and perineal surface water bodies. Two sensitivity analyses were performed to identify factors that most influence the overlay results and to determine the robustness of the AHP method (Figure 3).

Multi-Criteria Decision Analysis

Recently, GIS and remote sensing techniques have been combined with MCDA to aid in identifying potential MAR locations (Rahman et al. 2012; Gdoura et al., 2015; Bonilla-Valverde et al., 2016). For the MCDA within the Yakima River Basin, the following criteria were chosen:

Transmissivity

Transmissivity is a principal factor when identifying groundwater recharge projects. High transmissivity values are generally targeted to avoid unwanted mounding (Brown, 2005; Smith and Pollock, 2012; Singh et al., 2013; Chipongo and Khiadani, 2015; Russo et al., 2015) which may lead to groundwater flooding. Geologic geodatabases in the 1:100,000 scale (WA DNR, 2016) were downloaded and clipped to each structural basin. Attributes tables were exported, and transmissivity values assigned to each formation based on location. Transmissivity values were derived from Vaccaro et al. (2009) by calculating average thickness and horizontal hydraulic conductivity of each hydrogeologic unit, which was previously estimated by the United States Geological Survey (USGS) (Jones et al., 2006; Jones et al., 2008; Vaccaro et al., 2009).

Land use

Land use maps allow for the identification of vegetation cover, distribution of urban and rural developments, potential soil properties, and it assists in estimating runoff and evapotranspiration (Hsin-Fu et al., 2016). The landcover thematic layer was obtained from the Washington State Department of Ecology (2010) geospatial data catalog. The land use file is a tax parcel derived dataset that contains specified land use codes. Codes considered for suitability included agriculture, agriculture under legislative declaration, open space, timberland, and undeveloped land.

Lithology

Rock exposed at the surface is an important factor in recharge, percolation of water, and groundwater distribution (El-Baz et al., 1995; Shaban et al., 2006). The geologic polygon layer within the Washington Department of Natural Resources (2016) geodatabase was used to identify lithological formations within each structural basin. The polygon layer contained over 100 different geologic units and over 150 lithological descriptions. The geologic layer was clipped to each structural basin and its respective lithological attributes were exported in text format and processed within Excel to identify and remove lithological classes not suitable for MAR.

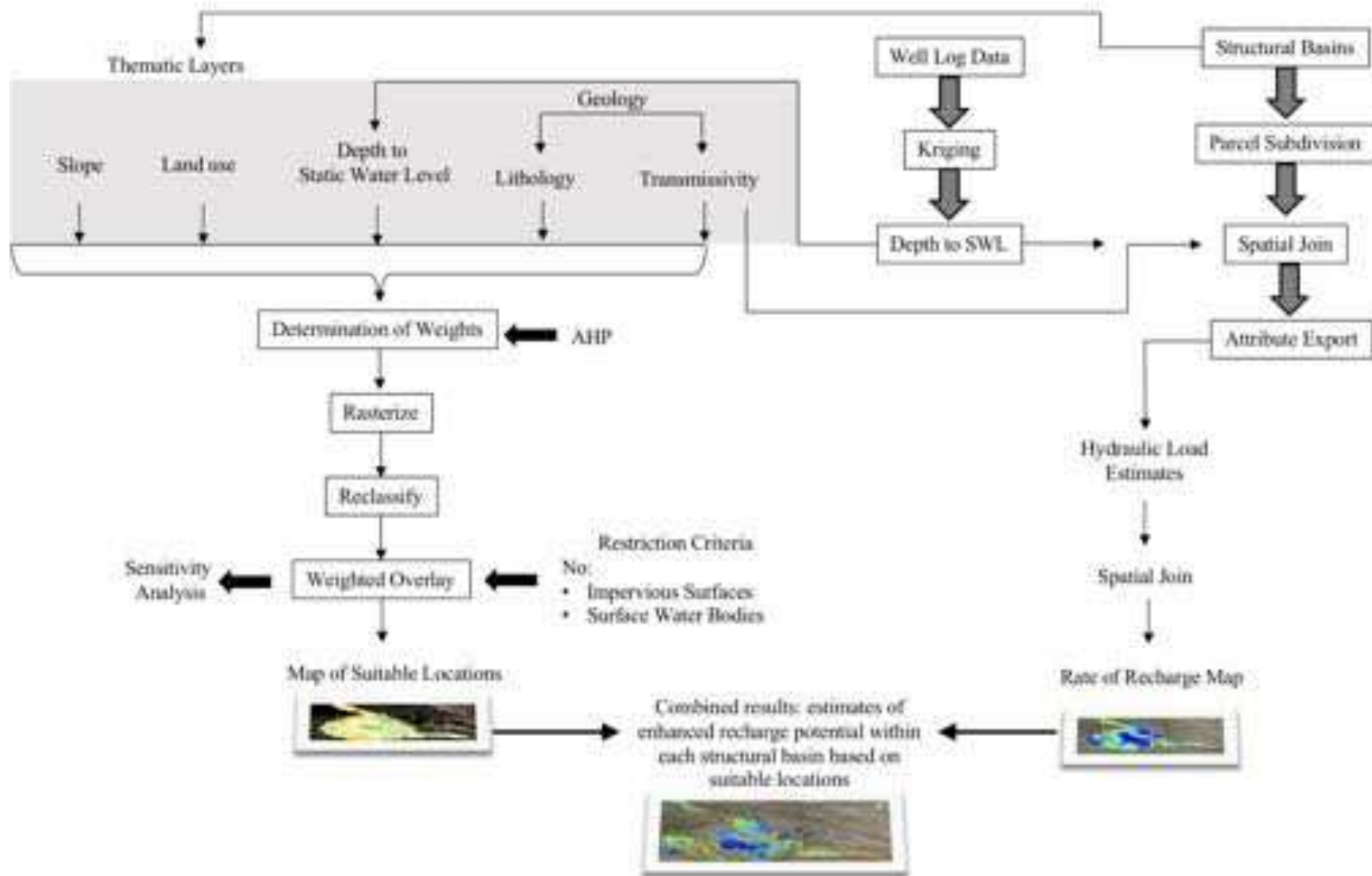


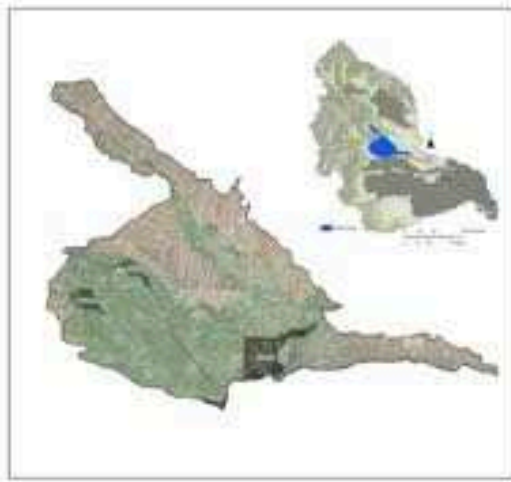
Figure 3. The method used to obtain the site suitability maps, hydraulic load estimates and overall potential for enhanced groundwater recharge within each structural basin.

Slope

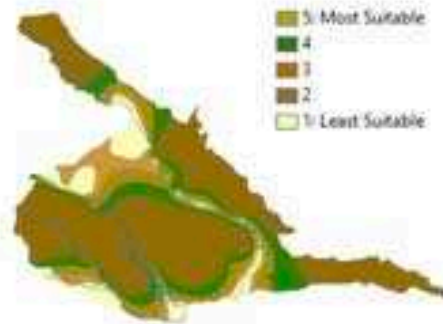
Slope is a relevant factor as it controls runoff potential (Magesh et al., 2012; Sener and Davraz, 2013; Selvam et al., 2014). Slope values were calculated from the USGS National Elevation Dataset (2015). Digital elevation models (DEM) were obtained from the USGS National Map (2018) and masked to the Yakima River Basin in ArcMap. A mosaic of raster files were created within geodatabases of each structural basin and contour maps with elevation data were derived. Slope was calculated using ArcMap 3-D analyst tool with output measurements obtained in degrees.

Depth to Static Water Level

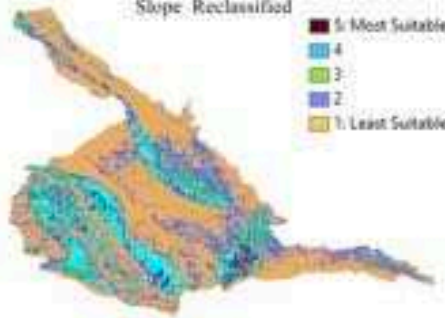
Depth to the static water level is a controlling factor used to identify potential groundwater rise (Brown, 2005; Pedrero et al., 2011; Smith and Pollock, 2012). Records of over 20,000 water well logs were obtained from geospatial data provided by the Washington State Department of Ecology (2018). The respective geodatabase was used to export attribute tables for wells built within the last 25 years, contain static water level information, and were constructed during the winter months (December to March). This point information was imported into ArcMap. Static water level maps were created by ArcMap's interpolation methods and digitized. Depth to static water level contours were compared to previous research. Updated maps were subsequently processed using ArcMap's raster calculator to subtract ground surface elevations from the static water level, thereby obtaining static water level elevations and depth to static water level rasters. Each thematic layer in Figure 4 was reclassified to a scale from 1 to 5, with 5 being the most suitable. For brevity, only the Selah structural basin is shown, however respective maps of each basin are presented in Appendix B. Table 1 lists the subcategories deemed appropriate for each basin and the sub-criterion factors for each thematic layer.



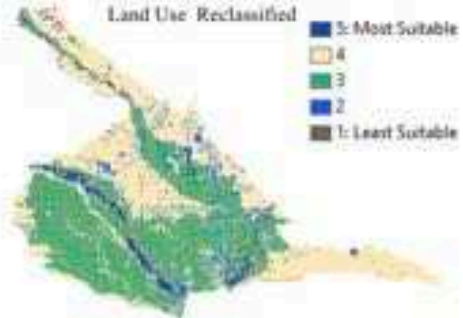
Depth to Static Water Level: Winter Months (Reclassified)



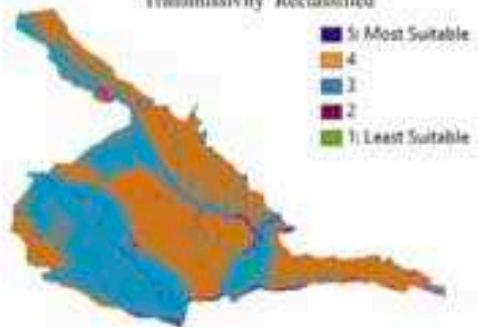
Slope - Reclassified



Land Use - Reclassified



Transmissivity Reclassified



Lithology Reclassified

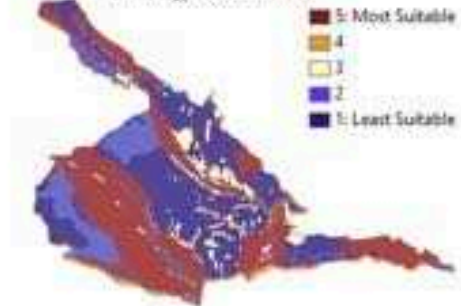


Figure 4. Raster datasets of the Selah basin. Thematic layers were reclassified to a scale from 1 to 5, with 5 being the most suitable for enhanced recharge. The thematic layers include slope, transmissivity, depth to static water level, land use, and lithology.

Criterion	Normalized Pairwise Weight	Sub-Criterion	Weighted Judgment	Normalized Pairwise Weight
Land use	0.11	Agriculture	3	0.16
		Agriculture under 84.34	3	0.13
		Open space	7	0.37
		Timberland	3	0.13
		Undeveloped Land	4	0.21
Slope (%)	0.2	0-1	6	0.34
		1-3	5	0.28
		3-5	4	0.20
		5-10	2	0.11
		10+	1	0.07
Lithology	0.23	Alluvial Deposits	5	0.27
		Basalt	5	0.24
		Gravels	3	0.16
		Ellensburg Formation	4	0.22
		Low Perm_Quat Deposits	2	0.11
Transmissivity (ft ² /d)	0.17	5,000 to 10,000	7	0.29
		10,000 to 15,000	6	0.26
		15,000 to 25,000	6	0.26
		T < 5,000	2	0.09
		T > 25,000	3	0.11
Depth to Static Water Level (ft)	0.29	0 to 5	1	0.06
		6 to 10	3	0.14
		10 to 25	4	0.23
		25 to 50	5	0.29
		+51	5	0.29

Table 1. Subcategory scores used in the AHP matrix

Analytical Hierarchy Process

The AHP weighing approach within a MCDA model was devised by the mathematician Thomas L Saaty (1980). Its purpose is to analyze complex decisions by creating pairwise alternatives. The AHP allows for relative measurement or proportions between elements. According to Brunelli (2014), AHP is utilized within the spectrum of decision analysis and operational research, where decision analysis is defined as an analysis that allows for individual choices among predefined alternatives,

and operational research is defined as using scientific and mathematical methods to problem-solve complex set of systems. The AHP method is also flexible enough to encompass subjective and objective components of the decision process while limiting bias in the decision-making process by incorporating a ‘consistency check’ (Saaty, 1980).

The AHP involves reducing the final goal of suitability into a hierarchy. Each criterion is assigned an appropriate weight (Table 1), which reflects expert opinion and available literature. Weighting allows for a degree of preference relative to the criterions. A 9-point scale of importance is implemented, with 9 being the most important. Once the assignment of weights is complete, quantification of criteria is conducted through pairwise comparison matrices within each hierarchal structure and then normalized.

Let $C_1, C_2, C_3, \dots, C_n$ is the “n” different and independent alternatives, and a_{ij} represents a quantified decision of a pair of alternatives C_i, C_j , which results in an $n \times n$ matrix A:

$$A = [a_{ij}] = \begin{matrix} & \begin{matrix} C_1 & C_2 & \dots & C_n \end{matrix} \\ \begin{matrix} C_1 \\ C_2 \\ \vdots \\ C_n \end{matrix} & \begin{bmatrix} 1 & a_{12} & \dots & a_{1n} \\ \frac{1}{a_{21}} & 1 & \dots & a_{2n} \\ \vdots & \vdots & \vdots & \vdots \\ \frac{1}{a_{n1}} & \frac{1}{a_{n2}} & \dots & 1 \end{bmatrix} \end{matrix} \quad (1)$$

where,

$$a_{ii} = 1, a_{ij} = 1/a_{ji}, i, j = 1, 2, \dots, n.$$

Assigning n alternatives to C_1, C_2, \dots, C_n to a set of weights (W_1, W_2, \dots, W_n) that corresponds to judgments (a_{ij}) . As a consistency matrix, A the relationship between the judgements and weights are $W_i/W_j = a_{ij}$ (for $i, j = 1, 2, 3, \dots, n$). Weight vectors are computed by $W = (W_1, W_2, \dots, W_n)$, Where W is the column vector as the principal right eigenvector of matrix A:

$$A_w = \lambda_{max} W \quad (2)$$

where,

λ_{max} is maximum value of the eigenvector

Each matrix is checked for consistency throughout the process by calculating the following consistency ratio from the consistency index (c_i) and dividing it by the random index (r_i) (Saaty, 1980):

Consistency index:

$$c_i = \frac{\lambda_{max} - n}{n - 1} \quad (3)$$

$$c_r = \frac{c_i}{r_i} \quad (4)$$

The random index (r_i) is a table developed by the Oak Ridge National Laboratory for matrices with up to 15 rows (Saaty, 1980). If the consistency ratio exceeds 0.1 then the weight of the theme is inconsistent. If $C_r < 0.1$ then it is considered an acceptable estimate.

The AHP pairwise matrix developed for the Yakima River basin is listed in Table 2.

Pairwise comparison	Land use	Slope	Lithology	Transmissivity	Depth to SWL	Normalized Pairwise	
Land use	2/2	2/3.5	2/4	2/3	2/5	0.11	
Slope	3.5/2	3.5/3.5	3.5/4	3.5/3	3.5/5	0.20	
Lithology	4/2	4/3.5	4/4	4/3	4/5	0.23	CI=0
Transmissivity	3/2	3/3.5	3/4	3/3	3/5	0.17	RI=1.11
Depth to SWL	5/2	5/3.5	5/4	5/3	5/5	0.29	CR=0

Table 2. The AHP pairwise matrix, subsequent normalized values, and the consistency check scores used in the Yakima River Basin.

Sensitivity Analyses

Two sensitivity analyses were applied to estimate the stability of the AHP weighting technique (Qureshi et al., 1999) and to estimate the thematic factors that most affect its outcome (Lodwick et al., 1990; Babiker et al., 2005). To analyze the robustness of AHP, scenarios were created where one factor was reduced 50% while the difference was evenly distributed among the others. Multiple simulations were conducted until all factors were affected. A separate factor removal process was applied where all criteria were assigned equal weights, then each factor was systematically removed and the weight of that factor was evenly distributed among the remaining criteria. Simulations were run until all factors were removed and compared to the initial run.

Groundwater Storage Recharge Rates: Analytical Methods

To estimate groundwater storage rates for SAR, each basin was subdivided into 0.5-acre circular parcels in ArcMap. The center of each cell was exported into Excel, with respective transmissivity

and depth to static water level values, which were required to solve the analytical solution (Glover, 1960). To estimate ASR potential, an equation rooted in Theis (1935) was applied to over 200 wells accessing the confined units of the Ellensburg Formation within the CRBG.

The results obtained from analytical solutions were imported into ArcMap and represented spatially within the basin.

Shallow Aquifer Recharge

Shallow Aquifer Recharge (SAR) is a tool utilized to hydraulically influence the water table by inducing recharge through infiltration from the ground surface. Groundwater mounding beneath an infiltration basin is reduced as the groundwater mound reaches the surface. Once the mound reaches the ground level, infiltration is no longer possible. Therefore, approximations of mound growth in response to infiltration rates and other hydrogeologic variables is required to determine locations capable of accommodating prospective projects.

Groundwater mounding beneath infiltration basins has been widely studied and estimated using analytical approximations (Glover, 1960; Hantush, 1964; Marino, 1974; Singh, 1976; Molden, 1982; Morel-Seytoux et al., 1989; Warner et al., 1989; Rai et al., 1998; Bouwer, 2002; Ilias et al., 2008; Zomorodi, 2009; Kormkmaz, 2013; Chipongo and Khiadani, 2015). Using the governing partial differential equation for groundwater flow, Glover (1960) was the first to predict mounding properties within circular basins under instantaneous recharge, assuming the initial saturated thickness was much greater than the mound height. The solution was later expanded to include continuous rates of recharge (Warner et al., 1989). To estimate recharge capacities for SAR, Glover's solution for a circular basin was utilized, since it is computationally less intense than rectangular basins yet can be approximated to an equivalent rectangular area (Asano, 1985).

Mound growth is predicted from the following:

$$H = C \left(\frac{1}{2\alpha t} \right) \int_0^a \xi \exp\left(-\frac{r^2 + \xi^2}{4\alpha t}\right) I_0\left(\frac{r\xi}{2\alpha t}\right) \quad (5)$$

where,

I_0 = the modified Bessel function of the first kind and order zero

ξ = dummy variable of integration

$\alpha = T/S$

T = Transmissivity (L²/t)

S = Storativity (dimensionless)

r = radius (L)

C = height of slug injected cylinder (L)

t = time (t)

And a continuous recharge rate for a cylinder of water of incremental height is expressed as:

$$dC = \frac{R}{S} dt \quad (6)$$

where,

R= Recharge rate, volume flux per unite area (L/T)

Substituting equation 6 for C in equation 5 provides estimates of incremental mound height, dH. Integrating with respect to time yields a solution for constant recharge (Molden, 1982):

$$H = \frac{R}{2\alpha S} \int_0^t \frac{1}{t-t'} \int_0^a \xi \exp\left[-\frac{r^2 + \xi^2}{4\alpha(t-t')}\right] I_0\left[\frac{r\xi}{2\alpha(t-t')}\right] d\xi dt' \quad (7)$$

where,

H = mound height (L)

The mound height at the center of the basin where r=0 is

$$H_o = \frac{RT}{S} (1 - e^{-u} + u_o W(u_o)) \quad (8)$$

Where, $u_o = \frac{a}{4\alpha t}$ (McWhorter and Sunada, 1977) and W(u) is the well function at the center of the basin H_0 (Warner et al., 1989).

If the mound has reached ground surface, the depth to the static water level (DSWL) will be equivalent to the height of the recharge mound:

$$\frac{DSWL}{H} = 1 \quad (9)$$

By substituting Q/A for R into equation 8, where Q is the rate of recharge (L^3/t) and using a polynomial approximation to calculate the well function (Huntoon, 1980), maximum recharge potential can be estimated.

This analytical approach was used to calculate potential recharge capacity within the Yakima River Basin by subdividing each structural basin into circular areas of 148 ft radiuses, executed in ArcMap with $t = 120$ days - assuming capture of water occurred for 3 winter months. The DSWL water level and T values were obtained at point locations from thematic layers derived in ArcMap. Values were exported in text delimited form, imported into Excel spreadsheets, and Q approximations were calculated.

Aquifer Storage and Recovery

The Theis (1935) equation and Cooper-Jacob (1946) approximation were used to predict injection rate capacities within the Ellensburg Formation located within the CRBG. The following equation assumes the aquifer is homogenous and of infinite lateral extent:

$$h_w - h_0 = \frac{Q}{4\pi T} \int_u^\infty \frac{e^{-u}}{u} du \quad (10)$$

$$W(u) = -0.5772 - \ln u + u - \frac{u^2}{2 \times 2!} + \frac{u^3}{3 \times 3!} - \frac{u^4}{4 \times 4!} + \dots, \quad (11)$$

$$u = \frac{r^2}{4Tt} \quad (12)$$

where,

r is the well radius (L)

$W(u)$ is the well function (dimensionless)

Q is the injection rate (L^3/t)

h_w is the hydraulic head during injection (L)

h_0 is the initial hydraulic head prior to injection (L)

The wells evaluated for suitability in all access the CRBG within their respective structural basin. A screening process of over 3000 well logs obtained from Washington Department of Ecology (2018)

was distilled down to 200 (Figure 5), as it was determined each report contained the required well test data and each was estimated to be screened in the lower, confined Ellensburg Formation of the CRBG. The injection potential rates were determined by rearranging the Theis (1935) equation to quantify the maximum rate of injection, as head values reached the ground surface. The lower Ellensburg formation was targeted for ASR as it had been previously assessed to be the most suitable local aquifer, in addition it is currently being recharged through two municipal wells retrofitted for injection by the city of Yakima. As with the Glover equation, depth to static water level was divided by the head values determined from Theis (1935) and Cooper-Jacob (1946). Since this is an injection equation, $h_w - h_o$ is positive. However, the Ellensburg Formation is generally overlaid by unconfined aquifers; therefore, the injection threshold is not ground surface, as it is in the Glover method, but is assumed to be the contact between the Ellensburg Formation and overlying unconfined aquifers.

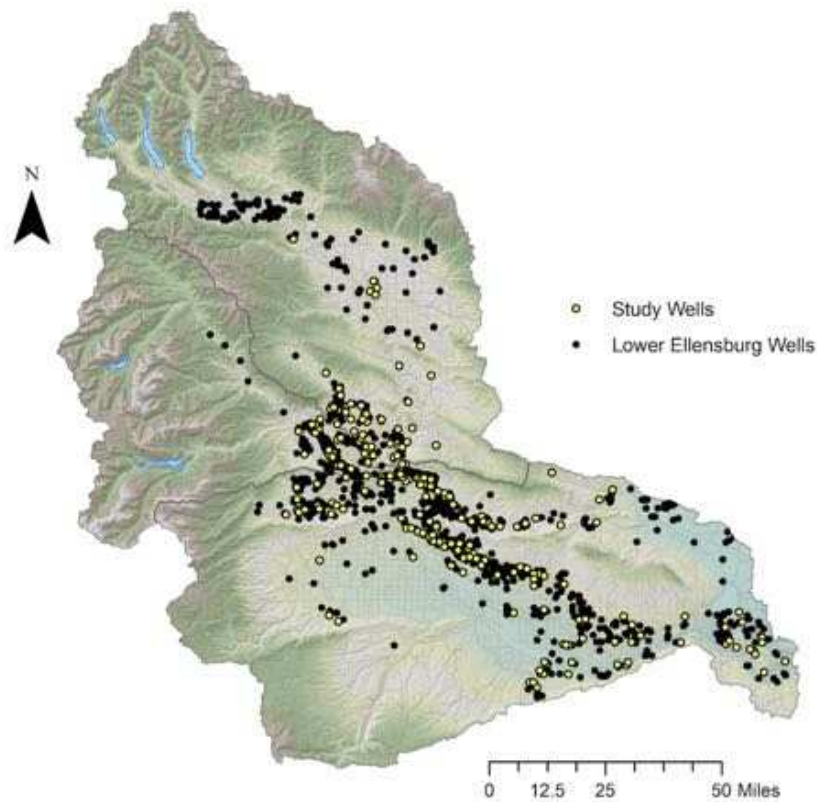


Figure 5. Location of wells surveyed, and subject wells used in this study.

Results

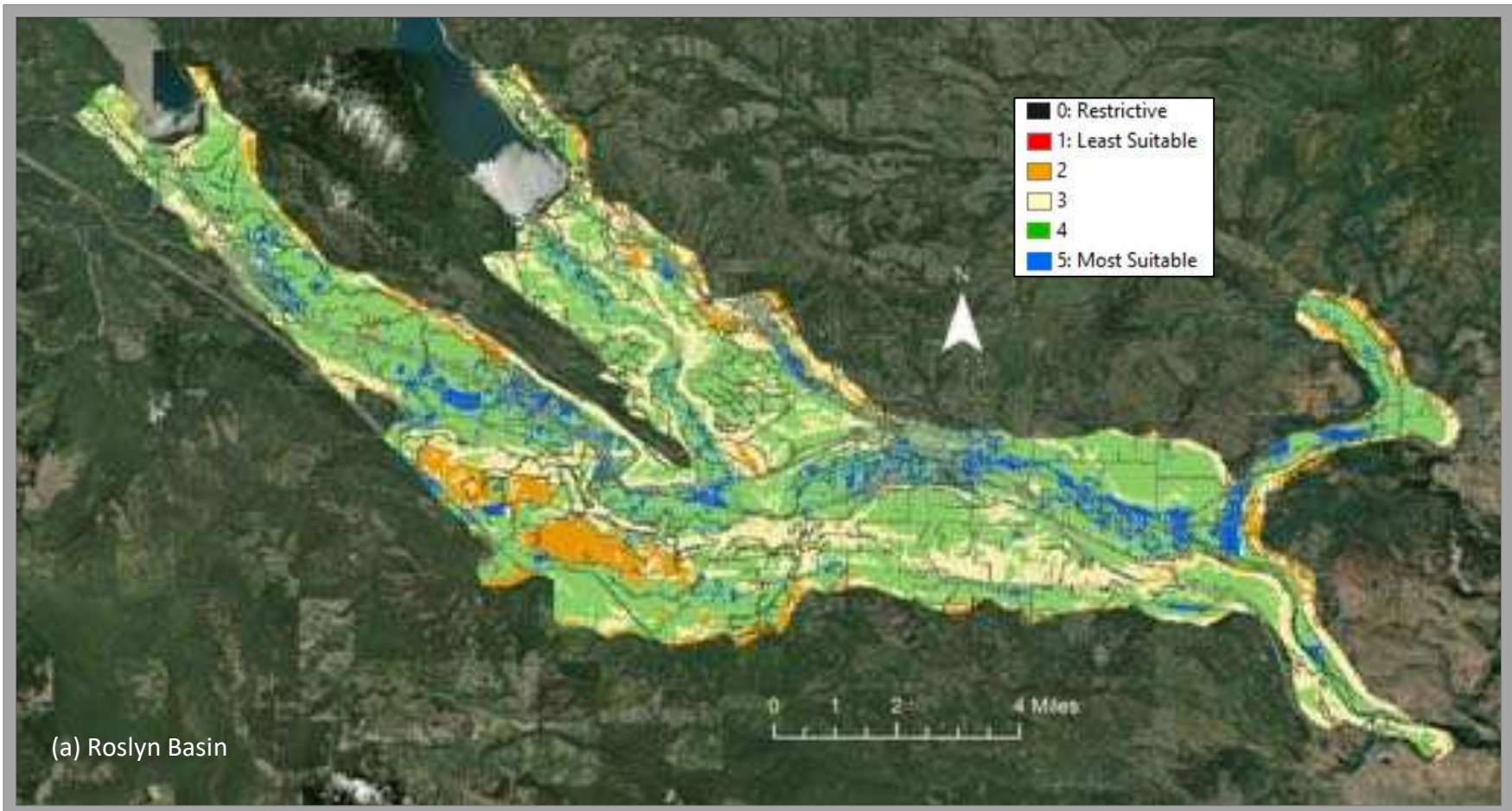
Analytical Hierarchy Results

An Analytical Hierarchy Process was developed within a Multi-Criteria Decision Analysis in the Yakima River Basin to spatially delineate locations most suitable. Results from the AHP weighted overlay method are expressed on a scale from 1 to 5, with 5 being the most suitable for SAR, indicating each location earned full points for all criteria. Criteria included slope, depth to static water level, transmissivity, lithology, and land use. The Roslyn basin scored a 5 out of 5 on less than 5.9% of its total area with 47% of the area earning a score of 4 out of 5. In the Kittitas basin, 4.5% of the area scored a 5 and 52% of the basin scored a 4 out of 5. In the Selah basin, 0.2% of the basin scored a 5, while 26% scored a 4 out of 5. The Lower Yakima basin had the least favorable conditions, as 0.1% of the basin scored a 5, while 18% scored a 4 out of 5. In the Toppenish basin, only 0.1% of the basin scored a 5, while 44% of the basin scored a 4. The Benton basin, 1.4% of the basin scored a 5 out of 5 and 46% of the basin scored a 4 out of 5. The results are summarized in Table 3 and spatially represented in Figure 6 (a-f).

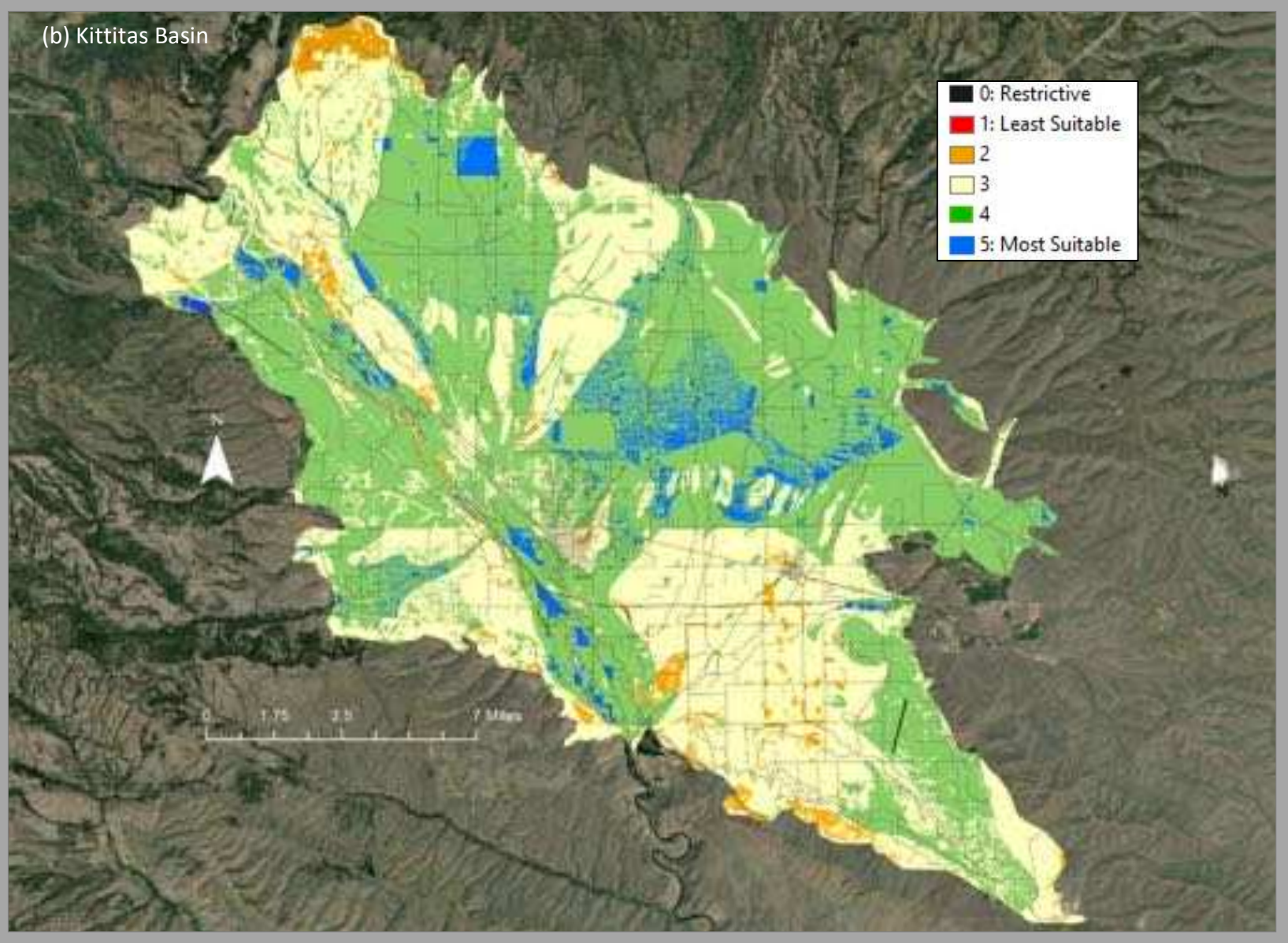
Basin	1: Least Suitable	2	3	4	5: Most Suitable	0: Restrictive
Roslyn	0%	7%	22%	47%	5.9%	18.8%
Kittitas	0%	2.3%	37%	52%	4.5%	4.4%
Selah	0.1%	14%	57%	26%	0.2%	2.5%
Yakima	1.8%	23%	52%	18%	0.1%	5.0%
Toppenish	0%	3.2%	49%	44%	0.1%	3.2%
Benton	0%	19%	32%	46%	1.4%	2.6%

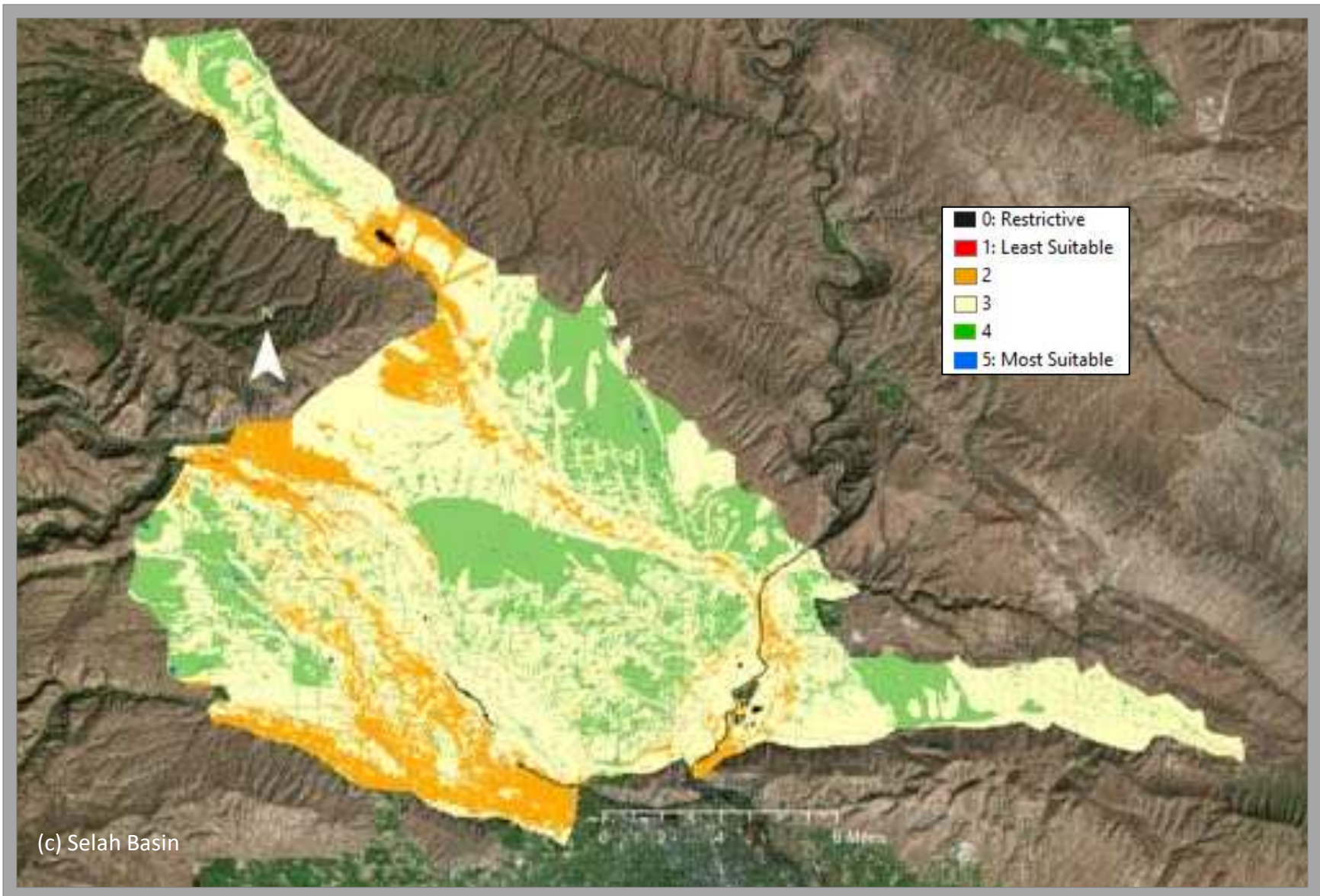
Table 3. Weighted overlay results by percent of basin area.

Figure 6. Results of the AHP Analysis: (a) Roslyn Basin, (b) Kittitas Basin, (c) Selah Basin, (d) Benton Basin, (e) Yakima Basin, and (f) Toppenish Basin. Areas in blue scored 5 out of 5, indicating all requirements for suitability were met. Areas in black were not included in the analysis as the locations represented impervious surfaces or surface water.

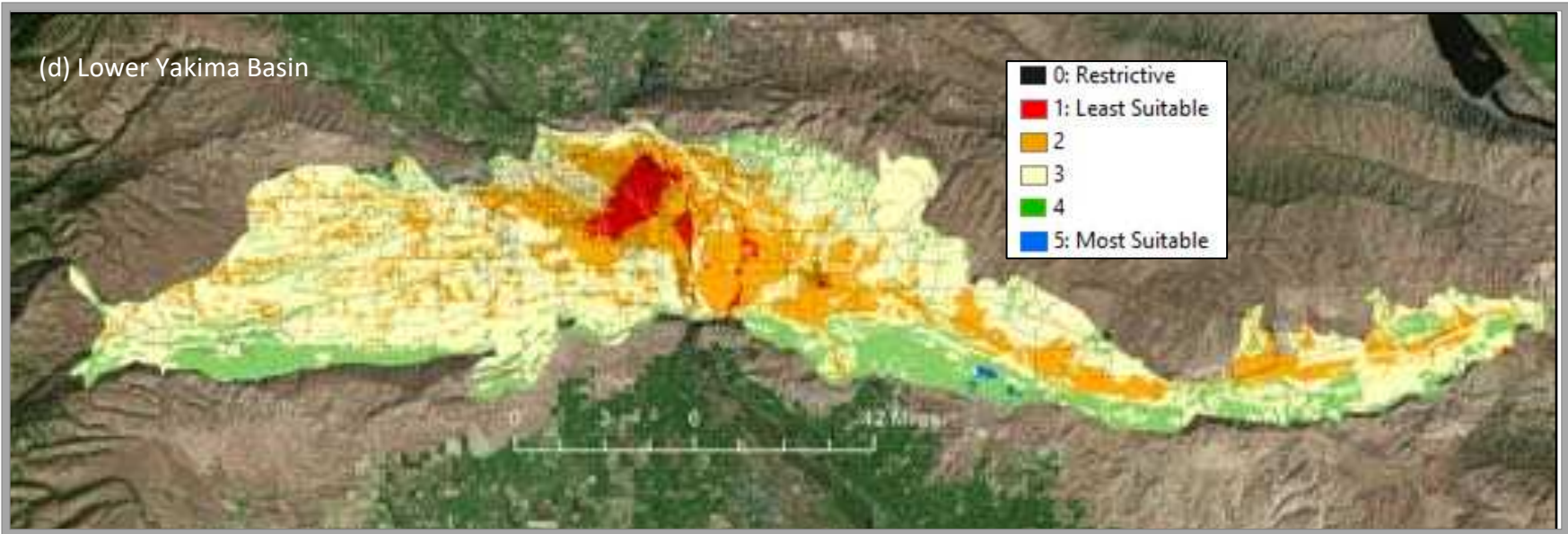


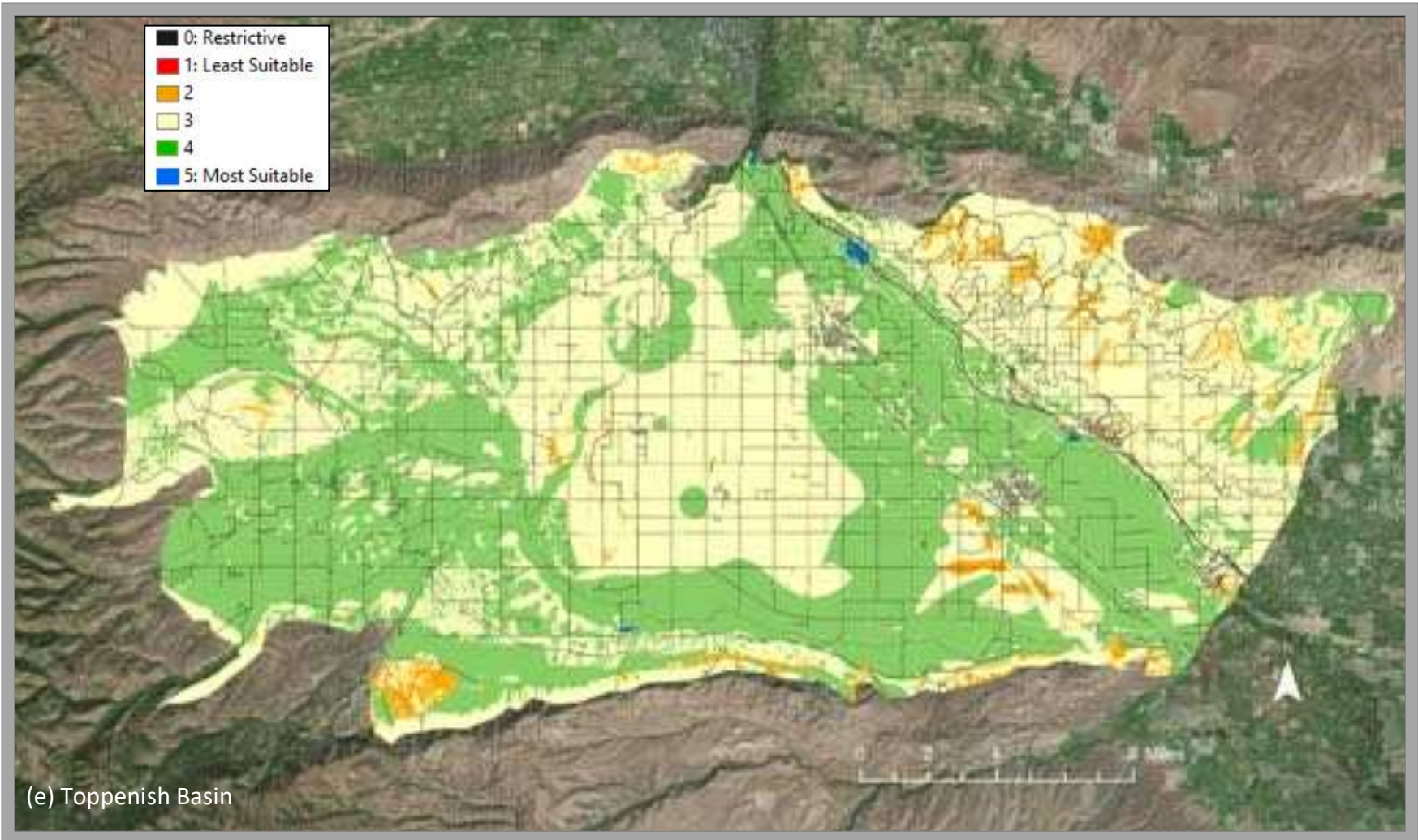
(b) Kittitas Basin



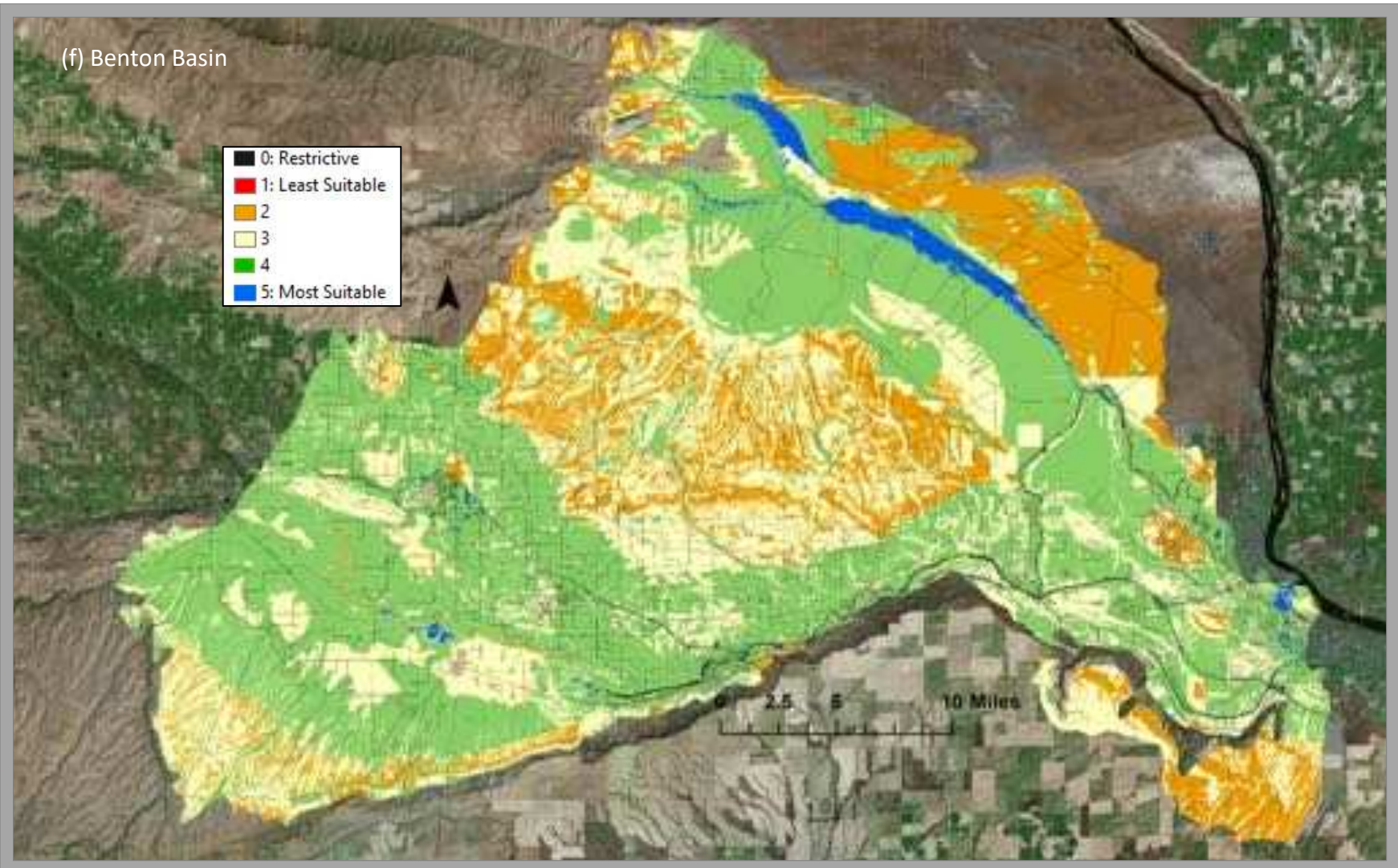


(d) Lower Yakima Basin





(f) Benton Basin



Sensitivity Analysis Results

Two sensitivity analyses were undertaken to understand the stability and robustness of the AHP method. Simulations of a 50% weight reduction of each criterion with equal distribution among remaining criteria predicted the system was most sensitive to transmissivity and least sensitive to land use. Percentage of suitable area under initial conditions equaled 22%. However, a 50% reduction in transmissivity increased suitable locations by 7%, whereas a 50% reduction in land use increased suitability by 1%. (Table 4). The second sensitivity analysis required the removal of each criterion within each structural basin. For simplification, Figure 7 are the results of the Lower Yakima Basin - results for all basins are in Appendix A.

50% reduction of criterion	Percent of suitable locations
Lithology	20%
Slope	24%
Transmissivity	29%
Land use	23%
Static Water Level	17%
Original	22%

Table 4. Results of sensitivity analysis with 50% reduction of criterion with equal distribution of weight to the criteria

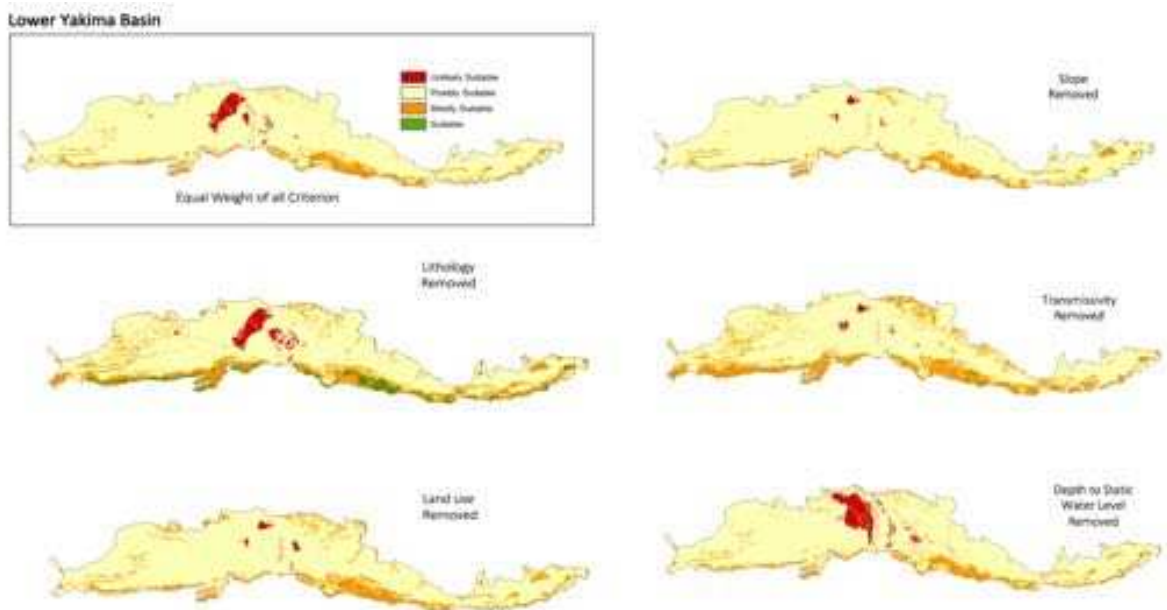


Figure 7. Simulation results of the sensitivity analysis where factor removal was exercised as a method to assess criterion influence and its implication on suitable locations. For simplicity, only the Lower Yakima Basin is shown. Sensitivity maps for each basin are available in Appendix A.

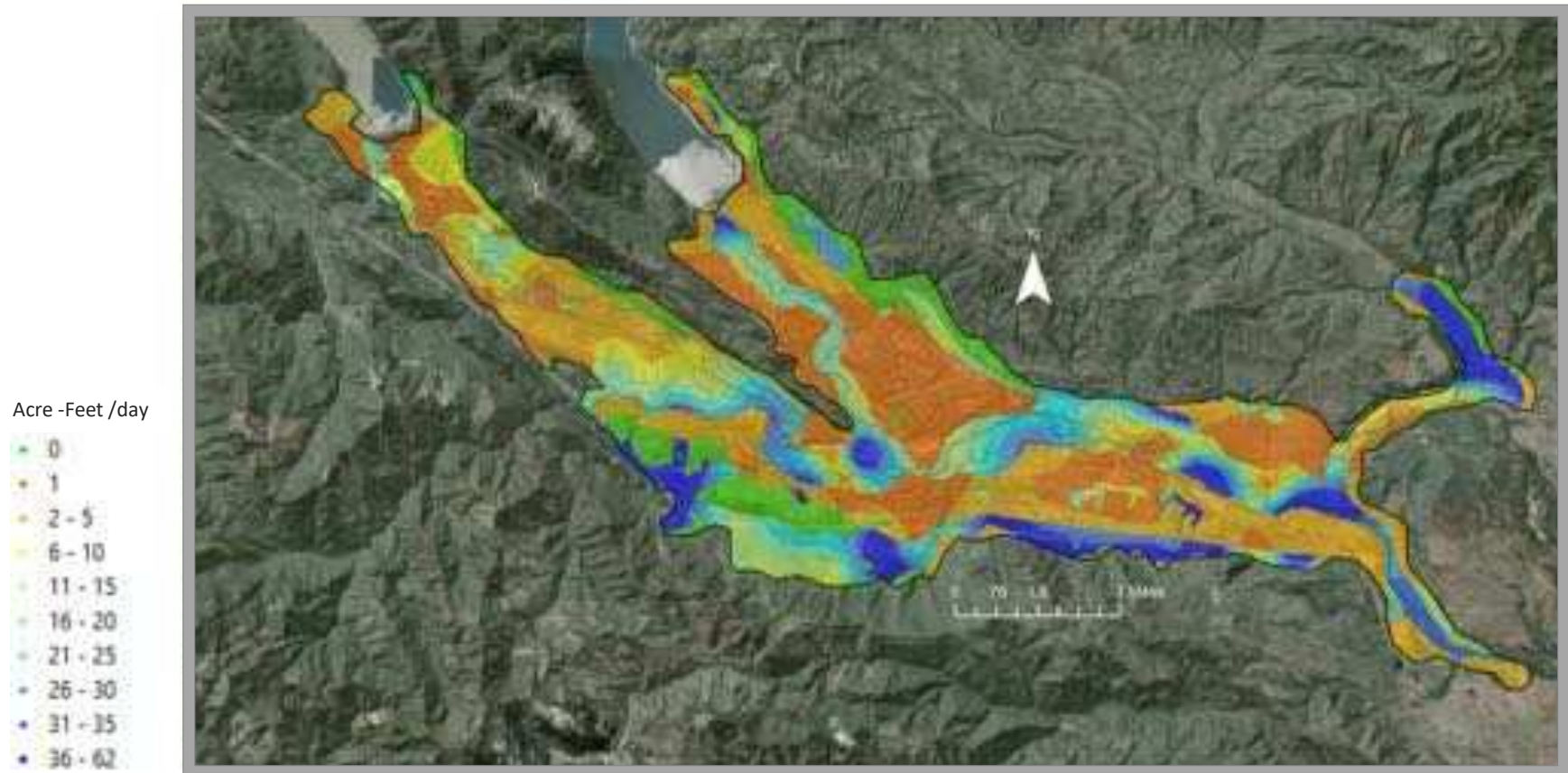
Analytical Results

Shallow Aquifer Recharge

Estimation of potential recharge capacities based on groundwater mounding were calculated from a derivation of Glover's (1960) solution within a circular infiltration basin. To estimate potential recharge storativity, transmissivity, radius of recharge location, and depth to static water level must be known. Spatial distribution varied among each basin and are represented in Figure 8 (a-f).

Figure 8. Spatial representation of potential recharge capacity of each structural basin within the Yakima River Basin. The six structural basins include (a) Roslyn, (b) Kittitas, (c) Selah, (d) Benton, (e) Yakima, and (f) Toppenish.

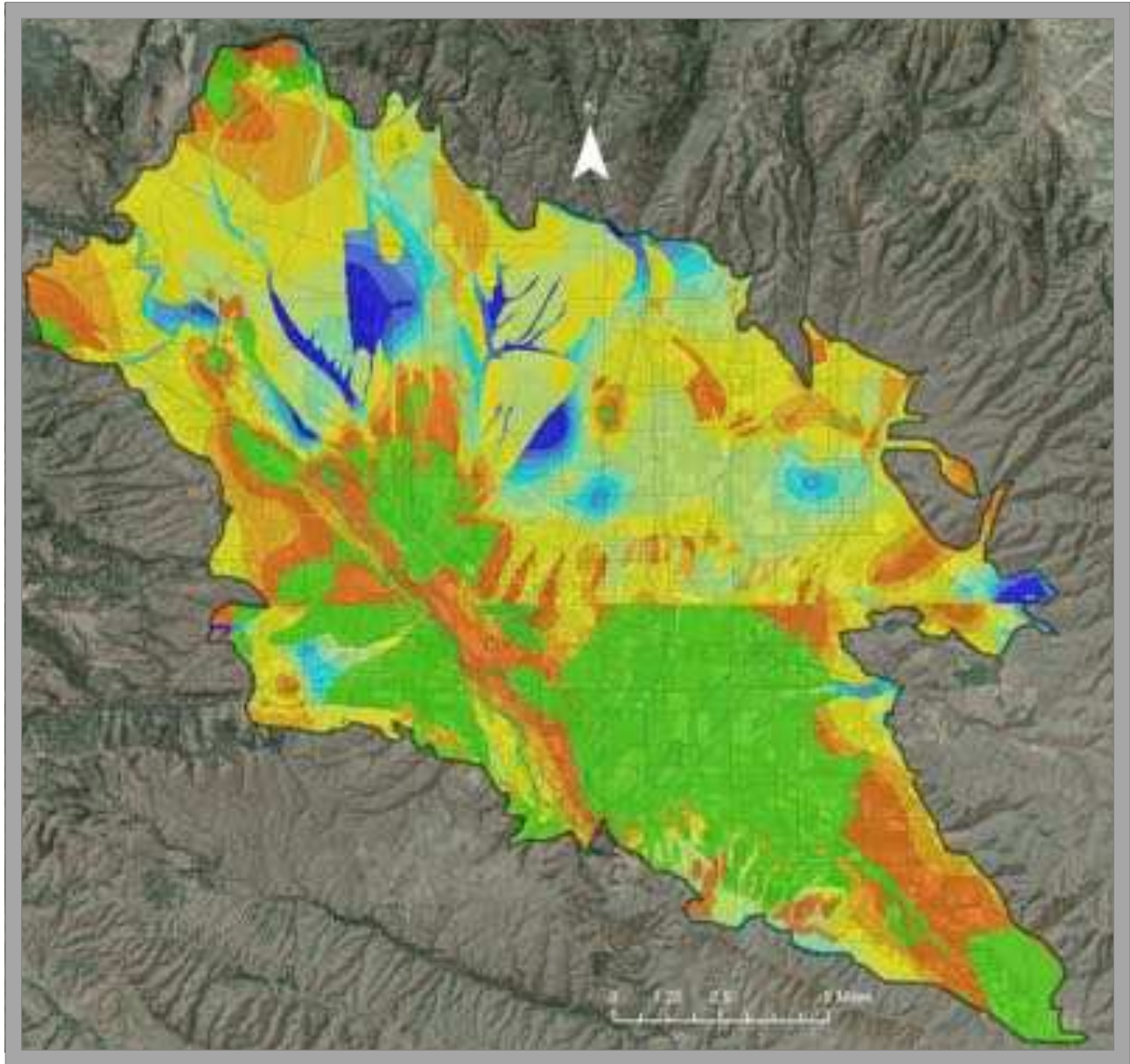
(a) Roslyn Basin



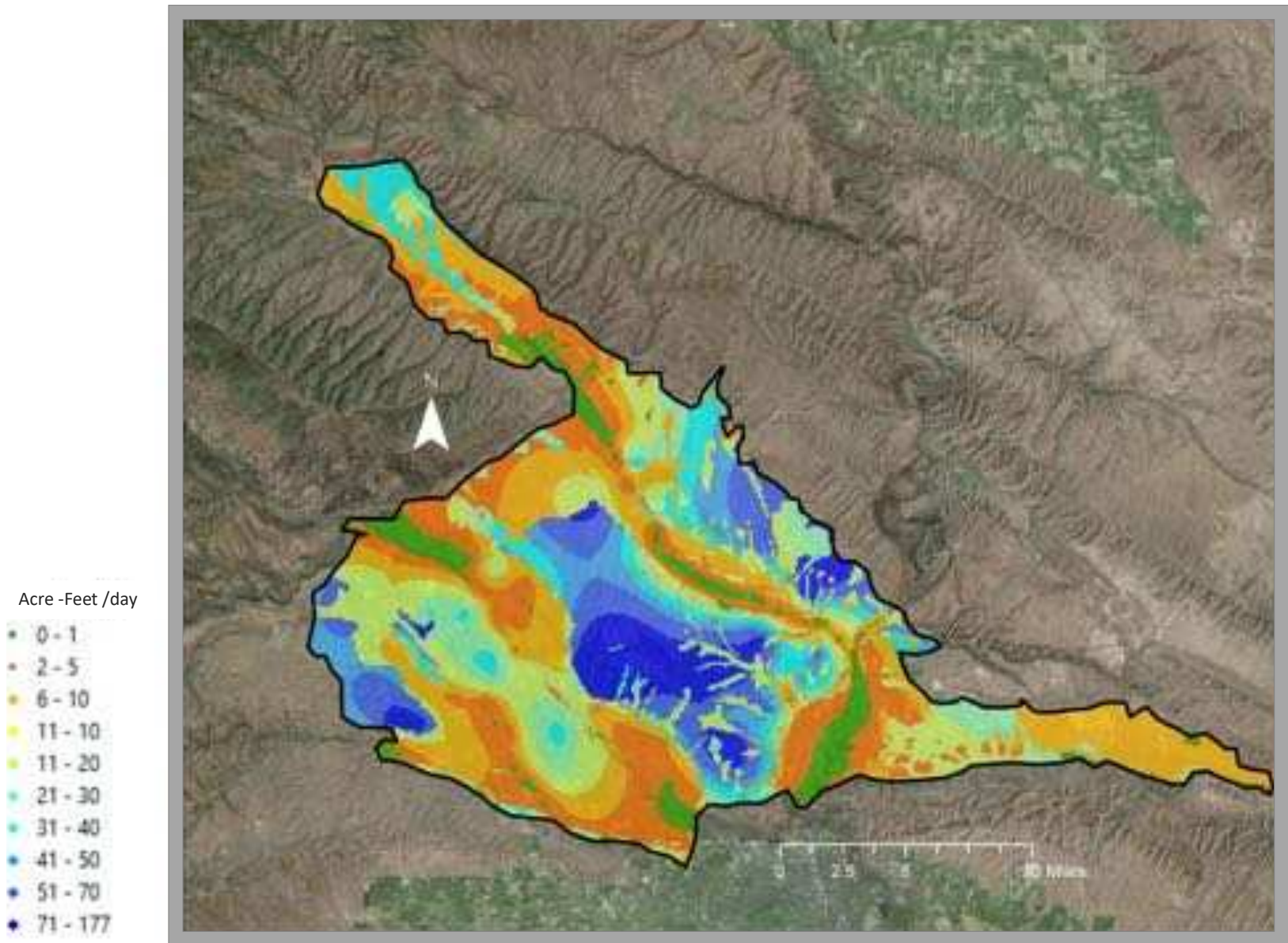
(b) Kittitas Basin

Acre -Feet /day

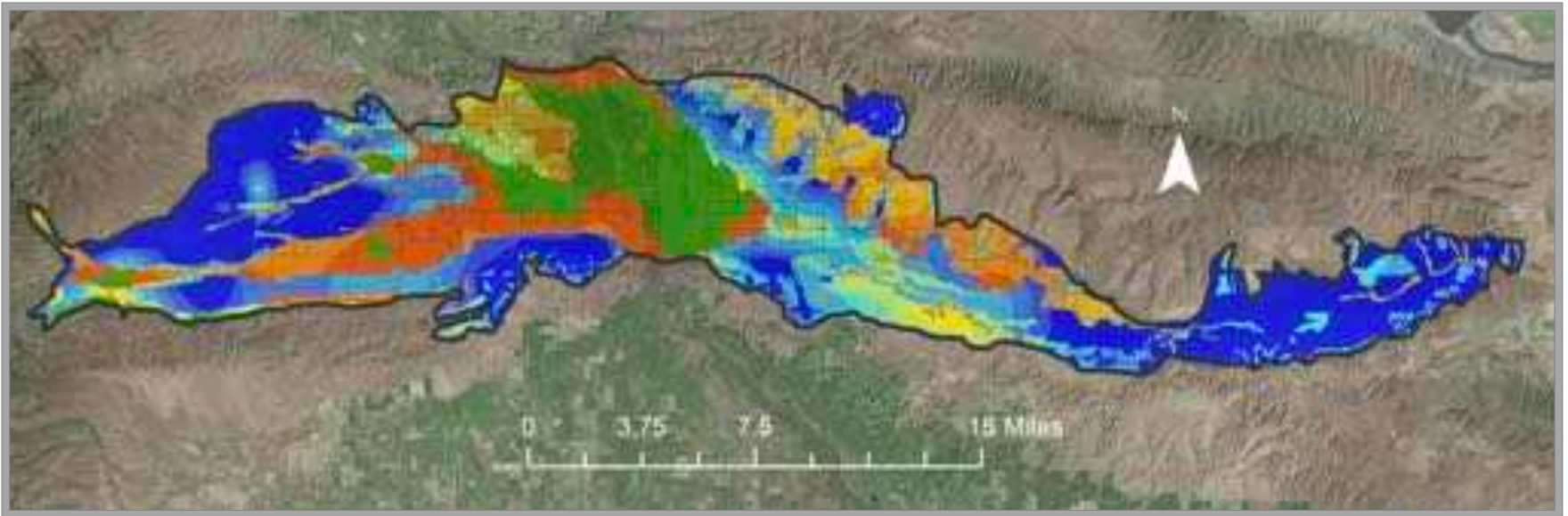
- < 1
- 2 - 3
- 4 - 5
- 6 - 10
- 11 - 15
- 16 - 20
- 21 - 25
- 26 - 30
- 31 - 35
- 36 - 62



(c) Selah Basin



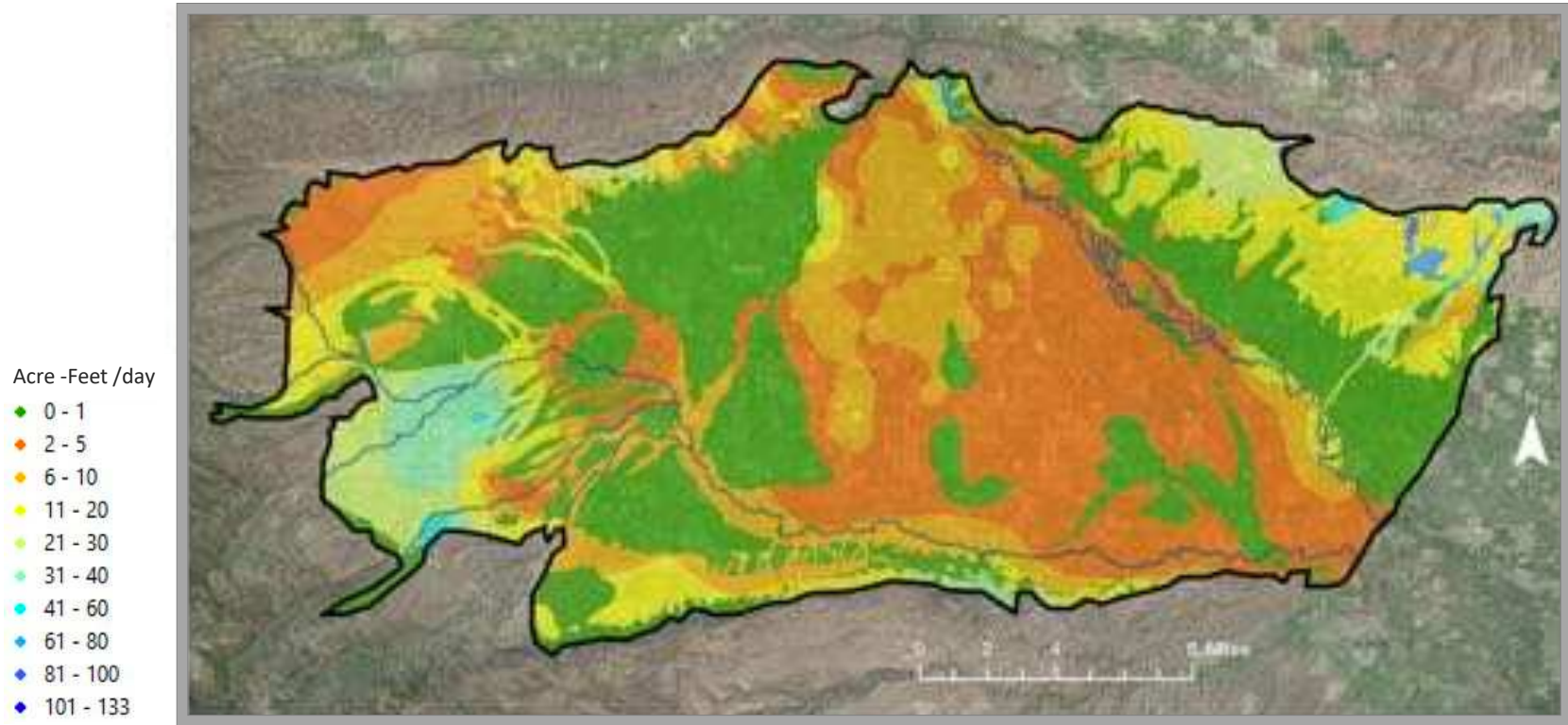
(d) Lower Yakima Basin



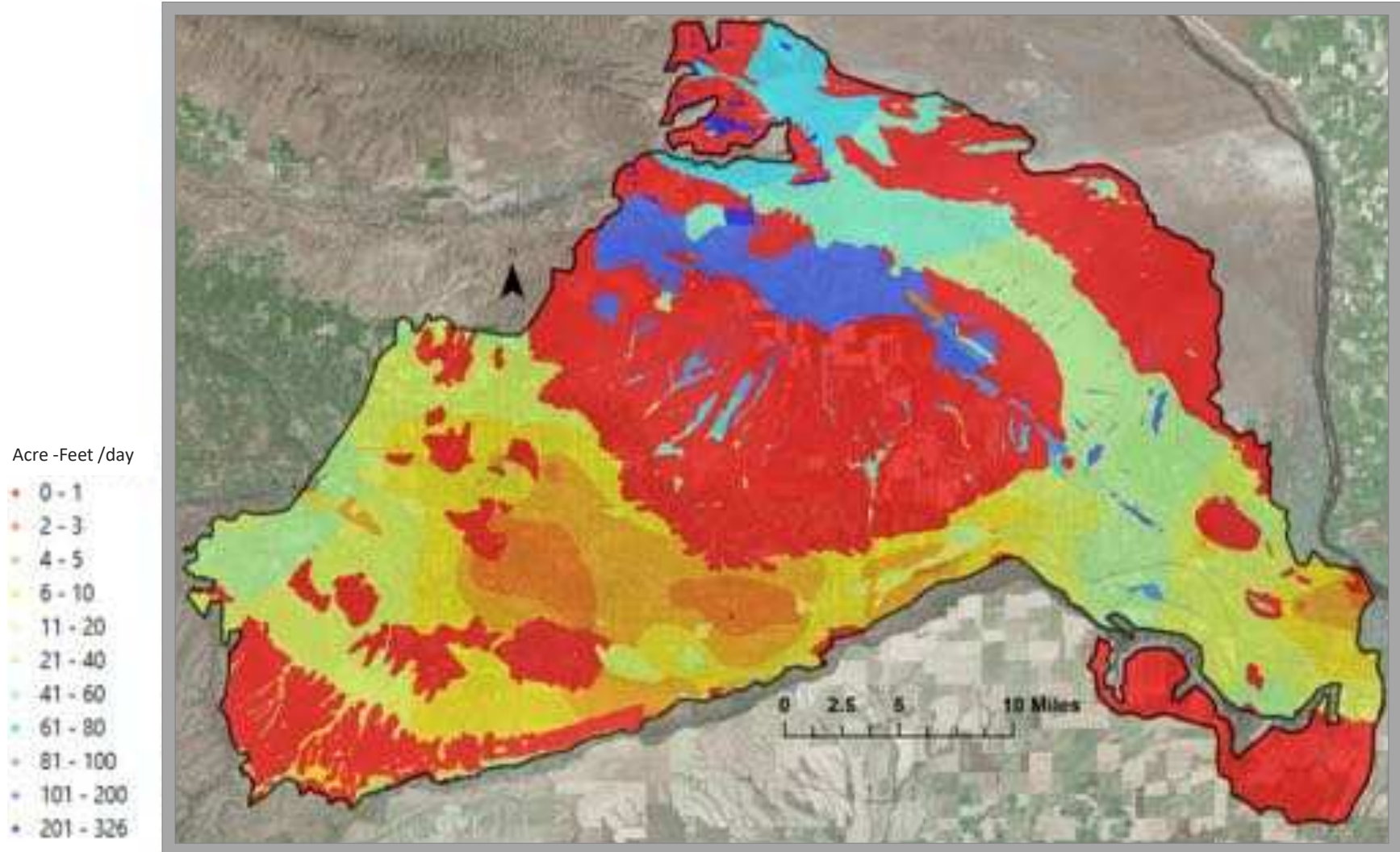
Acre - Feet /day

- 0 - 1
- 2 - 5
- 6 - 10
- 11 - 20
- 21 - 30
- 31 - 40
- 41 - 60
- 61 - 80
- 81 - 100
- 101 - 200
- 201 - 300
- 301 - 400
- 401 - 951

(e) Toppenish Basin



(f) Benton Basin



Combined Section Results

To elucidate areas of suitability for SAR within each structural basin, a coupled method was conducted in ArcMap that constrained the analytical solutions to the overlay locations with scores greater than 4. By combining the two methods, it allowed for reasonable comparisons of locations within and among basins (Table 5) (Figure 9 a-f). The smallest and most mountainous basin, Roslyn, has an area of 77 mi² with a potential annual recharge rate capacity of 104 TAF in Zone 4 and a 405 TAF capacity in Zone 5. Kittitas, the third largest basin (area 270 mi²), has a maximum recharge rate capacity of 243 TAF in Zone 4 and an 1865 TAF capacity in Zone 5. The Selah basin has an area of 170 mi², has a recharge rate capacity of over 4700 TAF in zone 4 and 24 TAF in Zone 5. The Yakima basin, with an area of 232 mi², has a recharge rate capacity of over 3600 TAF in Zone 4 and 11 TAF in Zone 5. Toppenish basin, which is the second largest basin (area of 1548 mi²) has a recharge rate capacity of over 2200 TAF in Zone 4 and a 3 TAF in Zone 5. The largest basin, Benton, has an area of 1004 mi² with a potential recharge rate capacity of 21484 TAF in Zone 4 and 730 TAF in Zone 5.

Recharge (TAF/year)	Roslyn	Kittitas	Selah	Yakima	Toppenish	Benton	Total
Zone 5	105	243	24	11	3	730	1116
Zone 4	405	1865	4783	3648	2270	21484	34455
Area of Basin (mi ²)	77	270	170	232	548	1004	2301

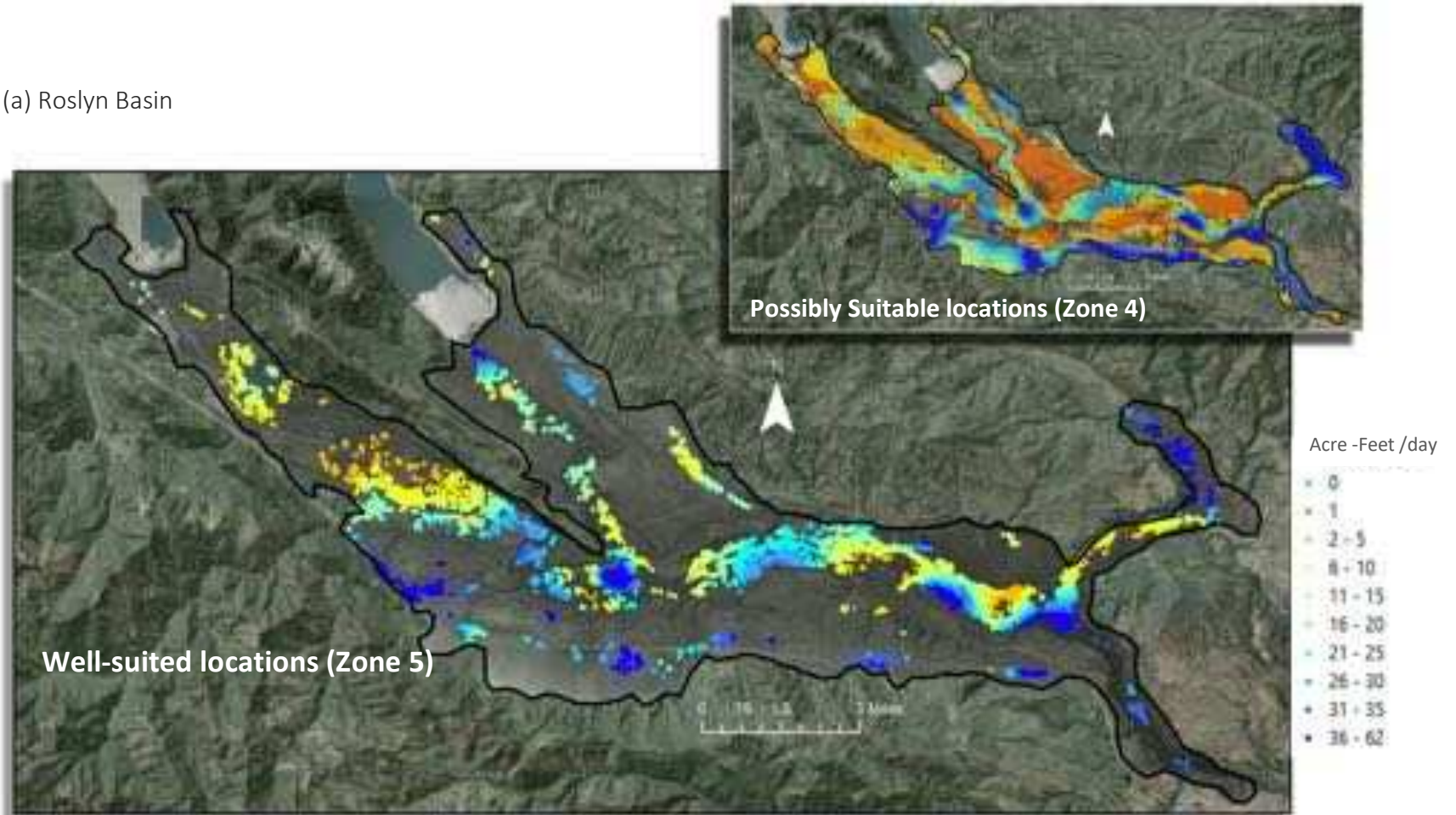
Table 5. The table represents estimated annual recharge capacity constrained to locations considered suitable for SAR within each structural basin. Zones of recharge are locations that met at least 4 out of 5 on the weighted overlay analysis

Infiltration Potential by Select Geological Units

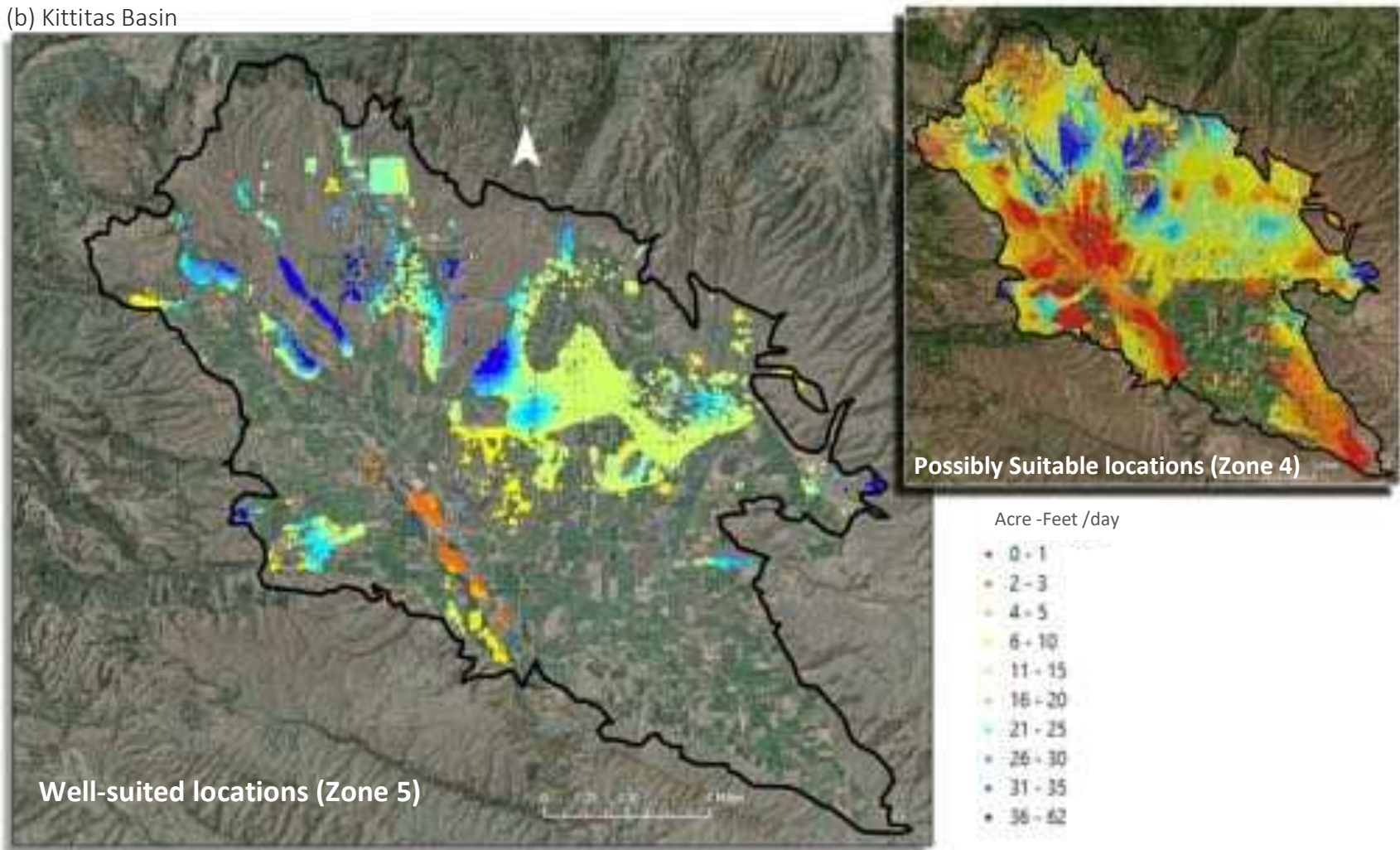
Infiltration potential for select geologic and lithologic units were assessed by estimating the mean and median values obtained from the recharge potential assessment. Values among each structural basin, values varied between 2 to 100 AF per day, with the highest mean and median value located within the continental sedimentary deposits of the Lower Yakima Basin. Charts of infiltration potential for each structural basin are in Appendix C.

Figure 9. Combined Results. Well-suited locations (Zone 5) met all criteria of the weighted overlay analysis. Possibly suitable locations (Zone 4) met 4 out of 5 criteria. The associated basin maps – (a) Roslyn, (b) Kittitas, (c) Selah, (d) Lower Yakima, (e) Toppenish, and (f) Benton – display recharge potential within Zone 4 and Zone 5.

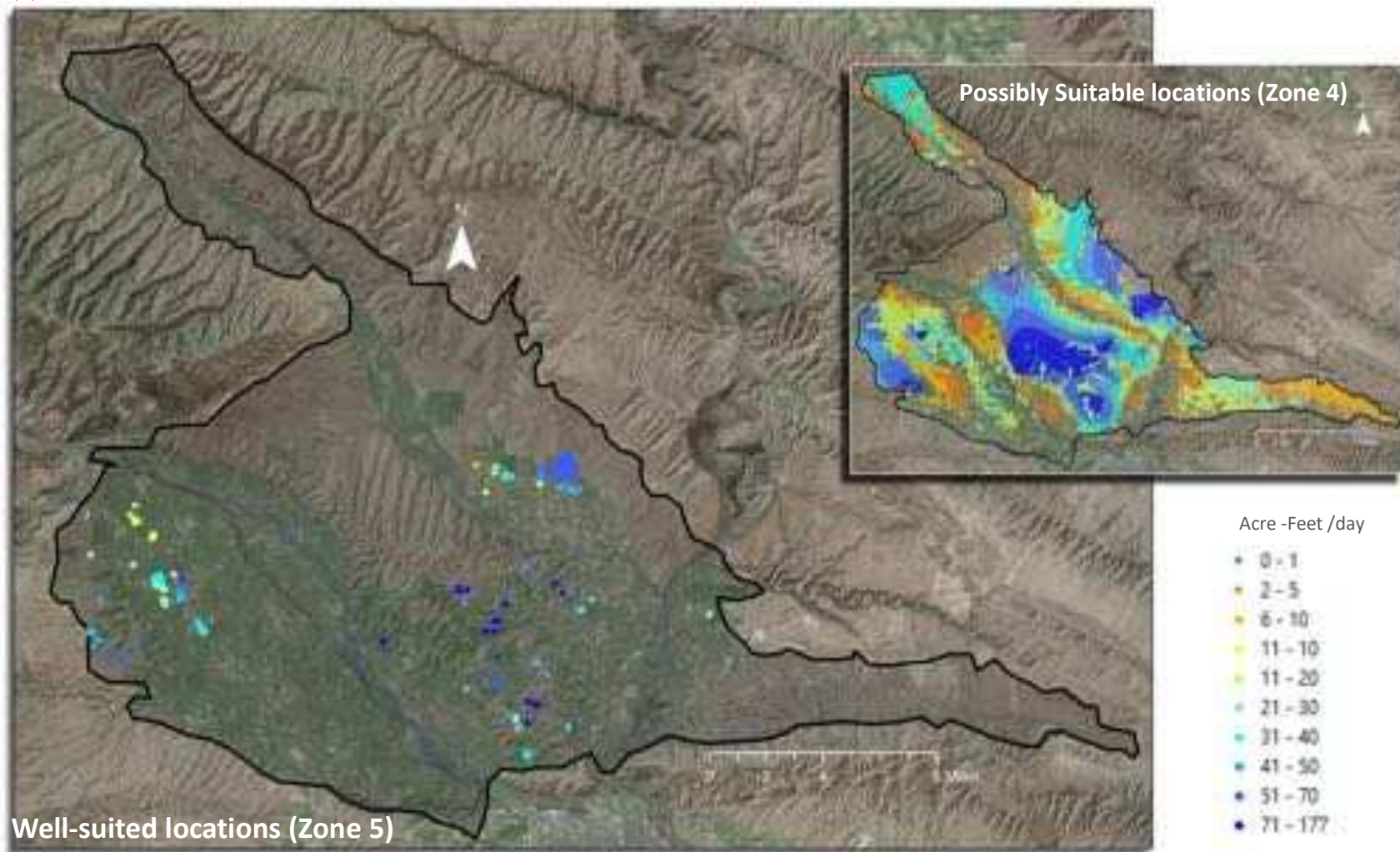
(a) Roslyn Basin



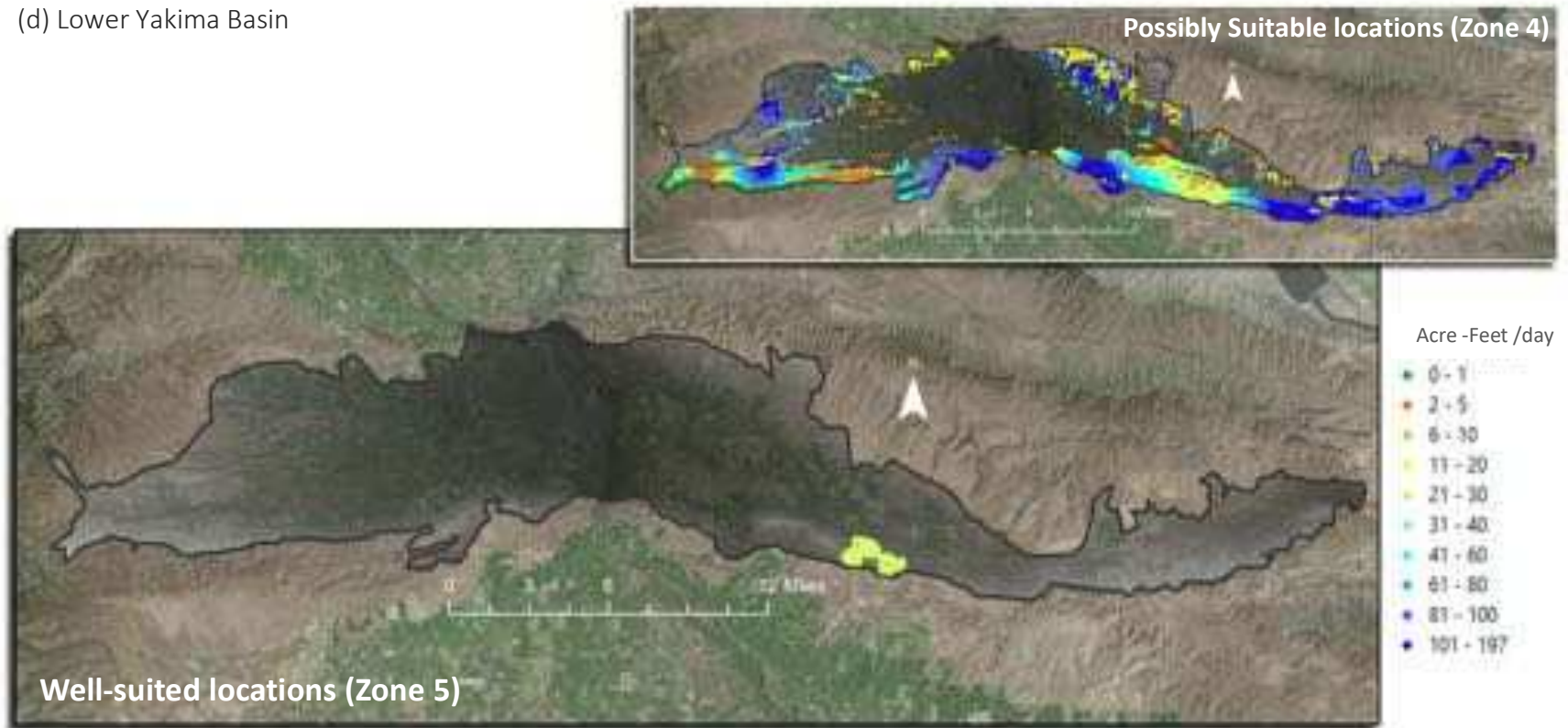
(b) Kittitas Basin



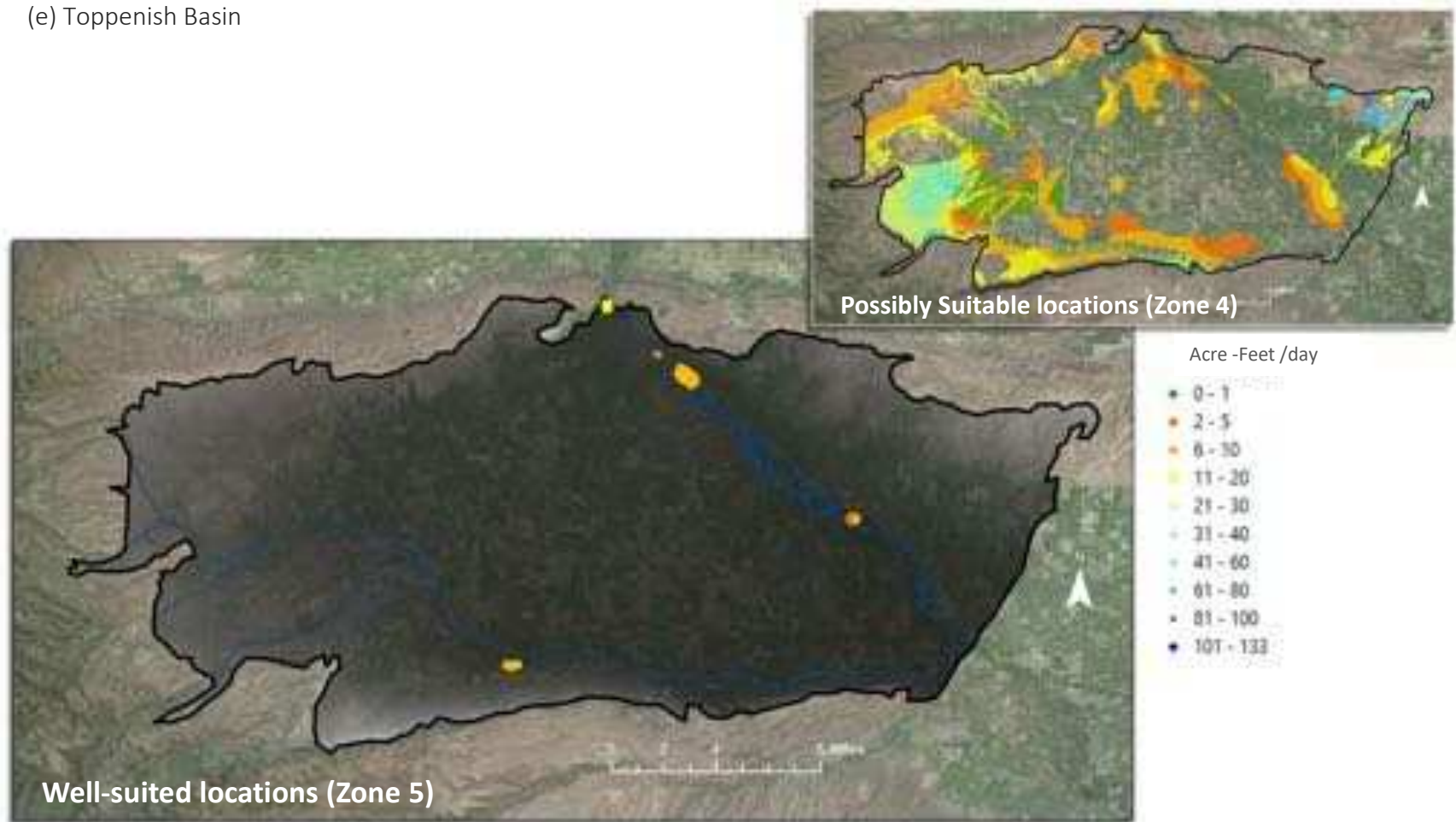
(c) Selah Basin



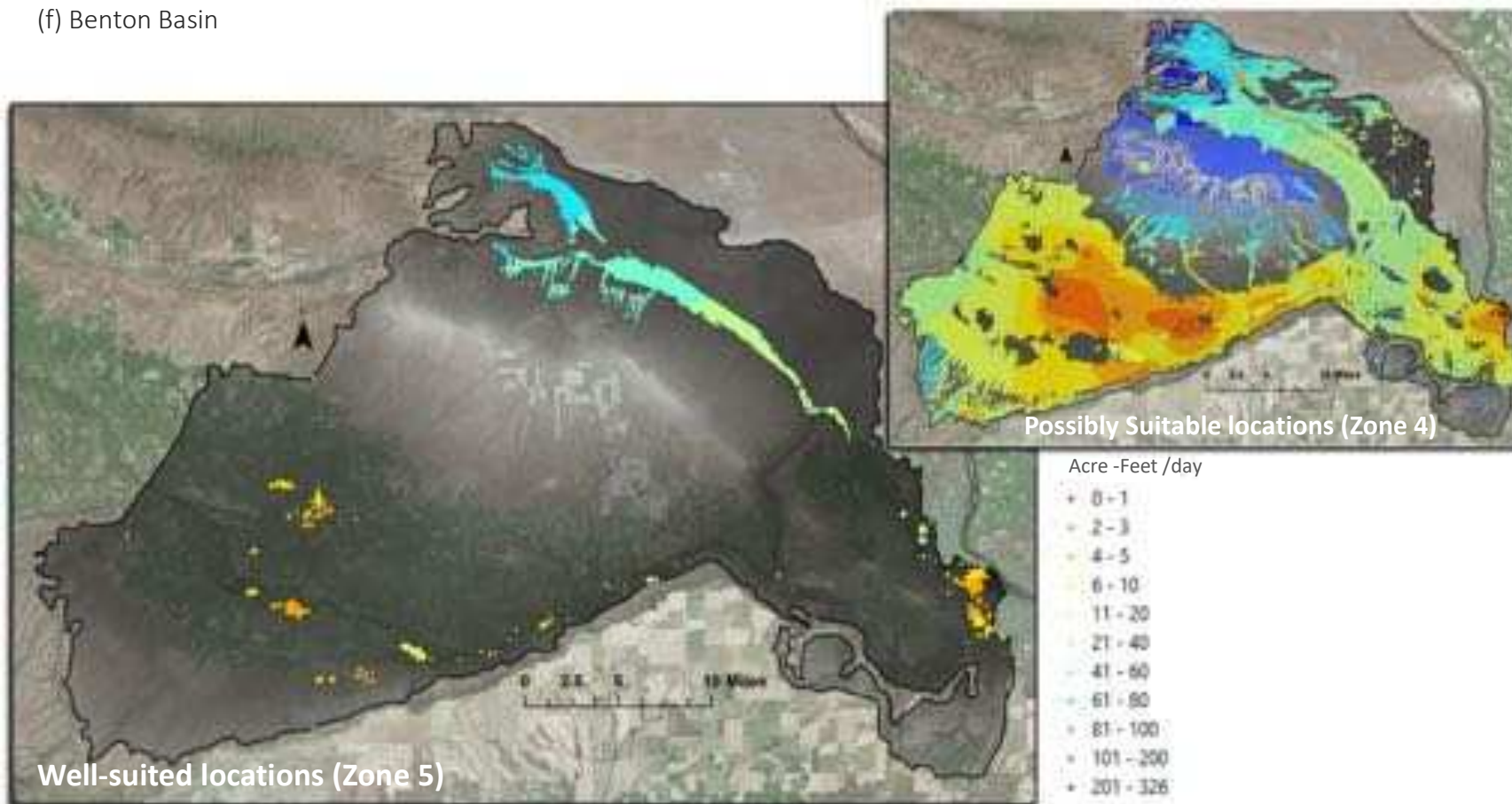
(d) Lower Yakima Basin



(e) Toppenish Basin



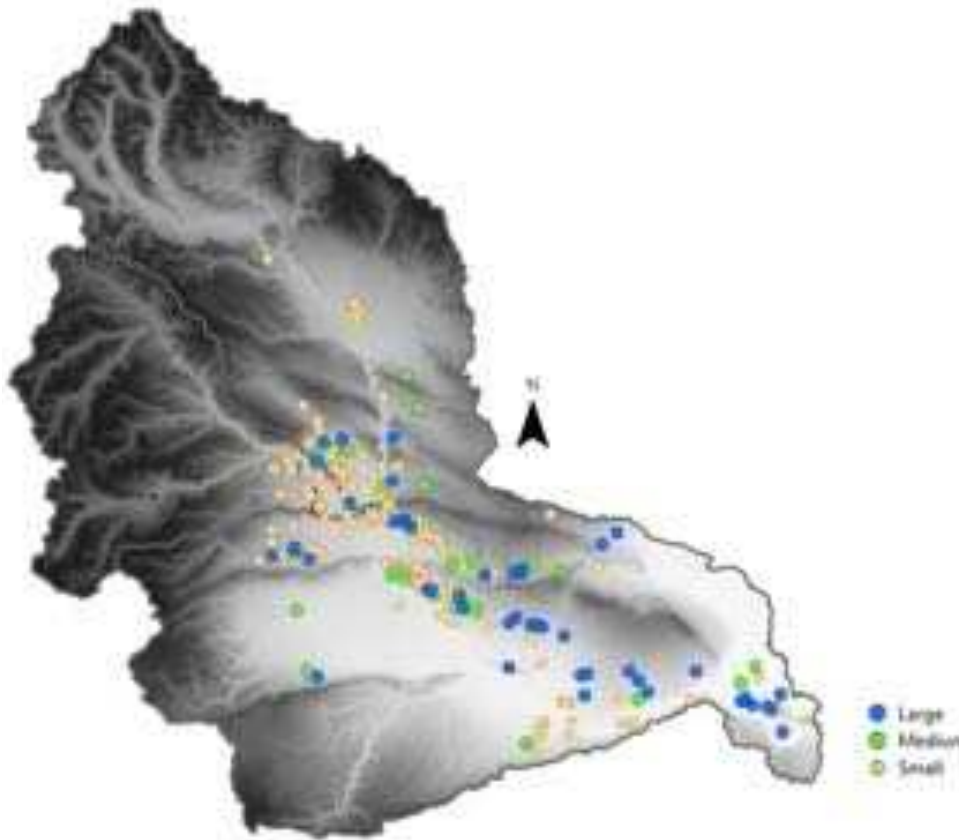
(f) Benton Basin



ASR Results

The Ellensburg Formation was targeted for ASR development. An assessment of local well logs and an analytical solution was used to identify potential injection rates. Injection rates were subdivided into small (less than 5 cfs) , medium (5 cfs to 15 cfs), and large (greater than 15 cfs). It is estimated the mean injection rate for the Ellensburg is up to 7 cfs. The maximum rate exceeded 245 cfs and the mean injection rate for large wells is estimated at 60 cfs. As a comparative measure, the City of Yakima operates the only ASR program within the Yakima River Basin and is permitted to inject up to 13 cfs into the Ellensburg Formation through 2 municipal wells. The injection rate varies among each structural basin and are shown in Figure (10)

Figure 10. Results of the ASR analysis targeting the confined Ellensburg Formation, with respective injection rates of each structural basin, with the exception of the Roslyn Basin, as no data were available in the basin to complete the analysis.



Kittias			
	Injection Rate (cfs)	Transmissivity (ft ² /d)	Well Depth (ft)
Mean	4	4109	863
Median	2	4308	761
Min	1	438	617
Max	10	8405	1205

Selah			
	Injection Rate (cfs)	Transmissivity (ft ² /d)	Well Depth (ft)
Mean	9	5338	656
Median	2	1679	576
Min	0.1	183	500
Max	91	59924	1955

Lower Yakima			
	Injection Rate (cfs)	Transmissivity (ft ² /d)	Well Depth (ft)
Mean	13	7413	834
Median	4	4001	676
Min	0.3	75	500
Max	123	61128	2213

Toppenish			
	Injection Rate (cfs)	Transmissivity (ft ² /d)	Well Depth (ft)
Mean	9	4507	871
Median	8	3569	710
Min	0.3	538	510
Max	48	16035	1945

Benton			
	Injection Rate (cfs)	Transmissivity (ft ² /d)	Well Depth (ft)
Mean	35	11801	965
Median	9	5676	888
Min	0	136	502
Max	254	85142	1690

2. System Dynamics Modelling: YAK-SDM

System Dynamics Modelling

Dynamic modeling of the Yakima River Basin was conducted within a system dynamics framework, which integrates proactive management strategies based on a system of equations. A system dynamics model connects causal mathematical models to observed, then predicted behavior (Forrester, 1987). Developed in the 1960s by Forrester (1961, 1969) to examine feedback theory in urban and industrial systems, it has since been applied in a wide field of disciplines including policy analysis (Pandey, 2002; Stave, 2002; Chi et al., 2009) sustainability, (Moffatt and Hanley, 2001; Slootweg et al., 2003; Bockerman et al., 2005; Antunes et al., 2006; Rehman et al., 2017), and water resources (Winz et al., 2009; Yang et al., 2015; Dhungel and Fiedler, 2016), including scarcity (Susnick et al., 2012). System dynamics modelling in water resources has also proven useful to managing conflict (Zomorodia et al., 2017; Pluchinotta et al., 2018), examining groundwater resources (Kotir et al., 2016; Susnik et al., 2017, Ohab-Yazdi et al., 2018), predicting groundwater sustainability and aquifer recharge (Niazi et al., 2012; Dhungel and Fiedler, 2016) and water quality management (Rivera et al., 2006).

The model development was conducted in the Structural Thinking Experimental Learning Laboratory with Animations (STELLA) software. It has been widely used in the field of SDM. Cassel and Clausen (1993) modeled phosphorus in agricultural environments to examine the long-term transport processes in surface water and groundwater, suggesting strategic variation in best management practices. Elshorbagy et al. (2006) modeled fecal coliform in surface water under various management scenarios at the watershed scale. A simulation model in STELLA was developed to analyze flow management options within an energy demand and climate framework in Ontario, Canada (Oni et al., 2012). In the Eastern Snake Plain Aquifer a system dynamics model was created in STELLA to conduct sustainable resource water scenarios with a MAR alternative when supply diminished (Ryu et al., 2012). The model aided in evaluating aquifer recharge and discharge associated with conservation, climate change, ET, and curtailment options, but MAR alternatives were not spatially assessed. In 2013, Jiao and Xu built a hydrological unit model for the Heihe River Basin in China to assist in spatially modelling runoff in mountainous regions. Groundwater depletion and fluctuation was modeled in STELLA for the Hamedan-Bahar plain in Iran in response to irrigation, energy pricing, and climate change (Balali and Viaggi, 2015). A system dynamics model was created in STELLA to evaluate water resources in the Zhengzhou City in China in response to sustainable scenarios (Li et al., 2018). The following analysis was conducted in STELLA to replicate the Yakima River IWRMP, estimate MAR potential, and understand its development in response to climate change.

System Dynamics Modelling (SDM) in STELLA uses interlinking compartments to account for the accumulation of material, known as *stocks* with *flows*, allowing for the movement of material in and out of stocks. Converters are used for the creation of system feedback or for modification of flows through connecting arrows (Figure 11).

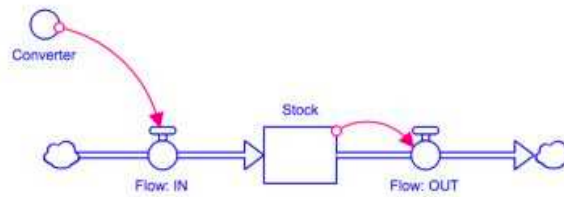


Figure 11. Core components of system dynamics modelling within STELLA. The converters allow for system feedback or modification of flows, while flows provide movement in and out of stocks. The cloud represents the boundary of the model where its influence is negligible.

Stocks are the state variable with the underlying following nonlinear differential equation within the model simulation:

$$X_i(t + \Delta t) = X_i(t) + f(X_i, R_i, A_i, C_i) \cdot t$$

Where,

$X_i(t)$ is the state variable vector

$f()$ is the vector-valued function

R_i is the flow variable vector

A_i is the auxiliary variable vector

C_i is the parameters vector

t is time

Δt is change in time

An SDM was developed for the Yakima River Basin (YAK-SDM). The YAK-SDM model analyzes capture potential against historical flow conditions, including two drought and one wet year. The modelling framework was designed to incorporate basin-wide estimations of capture and storage potential and provide alternative options to groundwater storage as a mitigation tool to accommodate projected hydroclimate alterations.

The YAK-SDM model (Figure 12) was created with a daily timestep, and a model run span of 13 years (1 to 4745 days) - beginning with water year 2005 and ending in 2017, with respective leap year days removed. The YAK-SDM model is fed by the Capture Potential Sector and MAR Sector. The Climate Change Sector was developed to estimate storage potential to accommodate hydrologic changes at the Parker Gauge for year 2040 and 2080. The IWRMP Surface Storage Goal Sector was built to compare groundwater storage potential against surface storage goals of the

IWRMP. Calibration of the model was conducted for 2 parameters: years of prorationing and mean annual precipitation. Table 6 shows values used and their source for specific converters in the YAK-SDM.

Type	TAF	Source
Mean Annual Precipitation	8900	Ely et al., 2011
Annual Groundwater Pumping	317	Vaccaro and Sumioka, 2009
Annual Groundwater Recharge	5200	Vaccarro and Sumioka, 2009
Conservation	97	HDR Engineering and Anchor QEA, 2011
Storage Potential Per Day for Zone 5		Gibson, 2018
Roslyn	105	
Kittitas	243	
Selah	24	
Yakima	11	
Toppenish	4	
Benton	730	
Storage Potential Per Day Zone 4		Gibson, 2018
Roslyn	413	
Kittitas	1865	
Selah	4783	
Yakima	3648	
Toppenish	2270	
Benton	21484	
Reservoir Storage Capacity		U.S Bureau of Reclamation and Washington State Department of Ecology, 2012
Keechelus	158	
Kachess	239	
Cle Elem	437	
Bumping	340	
Rimrock	198	

Table 6. Values and their source for specific converters in the YAK-SDM.

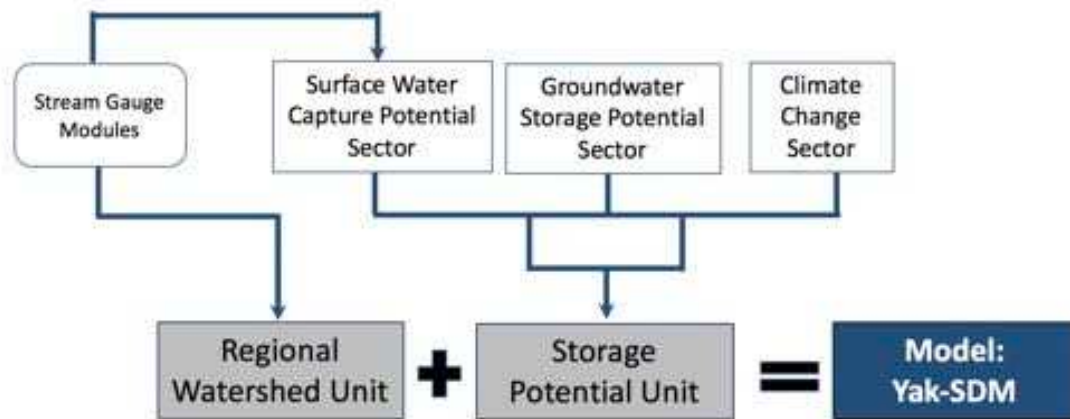


Figure 12. A simplified diagram of the YAK-SDM model with corresponding units and respective sectors and modules.

Model Construct

The YAK-SDM model is segmented into two sections connected by the “Precipitation Threshold Derived from Historic Data” and the “Total Managed Aquifer Recharge (MAR) Potential” converter. The left section of the model was developed to understand the relationship between groundwater storage, pumping, and natural recharge (Figure 13). Groundwater recharge is estimated at 5,100,000 AF per year, with an annual mean pumping volume of 324,000 AF (Vaccaro and Sumioka, 2009). Annual precipitation is estimated at 8,900,000 AF and evapotranspiration is believed to equate to ~54% of annual precipitation (Ely et al., 2011). It is also estimated that the 5 surface water reservoirs equal 30% of total annual runoff (U.S. Bureau of Reclamation and Washington Department of Ecology, 2012). Therefore, prorating was predicted from calibrated precipitation patterns obtained from historical reservoir release data. Evapotranspiration and uncaptured annual runoff were also calculated from historic precipitation patterns. The “Storage and Release Trends” were estimated from combined historic reservoir levels and reservoir release flows, both obtained from the U.S. Bureau of Reclamation (2018) Yakima Project Hydromet System. The “Estimated Yearly Precip Conditions” calculated the volume of precipitation at the end of each year from basin reservoir storage and was calibrated to annual precipitation for average years. The “Departure from Average” converter determined wet, average, and dry years based on divergence from normal conditions.

The remaining section of the YAK-SDM combined potential capture scenarios with potential storage (Figure 14) to calculate the percent the basin can meet precipitation deficits under varying

hydrologic conditions. This percentage was derived from “Precipitation Threshold Data Derived from Historic Data”, which is estimated from cumulative reservoir release volumes.

Figure 13. YAK-SDM: Regional Watershed Unit

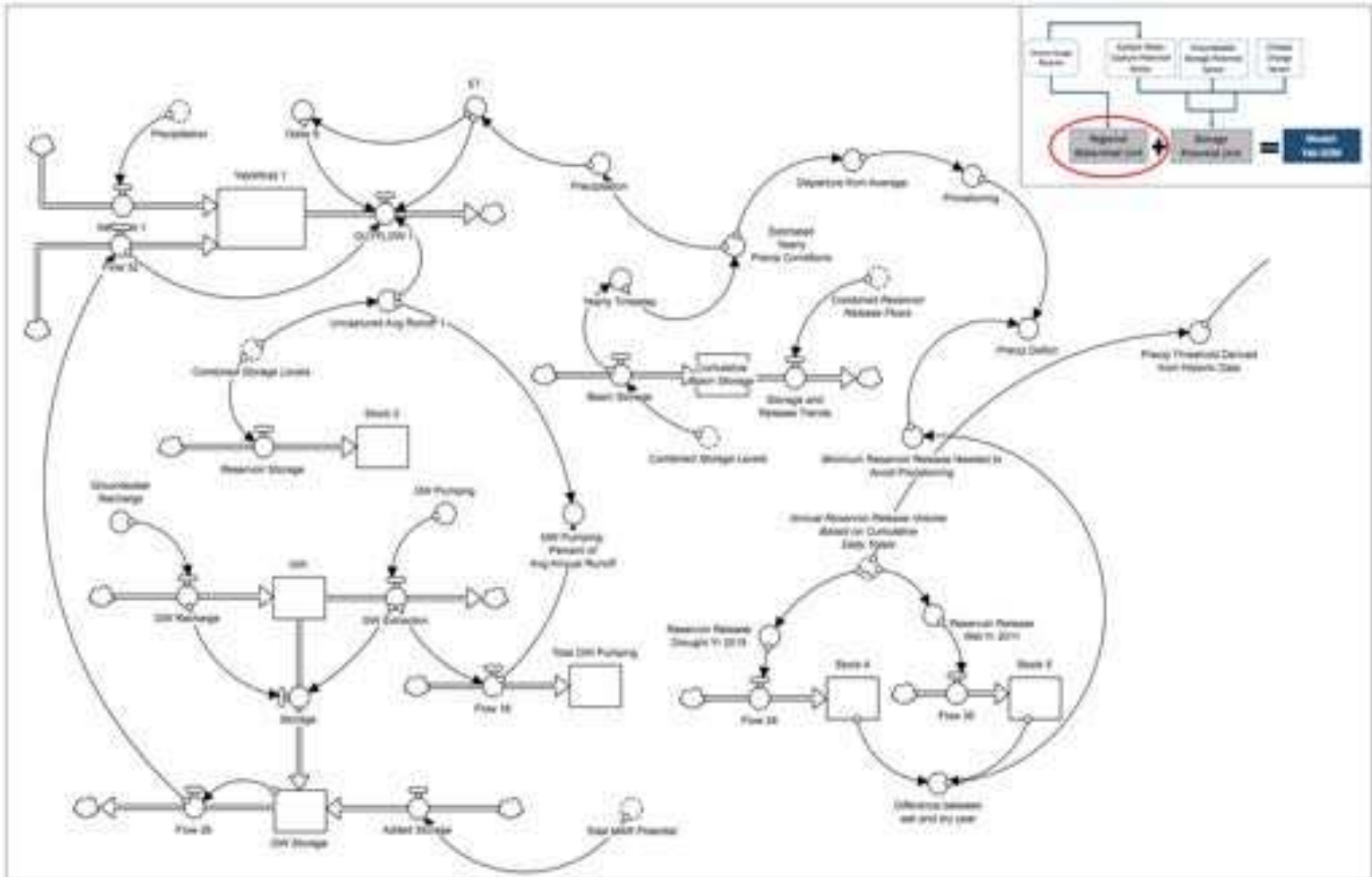
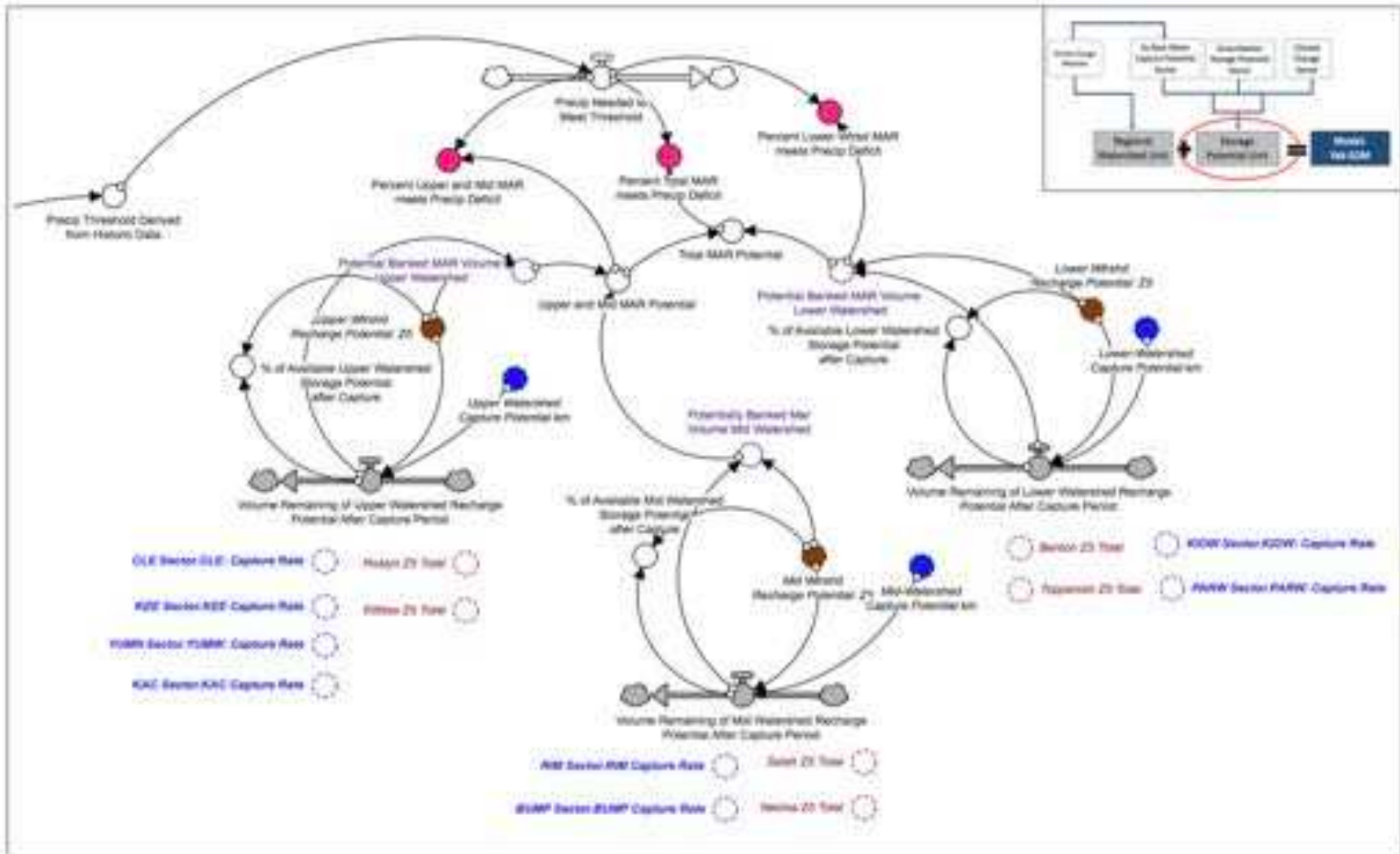


Figure 14. YAK-SDM: Groundwater Storage Unit



As a comparison approach, the minimum cumulative reservoir volume occurred in 2005, with the greatest occurring in 2011. The difference in value was calculated at 0.6 MAF and was also used as a precipitation threshold (Figure 15). This converter was used to vary the value up to the threshold to estimate the percent the basin can meet precipitation deficits under different scenarios. The model also estimated potential banked volume for upper, mid, and lower reaches of the watershed.

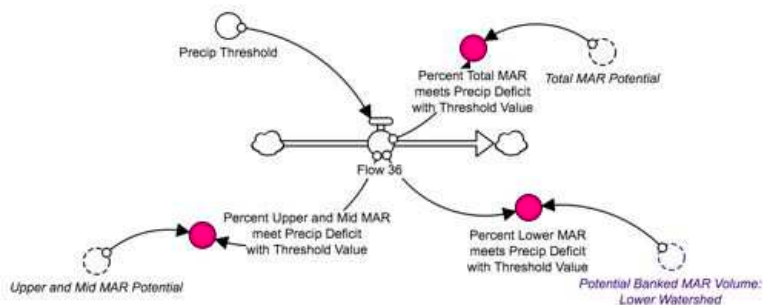


Figure 15. Percent estimates MAR can meet precipitation deficits based on a dialed “Precip Threshold”. The dashed converters are ‘ghosts’, which indicate the converter is also being applied elsewhere in the model.

Capture Potential Sector

To understand the funneling effect of reservoir release and streamflow response within the basin, 8 individual sub-modules were created that include 5 surface reservoirs and two stream gauges along the mainstem of the Yakima River. The 5 reservoirs include, Keechelus (KEE), Kachess (KAC), Cle Elem (CLE), Bumping (BUMP), and Rimrock (RIM), and the two stream gauges are Parker (PARW) and Kiona (KIOW) (Figure 16). The PARW site is of special interest, as yearly TWSA and prorationing is estimated from predicted flows and basin surface reservoir storage at this location.

The Capture Potential Sector allowed for rapid calculation of daily and yearly volume that may be available for groundwater storage during dry, average, and wet years. This sector fed the YAK-SDM model through sub-modules that are calibrated to water year 2005 through 2017. This sector calculated the basin-wide capture potential at specified locations by analyzing historical flow patterns in relation to instream flow requirements, which vary by location. Flows in excess of instream targets were analyzed for capture when demand was at its lowest and/or when flows were required to ramp down during irrigation season to optimize fish rearing habitat. The Capture Potential Sector also spatially calculated capture scenarios for the upper, mid, and lower stretch of the watershed. Estimates were based on capture rates that could be dialed from 0 to 100% of estimated available water (Figure 17).

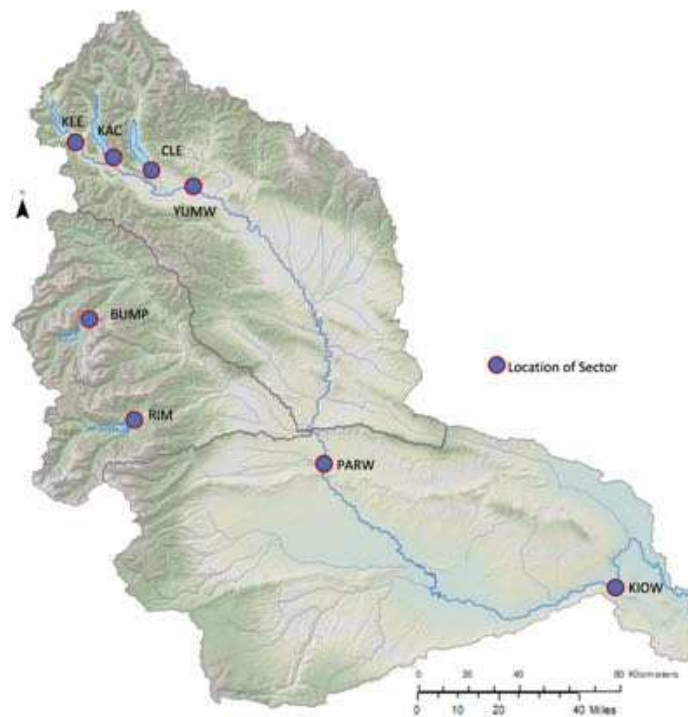
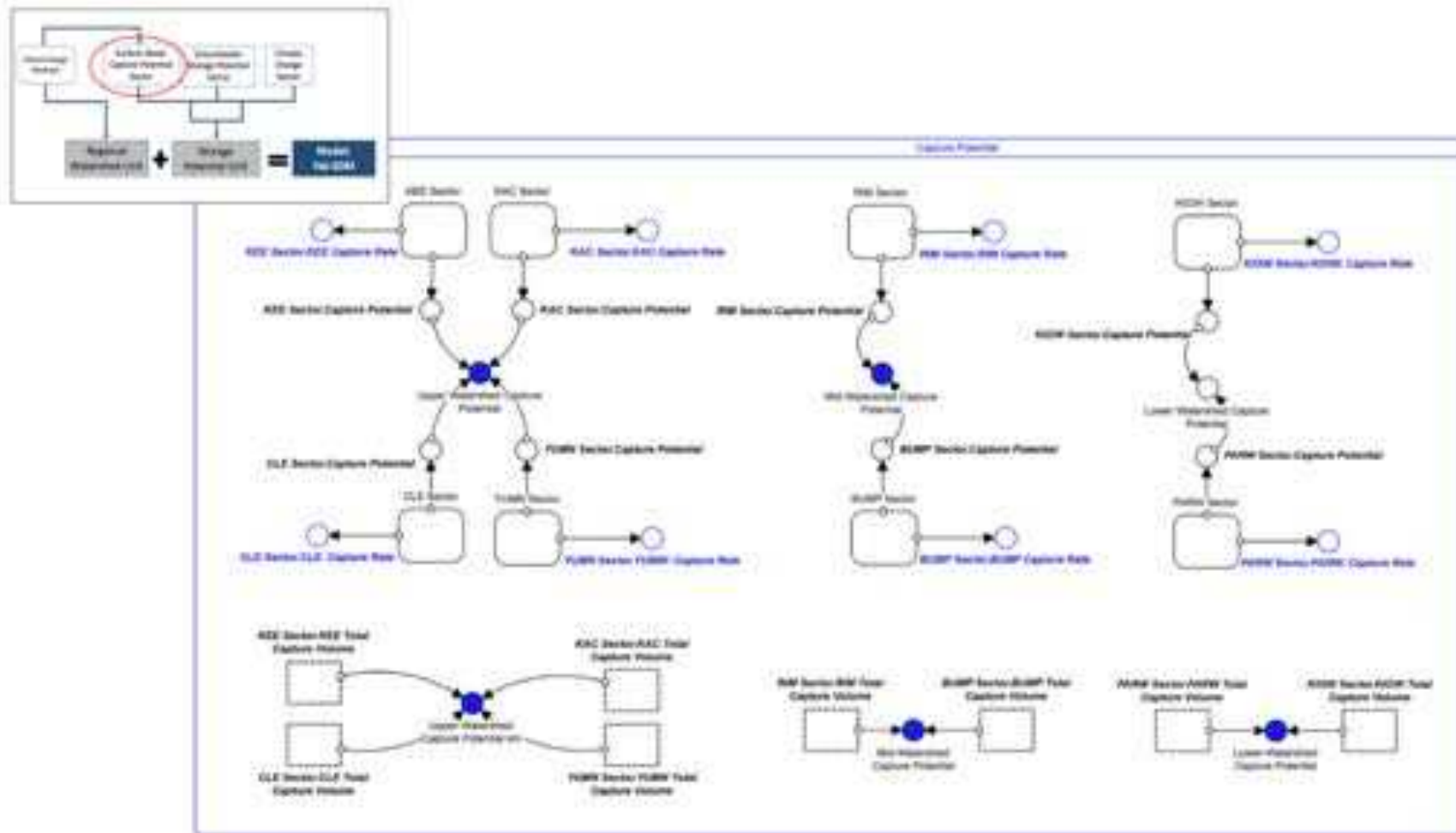


Figure 16. Stream gauges within YAK-SDM.

Figure 17. The capture potential sector in the YAK-SDM. Each sector is a module representing stream gauges where capture potential was evaluated.



Capture Potential Modules

Two types of modules are housed within the Capture Potential Sector - one to characterize reservoir release locations and the other to characterize streamflow gauges. Figure 18 depicts the KEE reservoir release module, and Figure 19 represents the Parker gauge (PARW) module. The two types of modules varied in construction due to instream flow targets differing based on precipitation-type years. Historical and climate change streamflow data were incorporated into graphical converters for water year 2005 to 2017. Each module analyzed divergence from instream flow requirements, divergence from natural conditions, potential capture period and potential (Figure 4.6), and altered flow patterns under two climate scenarios.

Within the modules, cumulative capture estimates under two climate change scenarios - intermediate and high modelled emissions - were also analyzed based on historical conditions at the PARW. Climate data were obtained from the University of Washington Hydro Columbia River Climate Change database (UW Hydro, 2018). The multivariate adaptive constructed analog (MACA) downscaling technique (Abatzoglou and Brown, 2012) was chosen, as it utilized analog methods to spatially match global climate model outputs at fine scales and used daily, rather than monthly, outputs. The Precipitation Runoff Modeling System (PRMS) was the preferred hydrologic model chosen as it has been bias-corrected and calibrated by the University of Washington to the no-regulation, no irrigation streamflow dataset obtained by the federal River Management Joint Operating Committee (UW Hydro, 2108). Global climate model output is based on the IPCC, 2014 (Pachauri et al., 2014) representative concentration pathways (RCP).

Figure 18. The KEE module. The KEE sector is a stream gauge located at the base of the Keechelus Reservoir

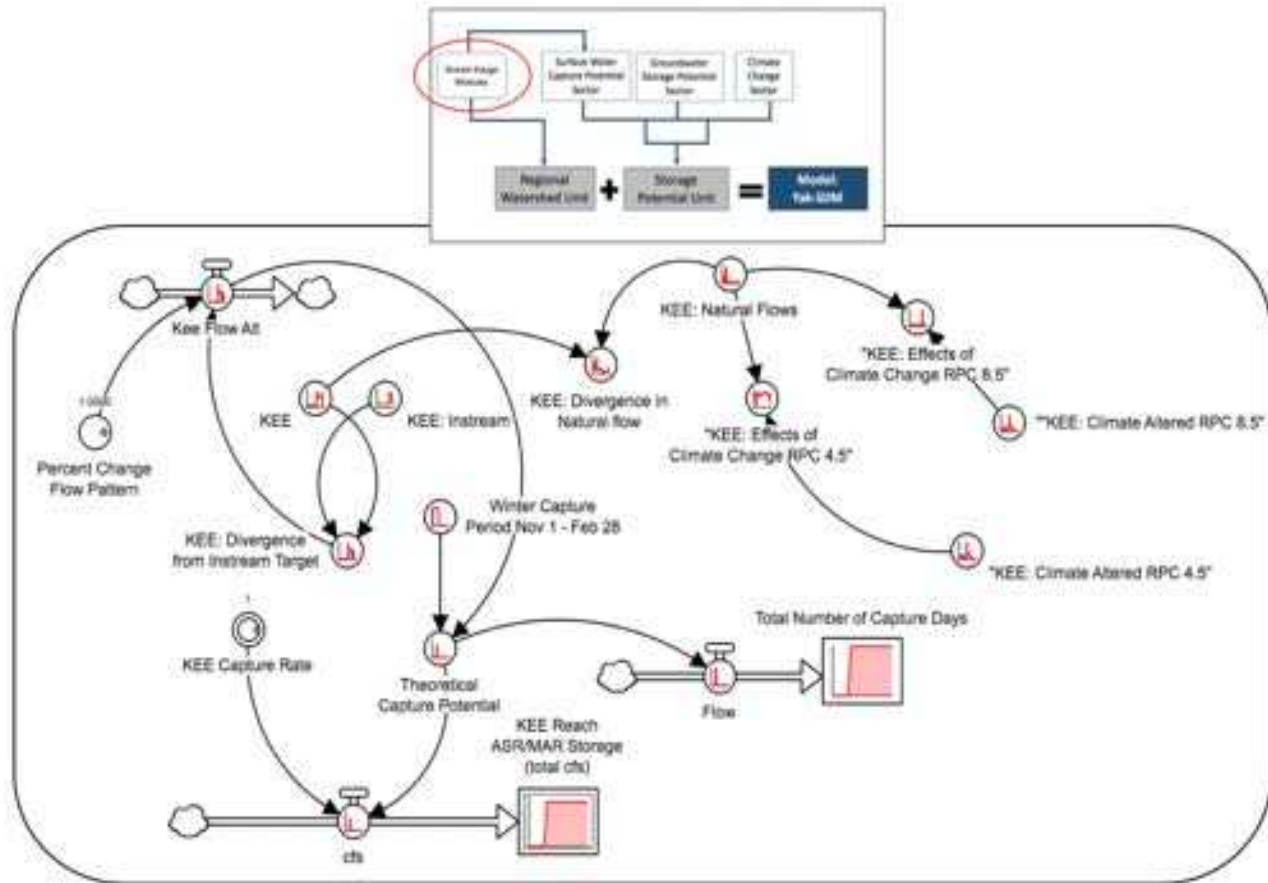
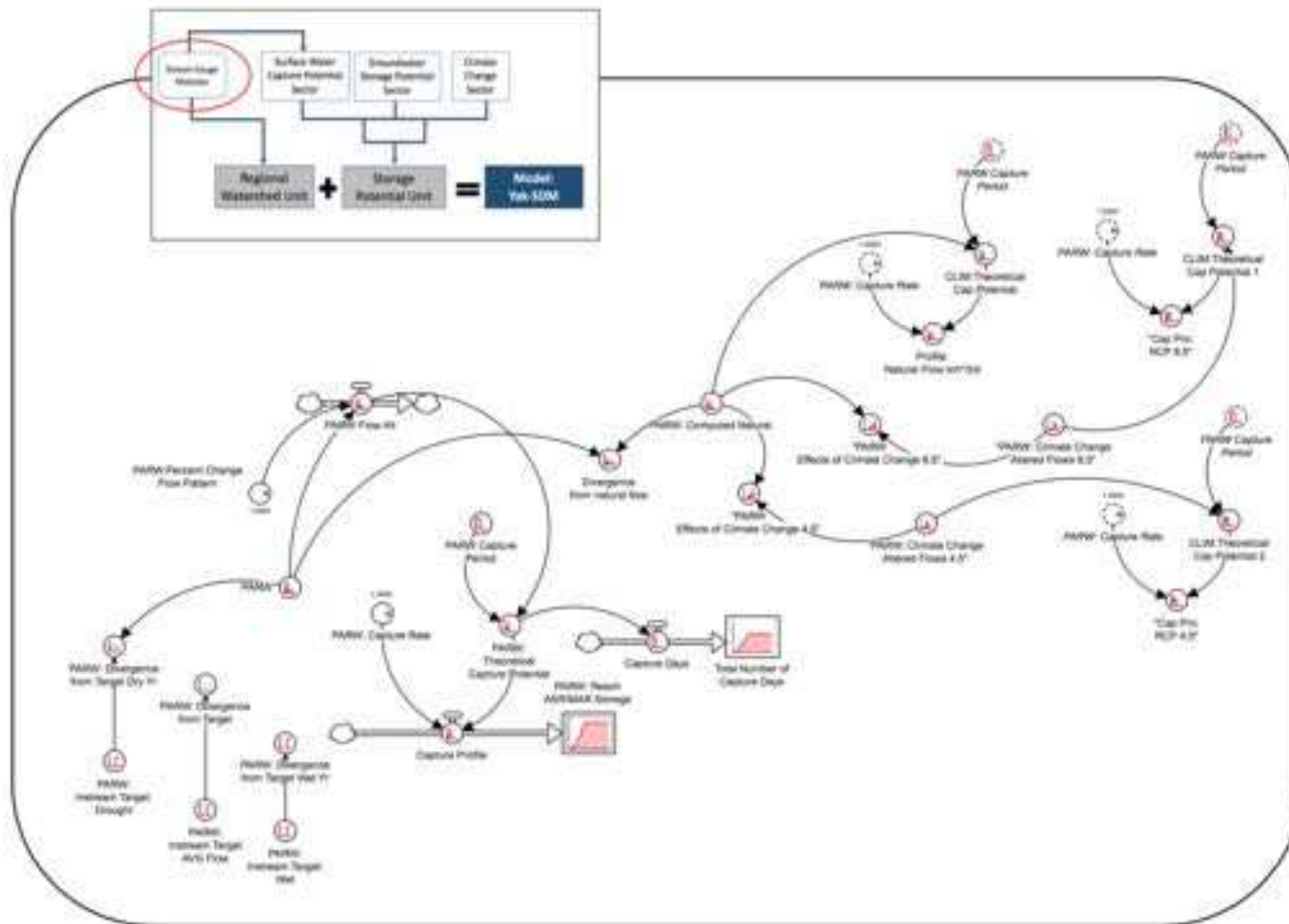


Figure 19. The PARW module. The PARW sector represents a stream gauge along the mid-section of the Yakima River



Instream Flow Targets

Instream flow targets within YAK-SDM were values obtained by HDR (2014) that were established as goals of the IWRMP. General instream flow objectives include reducing flows, increasing base flows, establishing pulse flows, and estimating target flows for dry, wet, and average years. Target flows for each sector were calculated on a daily timestep in Excel and imported into STELLA's graphical converter function for 1 to 4745 days. Figure 20 represents flow for water year 2005 for KEE, its associated target, and the surface water capture period.

Historical Streamflow Data

The streamflow data for historical water year 2005 to 2017 was obtained from the U.S. Bureau of Reclamation (2018) Yakima Project Hydromet System, which provides daily data access in tab-delimited form. Average daily flow values were imported into Excel spreadsheets and uploaded into STELLA's model view, graphical converter function. The assigned timestep began at day 1 and ended at day 4745, with leap year dates removed.

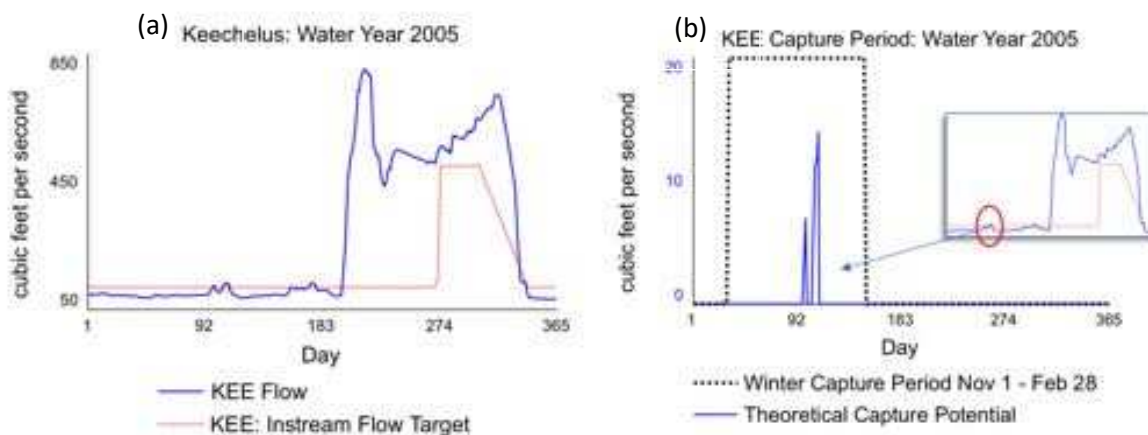


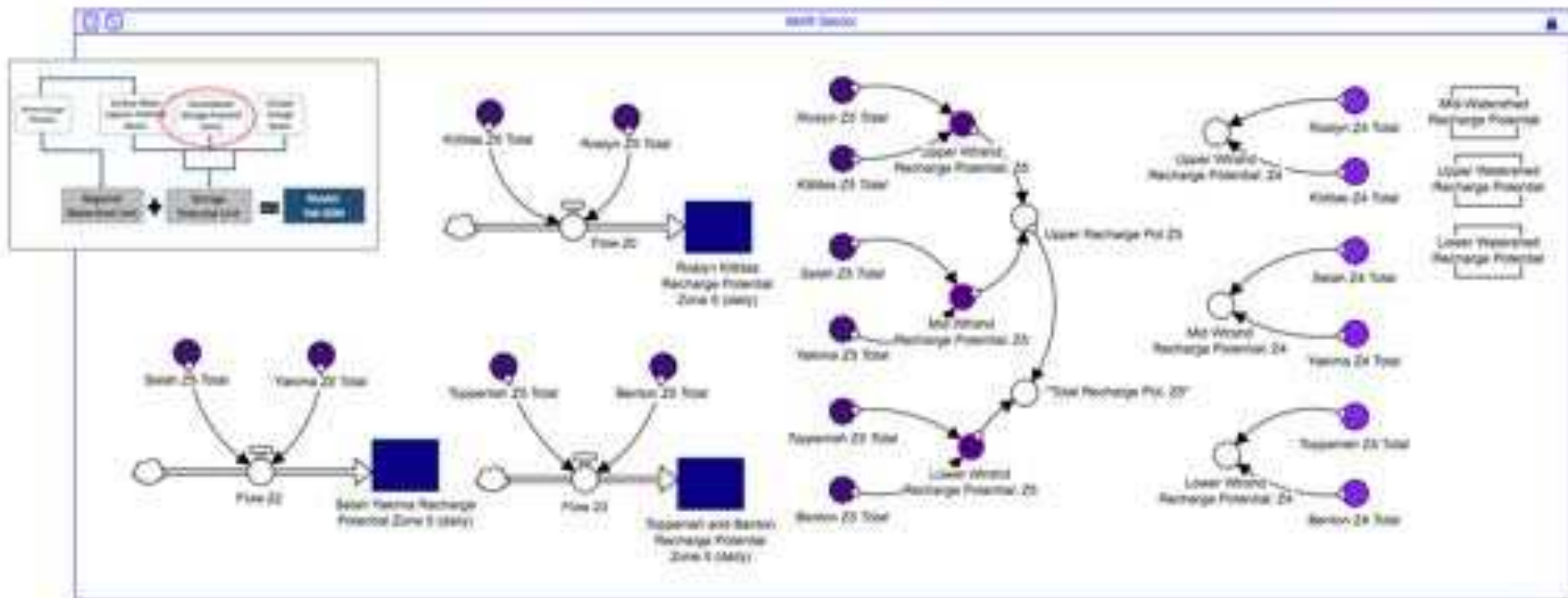
Figure 20. (a) Daily flows from KEE sector associated instream flow targets. (b) Capture period for KEE during drought year 2005. The capture period runs from day 32 to day 151, which correspond to November 1st through February 28th, 2005. Day 1 is October 1, 2005. Capture potential at KEE during this time was determined from excess flows and with respect to instream flow requirements.

Groundwater Storage Potential Sector

Estimates of storage potential were obtained Section 1 of this report. Within each sub-basin, potential storage estimates were calculated. Storage potential estimations were yielded

through a spatial overlay assessment coupled with analytical evaluation of aquifer conditions. Two zones were identified as potentially suitable: Zone 4 (Z4), which scored well and Zone 5 (Z5), which met all the criteria associated with suitability within its respective sub-basin (Figure 21).

Figure 21. The Groundwater Storage Potential Sector. Storage potential is based on a sub-basin relationship. The upper watershed consists of the Roslyn and Kittitas basin; the mid-watershed region consists of the Selah and Lower Yakima basin; and the lower watershed consists of the Toppenish and Benton basin. The potential storage values were obtained from Section 1 of this report.



Climate Change Sector

Climate change will likely alter precipitation patterns in the basin. Work conducted by Vano et al. (2010) indicates disruption of the system will be evident at the PARW gauge for year 2040 and 2080 (Figure 22). As climate alters snowpack runoff, the two-peak hydrograph as seen in many transition (snowpack-rain dominated) watersheds will likely evolve to a single-peak that occurs earlier in the season. To estimate the extent in which these changes can be buffered by MAR projects, comparison of historical, 2040, and 2080 data were analyzed.

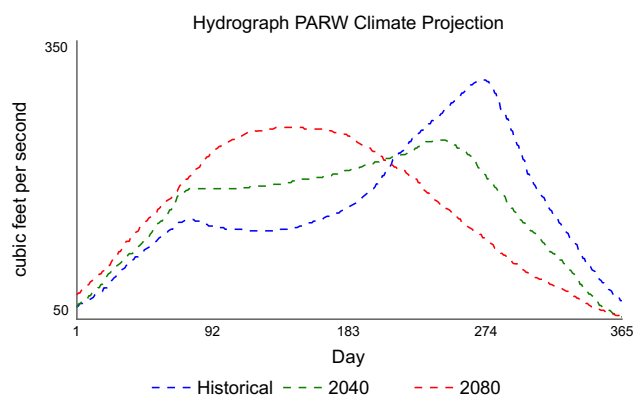


Figure 22. Historical, 2040, and 2080 predicted hydrograph for the PARW location. Modified from Vano et al. (2010).

Two climate change sectors (Figure 23) were constructed for year 2040 and 2080. To estimate groundwater storage potential with respect to current infrastructure, reservoir operations were incorporated into the model, which allowed for estimation of potential based beyond what current surface reservoir capacities meet (Figure 24). The model estimated capture and recovery trends that are required to mimic historic flows at PARW for 2040 and 2080, modified from Vano et al. (2010). Values were then compared to storage potential within the upper and mid reaches of the Yakima River Basin.

Figure 23. The 2080 Climate Sector used to estimate MAR potential based on available storage within the Yakima River Basin. The 2040 Climate Sector is not shown.

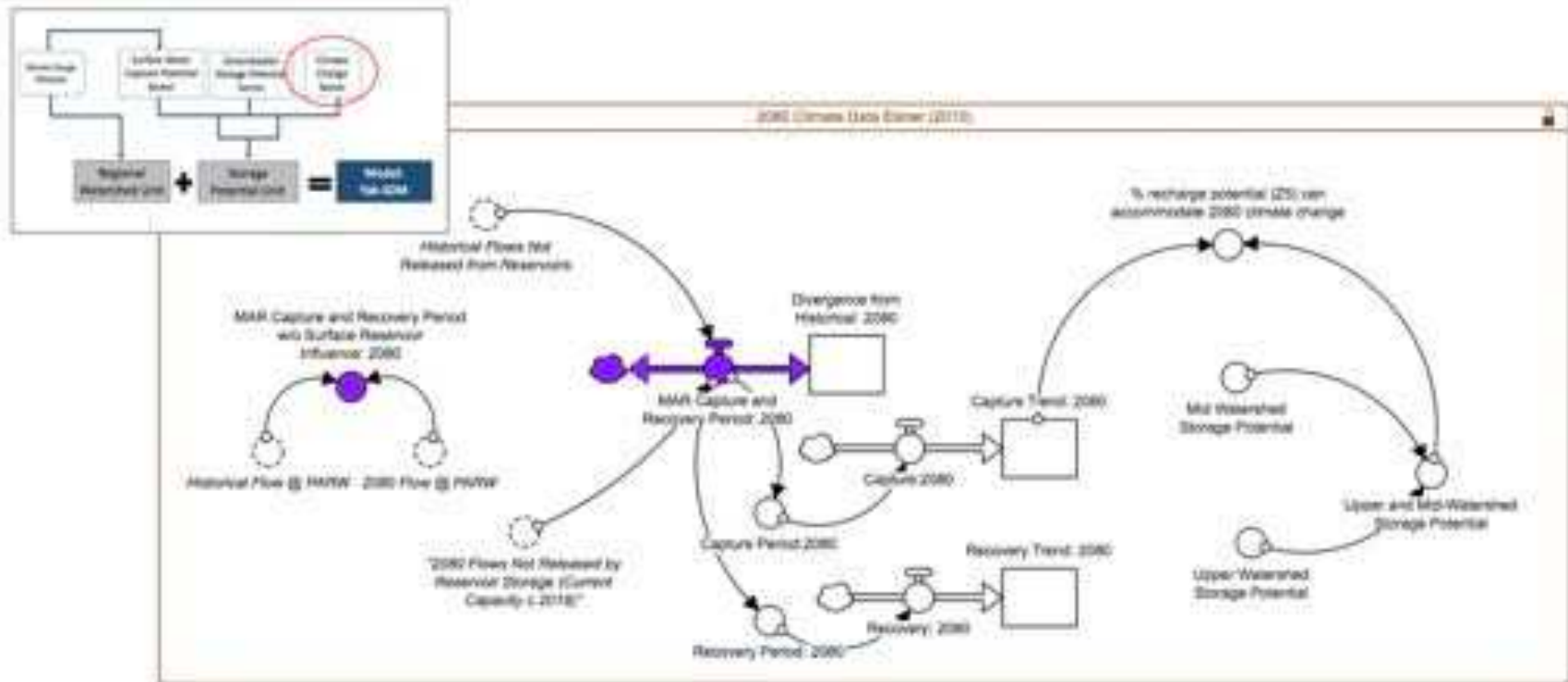
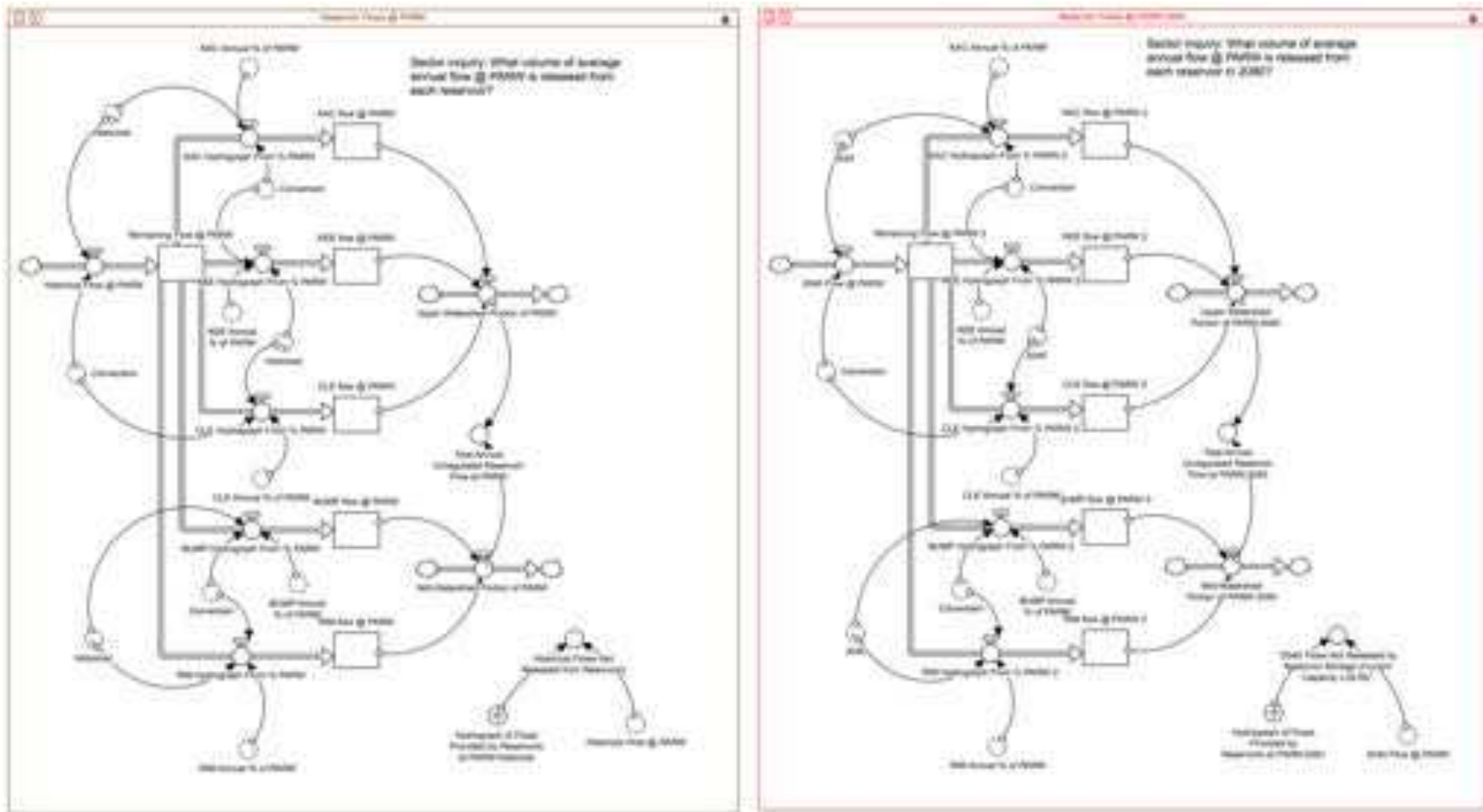


Figure 24. The sub-model of the Climate Sector that removes unregulated stream flow, with respect to current reservoir operations and historical conditions, at the PARW gauge, used to estimate MAR potential against climate change projections for 2040 and 2080 with current infrastructure. For simplicity only the historic and 2040 sub-model are shown.



Model Validation

The model was validated by its ability to predict historic trends in precipitation, and proration years. Historic departure from normal conditions is predicted in year 2005 (day 365), 2011 (day 2555), and 2015 (day 4015) (Figure 25). In year 2005 and 2015 the state of Washington, including the Yakima River Basin experienced drought conditions, and in 2011 the Yakima River Basin had a “wet” year - all three were predicted in the “Divergence from Average” for year 2005 to 2017.

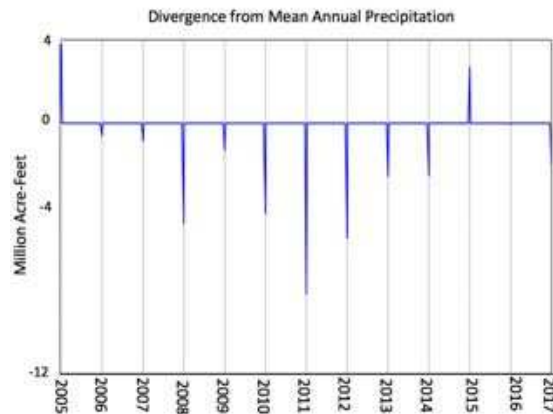


Figure 25. The departure from average precipitation conditions calculated by the YAK-SDM. Estimates show the 2005 and 2015 drought conditions and wet year 2011.

During dry years prorationing is enforced, which reduces the percentage of the proratable water delivery. This indicator and degree of prorationing, is calculated from a variety of hydrologic predictors estimated by the United States Bureau of Reclamation (U.S. Bureau of Reclamation and Washington Department of Ecology, 2012). When prorationing is in effect the basin stakeholders are assumed to undergo substantial economic loss. Although the YAK-SDM predicted prorationing for year 2005 and 2015 (Figure 6), an accurate percent of prorationing of entitlements was not achieved.

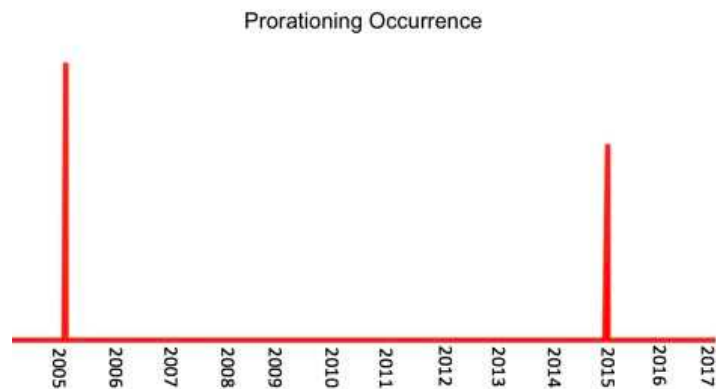


Figure 26. Predicted prorating for 2005 to 2017. Prorating occurred in year 2005 (day 365) and year 2015 (day 4015).

Additional Applications of YAK-SDM

The YAK-SDM also allows for quick policy viewing using hydrographs. The 1980 Quackenbush decision requires reducing water in the upper reaches, while increasing water in the lower reaches to promote fish spawning habitat. This is known as the flip-flop (U.S. Bureau of Reclamation and Washington Department of Ecology, 2012). Figure 27 shows the flip-flop for 2006 in the Cle Elem and RIM reservoirs.

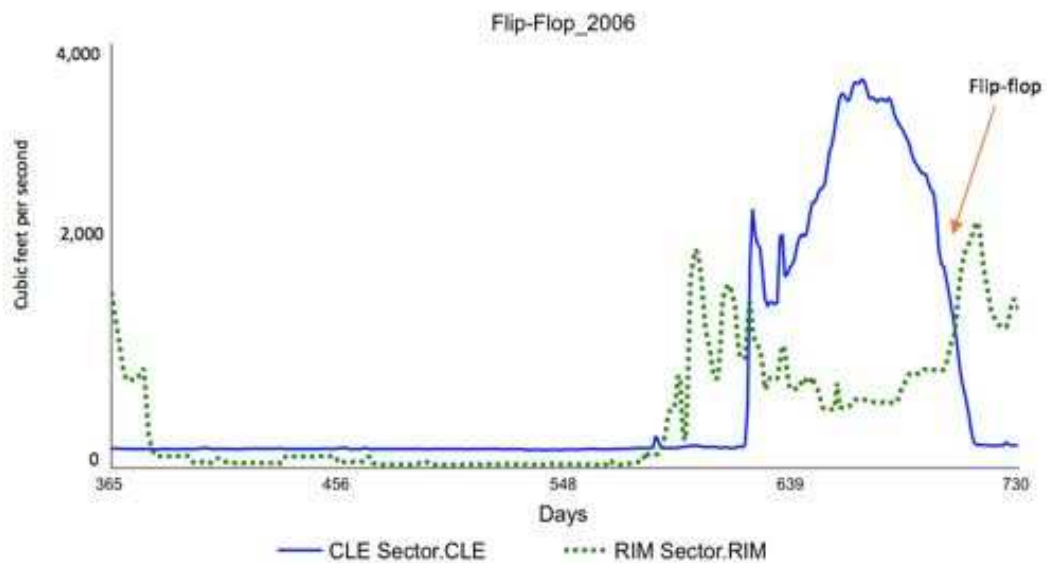


Figure 27. The hydrograph flip-flop of the Yakima River watershed for year 2006.

Environmental flows in the IWRMP are represented by instream flow targets. The YAK-SDM model can compare flows to calculate and visually inspect instream targets with current conditions and the degree they are met by reservoir releases. For example, the instream flow target for KEE is represented by the red dashed line in Figure 28.

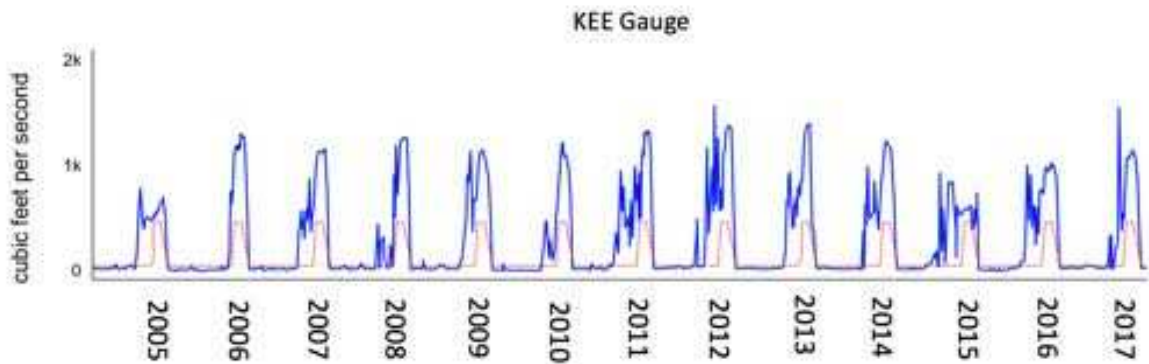
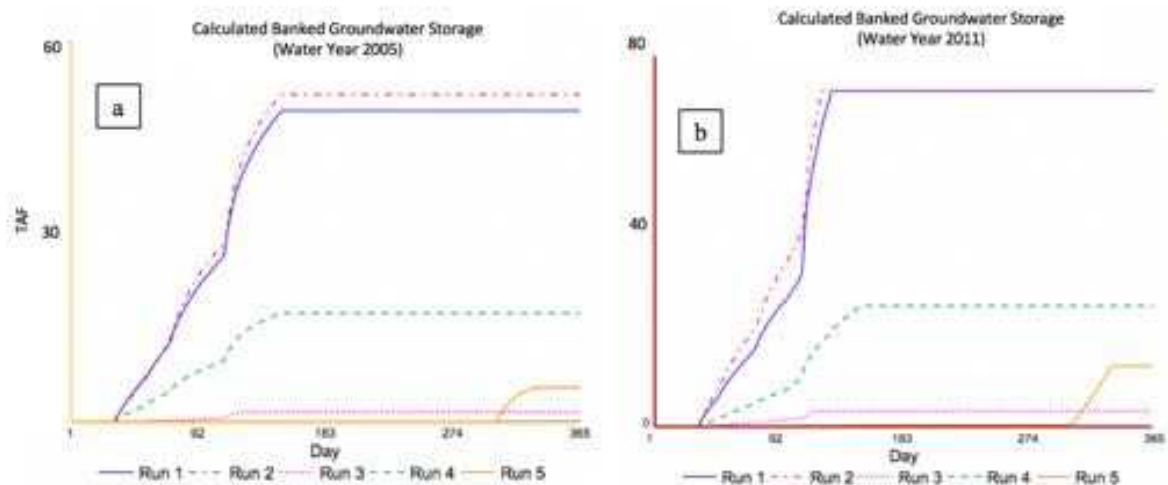


Figure 28. Hydrograph of KEE in comparison to instream flow target goals.

Section Results and Discussion

A set of indicators were identified to calculate groundwater storage potential in the Yakima River Basin: the estimated banked volume for a drought year, comparison of storage potential at full capture capacity for year 2005, 2011, and 2015; and number of capture days.

The estimated banked volume for drought year 2005 in different reaches of the watershed are shown in Figure 29. As capture will influence downstream potential, the following locations were analyzed for potential banked volume of water occurring only at one location, based on year 2005: run 1 is at the mouth of the river at KLOW, which totals 51 TAF; run 2 at the PARW gauge totals 49 TAF; run 3 at the BUMP and RIM reservoirs total 1.45 TAF; run 4 at the upper stream gauge YUMN totals 17 TAF; and run 5 at the upper watershed reservoirs (KAC, CLE, KEE) totals 6 TAF. The percent groundwater storage can meet precipitation deficits to avoid prorationing is as follows: run 1) 70% at PARW; run 2) 74% at KLOW; run 3) combined 2.1% at BUMP and RIM; run 4) 24.6% at YUMN; and run 5) combined 7.7% KEE, KAC, CLE.



Run 1: Lower Watershed Banked Volume at PARW
 Run 2: Lower Watershed Banked Volume at KLOW
 Run 3: Mid-Watershed Banked Volume at BUMP and RIM
 Run 4: Upper Watershed Banked Volume at YUMN
 Run 5: Upper Watershed Banked Volume at KEE, KAC and CLE

Figure 29. Banked groundwater storage. A) Estimates of banked MAR volume at distinct locations in the Yakima River watershed for drought year 2005. B) Estimates of banked MAR volume at different locations in the Yakima River Basin for wet year 2011, which starts on October 1st, 2010 (model day 2191) and ends Sept 30, 2011. Banked volume is based on the location of potential capture, potential capture with respect to timing of flows, and local MAR storage potential.

Capture Days

Another useful indicator of capture potential is the number of capture days recharge can occur. Values are based on non-reservoir storage control periods, typically in winter months, where instream flow goals were not assigned or where flow targets were met by flow conditions (Table 7). The least number of capture days occur in 2006 and the greatest in 2009.

Table 7. Number of potential capture days for each module for year 2005 to 2017.

	Capture Days												
	2005	2006	2007	2008	2009	2010	2011	2012	2013	2014	2015	2016	2017
KEE	7	0	0	7	32	0	17	0	0	0	47	0	16
KAC	2	1	4	33	120	0	120	120	120	111	120	36	108
CLE	31	31	31	21	31	31	31	31	31	31	31	31	31
YUMN	120	120	120	120	120	120	120	120	120	120	120	120	120
BUMP	111	67	117	119	119	119	119	119	19	119	119	113	75
RIM	21	56	119	119	119	119	119	119	119	119	119	102	119
PARW	120	120	120	120	120	120	120	120	120	120	120	120	120
KIOW	120	120	120	120	120	120	120	120	120	120	120	120	120
TOTAL	532	515	631	659	781	629	766	749	649	740	796	642	709

Climate Change

Capture and recovery trends were evaluated for 2040 and 2080 conditions. Climate data are based on work conducted by Vano et al. (2010), which represent the PARW hydrograph from day 1 to 365 days beginning January 1 and ending December 31. The trends were designed to capture and recover water to mimic historical flows. For 2040, the capture period is gradual and ends at day 215 and equals a volume of $\sim 0.28 \text{ km}^3$. For 2080 the capture period ends 8 days earlier (day 207) and equals a volume of 4.5 TAF. Recovery of stored water peaks at day 346 for year 2040, and at day 353 in year 2080. The rate for both capture and recovery in 2080 is greater than 2040 (Figure 30)

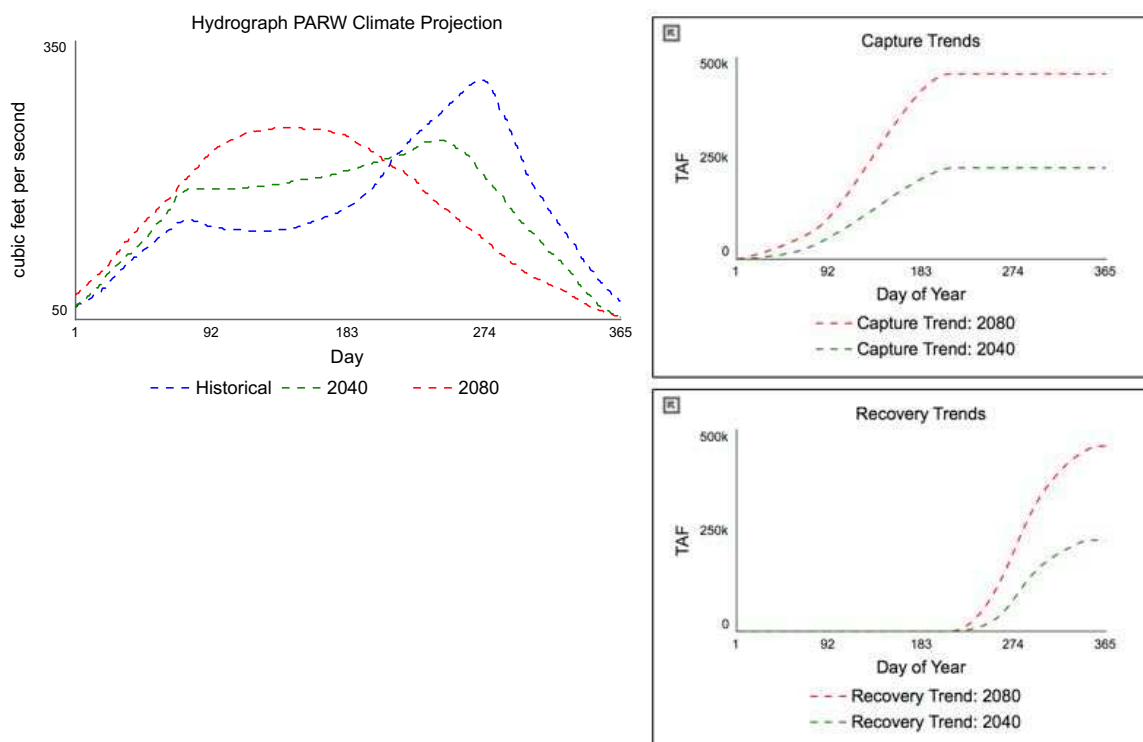


Figure 30. Hydrographs at PARW with respect to historical conditions and climate change (Modified from Vano, et al., 2010) and its associated capture and recovery trends. Capture and recovery trends to mimic natural flows at PARW under two climate change scenarios for year 2040 and 2080.

To understand how climate may impact surface water capture at PARW, two climate models were used in the YAK-STD Capture Potential PARW module – RPC 4.5 and RPC 8.5. The RPC 4.5 is an intermediate climate emissions scenario and the RPC 8.5 is a scenario with the most modelled emissions (Pachauri et al., 2014). In summary, the hydrologic model, PRIMIS-P1 downscaled with MACA under the RCP 4.5 and RCP 8.5 scenarios (UW Hydro, 2018) were adapted for use at this location.

Capturing surface water for groundwater storage was analyzed in YAK-SDM for water year 2005 to 2017 under historical flow conditions obtained from US Bureau of Reclamation (2018); against computed natural flow, which was based on pre-storage conditions; and climate scenarios RCP 4.5 and 8.5. Cumulative capture potential for water year 2005 to 2017 indicate capture potential is greater under RCP 8.5 (more adverse) climate conditions, which suggest additional runoff will be available in winter months due to changes in snowpack.

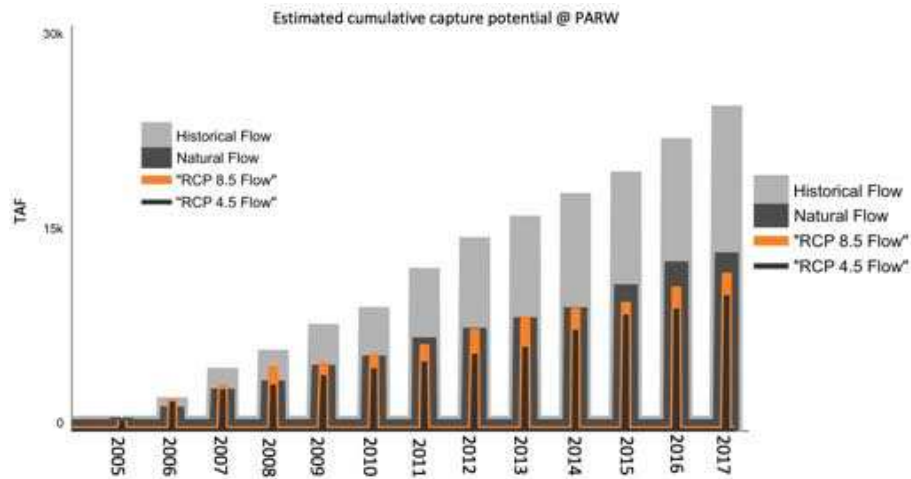


Figure 31 . Cumulative historical capture potential compared against the following: natural flows, which are calculated based on pre-storage conditions; RCP 8.5 Flow, which is the more adverse climate scenario; and RCP 4.5 Flow, which is the less adverse climate scenario (US Hydro, 2018). Historical flows were obtained from US Bureau of Reclamation (2018).

Capturing surface water for groundwater storage is greatest during the winter months. To understand capture potential under different conditions, a comparison of capture potential under two drought years (water year 2005; 2015), one wet year (water year 2011), and water year 2017 was conducted at YUMN, PARW, and KLOW gauges (Figure 32). Although capture potential is lowest during drought years, surface water is available for groundwater storage, which increases in volume downstream.

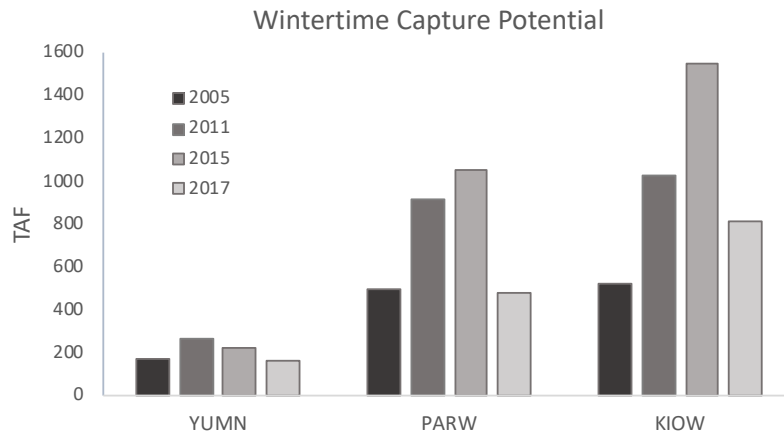


Figure 32. Potential surface water capture for groundwater storage during two drought years (water year 2005; 2015), wet year (2011), and current conditions (2017).

Mutual Gains Approach to Groundwater Storage

Public opposition of groundwater storage projects can dismantle prospective ventures, and in extreme cases result in regulation against future proposals (Seerly, 2003). Although it has also been shown that opposition can come from the public’s lack of scientific and technical knowledge, cultural heritage plays a greater role, as land use is of great significance to stakeholders but often not realized by technical experts (Kurki and Katko, 2015). Due to the geological structure of the Yakima River Basin, downstream users are generally isolated from upstream groundwater. As each sub-basin largely acts as individual containers, delayed recharge by human redistribution of natural flows is mostly realized downstream through surface water connections. To increase complexity, the spatial location of senior, proratable, and junior users do not coincide with the step-down configuration of the sub-basins, therefore no upstream-downstream hierarchy exists. In order to understand the subtle complexities of adding groundwater storage to the basin, informal interviews among land owners and others were conducted between in 2017-2018, through a mutual gains approach (Susskind, 1996). The MGA is guided by 6 basic principles: 1) acknowledge the concerns of the other side; 2) encourage joint fact finding; 3) offer contingent commitments to minimize impacts – compensate knowable but unintended impacts; 4) accept responsibility, admit mistakes, and share power; 5) act in a trustworthy fashion, and 6) focus on building long-term relationships. The findings suggest the IWRMP maintains many of the MGA characteristics to support collaborative groundwater expansion based on historical relationships, however:

- Many local stakeholders are generally unfamiliar with enhancing groundwater storage to increase supply, although some are familiar with the city of Yakima’s ASR program, the Toppenish alluvial fan recharge project was relatively unknown. Since it has been shown that social acceptance of groundwater projects is tied to communication and education (Mankad et al. 2015), a focus on community outreach might be warranted.

- The most contentious subject regarding increasing water supply is the surface water component of the IWRMP, specifically the Bumping Reservoir expansion. Others want to see the Black Rock Reservoir project re-evaluated, as it has since been dismissed as an option. Enhancing fish habitat was a concern, and conservation of water seemed preferable over reservoir expansion by some. In terms of groundwater storage expansion, a fear of unequal distribution of benefits exists, as it was unclear how groundwater storage relates to surface water enhancements, under unseen conditions. Since it has been argued that stakeholder participation should occur early in the process (Reed, 2006), further development of groundwater storage projects should consider community education regarding technical aspects and also solicit community feedback.
- Managing large-scale groundwater storage projects will require transparency and trust between the community and any decisions made by project management. Alternatives that meet the same goals should also be discussed. The step-down pattern of the sub-basins isolates communities too; therefore, project managers also need to consider perceived unfairness by communities where these projects are not feasible, even though benefits will be observed through indirect means.

3. Recommendations

Recommendations are based on a location considered for short-term groundwater storage, to enhance surface reservoir carry over supply (Figure 33). Well-suited locations (Zone 5) were chosen, as these locations met all criteria of the weighted overlay analysis - slope, lithology, geology, transmissivity, and depth to static water level. The respective recharge rates were obtained from the analytical methods in section 1. The results were coupled with a stream depletion factor (SDF) to estimate timing of groundwater storage and streamflow improvements. Basins with well-suited locations that did not fall within the SDF include recommendations based on Zone 4 locations. Maps of SDF for each basin are available in Appendix D.

Site-Specific Carry over Storage and Climate Change Scenarios

To increase carry over storage under current surface water reservoir conditions, a stream depletion factor (Jenkins, 1968) approach was taken to define locations suitable for groundwater storage. The SDF estimates the timescale recharged water will propagate through an aquifer connected to a stream, albeit via infiltration basins or injection wells. Since capture potential is greatest in winter, locations were identified that allowed for passive recovery to reach the stream by the beginning of the irrigation season (April 1).

$$SDF = \frac{a^2 S}{T}$$

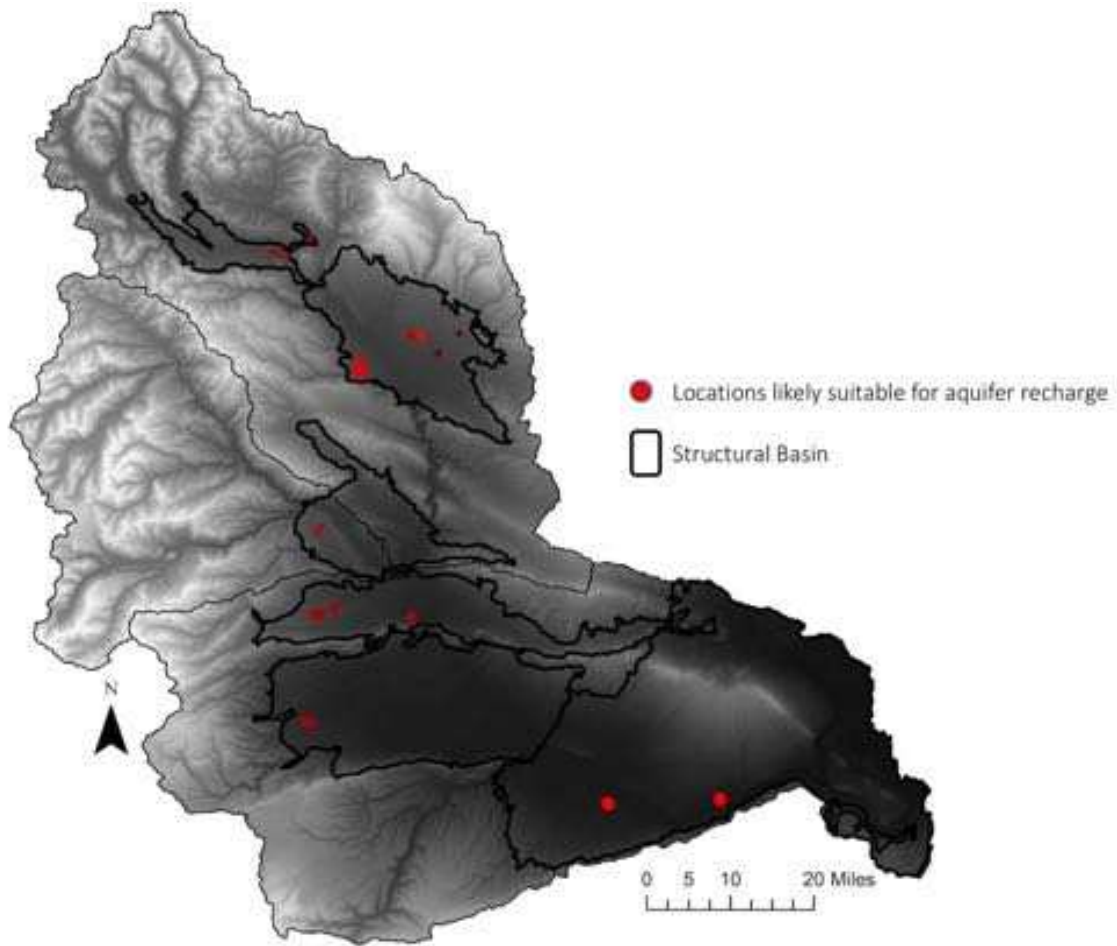
Where,

a is the distance between an infiltration basin or well and the stream (L)

S is the storage coefficient (dimensionless)

T is the transmissivity (L²/t) of the aquifer

Figure 33. Locations identified as well-suited or suitable for groundwater recharge based on the weighted overlay, analytical recharge method, and stream depletion factor approach; with adjustments due to climate change. Results within each basin include: (a) Roslyn, (b) Kittitas, (c) Selah, (d) Lower Yakima, (e) Toppenish, and (f) Benton. Well-suited locations are areas that scored 5 out of 5 for slope, transmissivity, lithology, geology, land use, and depth to static water level. Location of results with respect to local streamflow are within the appropriate distance and maintain recharge capacity to enhance carry over storage.



Roslyn Basin

Among the 6 structural basins, the Roslyn Basin is highest in elevation. During the winter, snowfall can blanket the region and, depending upon the infiltration system, low temperatures can reduce infiltration capacity of recharge basins. Although experimentation of infiltration basins in subarctic conditions have taken place (Anderson, 1977) most groundwater storage schemes using infiltration basins are found at lower elevations with the United States (IGRAC, 2018). Suitability of ASR was not identified as few wells with the pump test data exist within the basin. However, the lower basin may be suitable for infiltration (Figure 34).

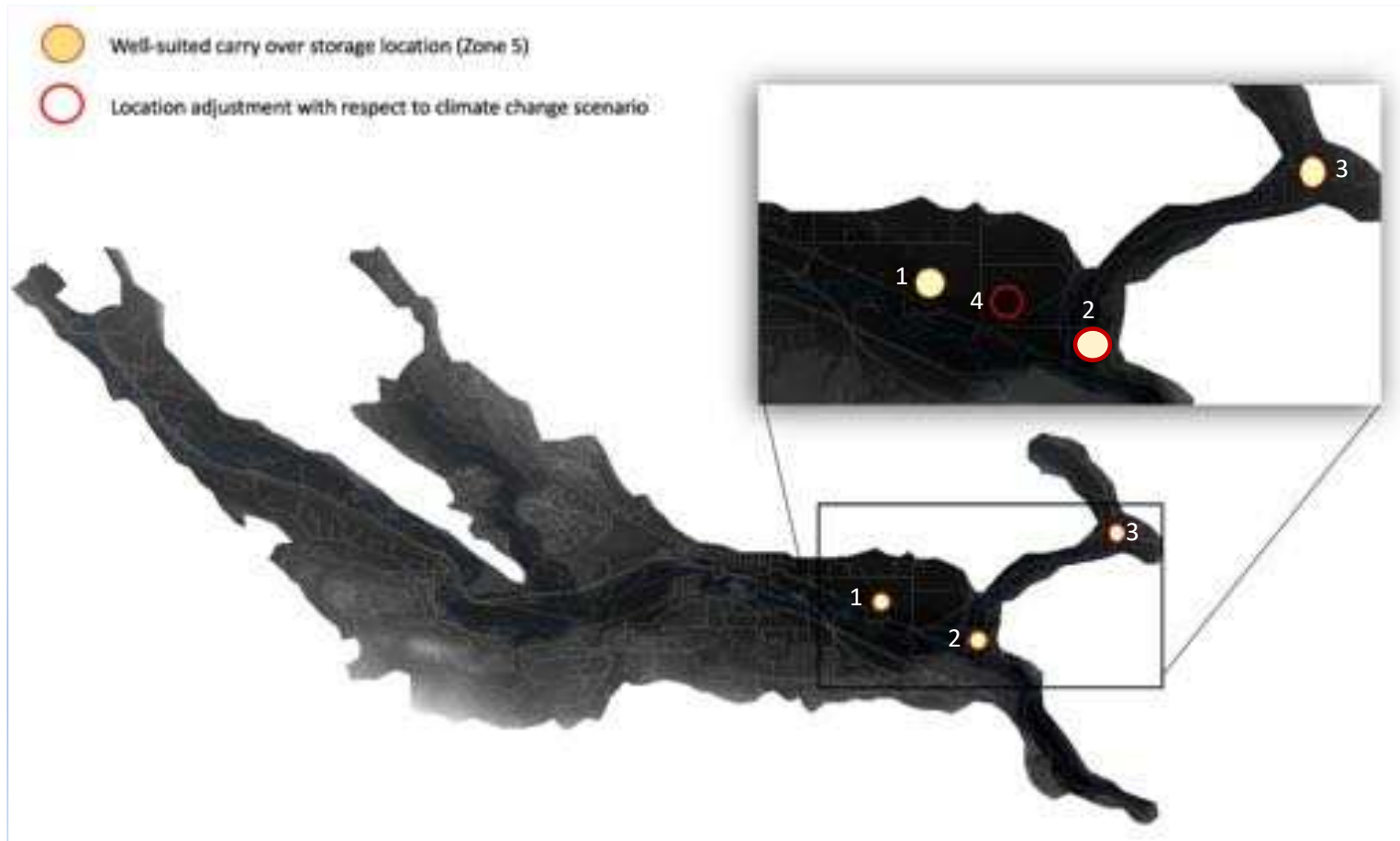
Location 1: This area overlies alpine glacial outwash of the Lakedale Drift. Transmissivity within this unit is estimated at 7520 ft²/day, depth to static water during winter is calculated at 33 below ground surface, and the SDF indicates recharged water will propagate to the Yakima River from this location in 120 days at a recharge rate of 2 AF per day. Land use is predominantly designated forest. It is projected that the YUMN gauge has a capture potential of 120 days during winter months. To reduce the need for surface reservoir release, thereby increasing carry over storage, recharge will need to occur through the end of February to increase surface flows until the end of June.

Location 2. This location is underlain with Quaternary alluvium, has an estimated transmissivity of 7520 ft²/day, and the depth to static water level is estimated at 100 ft below ground surface. The SDF indicates recharge water will propagate to the Teanaway River in 80 days with a groundwater storage rate of 2 AF per day; therefore, recharge is predicted to increase stream flow by the beginning of irrigation season with recharge ending in February.

Location 3. This area is underlain by Quaternary alluvium, has an estimated transmissivity of 7520 ft²/day, and the depth to static water level is estimated at 100 ft below ground surface. The SDF indicates recharge water will propagate to the Teanaway River in 150 days at a groundwater storage rate of 1.5 AF per day. Recharge is predicted to increase stream flow through July, if recharge begins in November.

Location 4. This location was chosen in response to altered capture days due to climate change. Location 2 is considered not suitable under climate scenarios. Location 4 maintains similar characteristics as Location 1; however, a greater radius of recharge rate exists (2.25 AF per day) and an SDF of 180 days. The increase recharge rate and greater SDF is estimated to allow for more flexibility under climate scenarios. Land use in this area is considered agricultural.

Figure 34. Suitable locations for groundwater storage in the Roslyn Basin.



Kittitas Basin

Within the Kittitas Basin, five locations were identified as meeting criteria assumed suitable for groundwater recharge. However, after surveys conducted with local building contractors, standing water during winter and return flows through seasonal irrigation were identified as problematic. Therefore, an additional survey was conducted to estimate water logged regions during wintertime in the Kittitas Basin. As a basin-wide scale is difficult to assess through on-site field investigation, a water index was calculated using satellite imagery to enhance water bodies where possible. A survey of Landsat 8 OLI Level-1 images was performed for all wintertime months since 2014 with reduced cloud cover. Only 1 image met the required characteristics to conduct the analysis. A raster image obtained for January 4, 2014 was processed using a modified normalized difference water index (MNDWI) to limit build-up of land, suppress soil and vegetation noise, and enhance standing water (XU, 2006).

The MDVI suggest water logged areas are present throughout the basin. No precipitation was observed near the city of Ellensburg for the previous 10 days (NOAA, 2018). In comparison to a May 12, 2014, waterlogged regions are reduced.

Figure 35. Kittitas Basin: Standing water present January 2014. Standing water is highlighted in white.

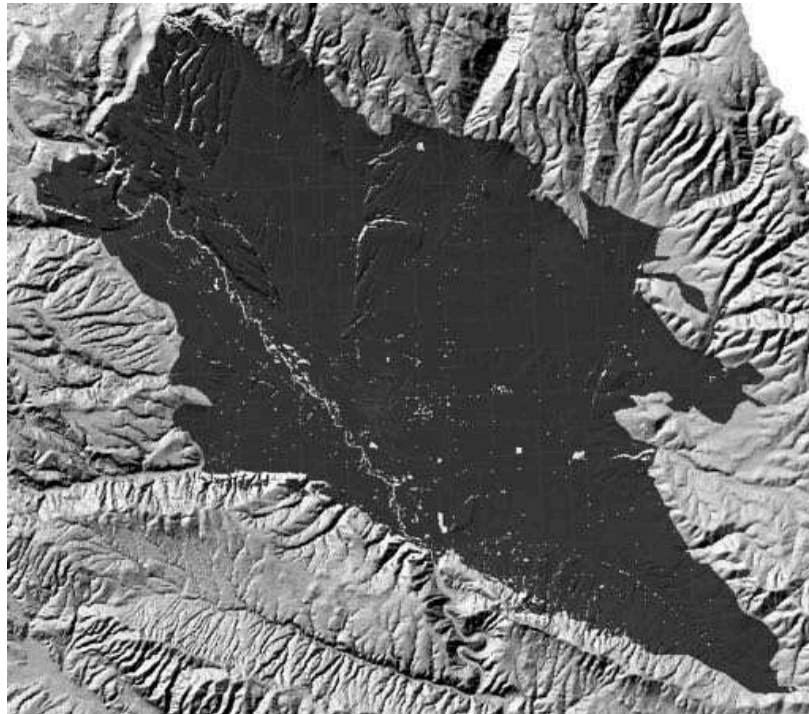
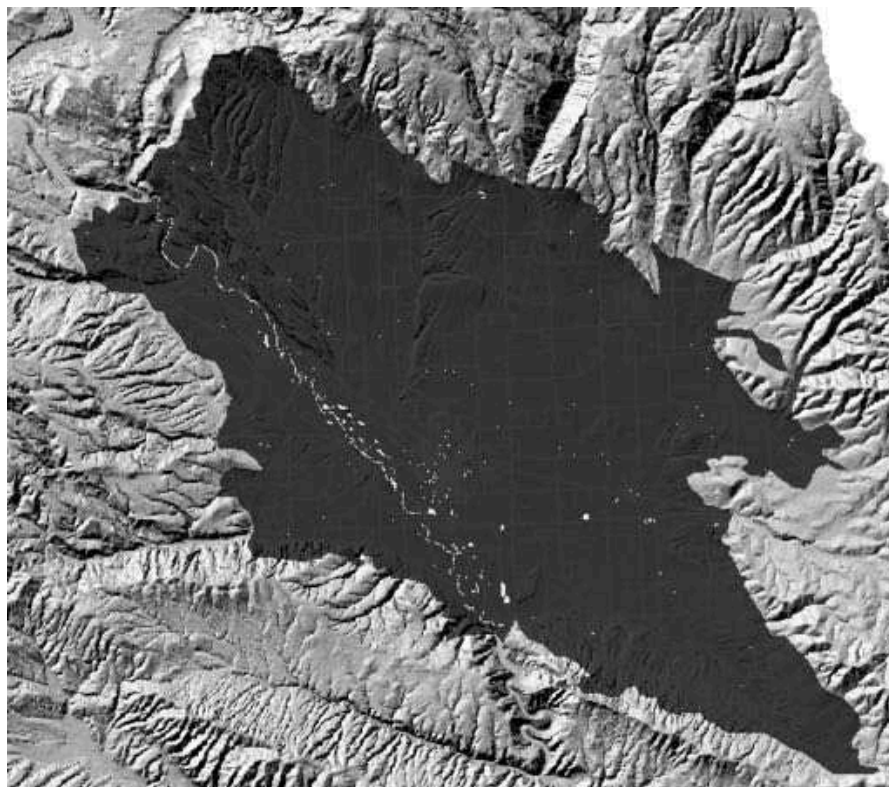


Figure 36. Kittitas Basin: Standing water present May 2014. Standing water is highlighted in white.



Locations (Figure 37):

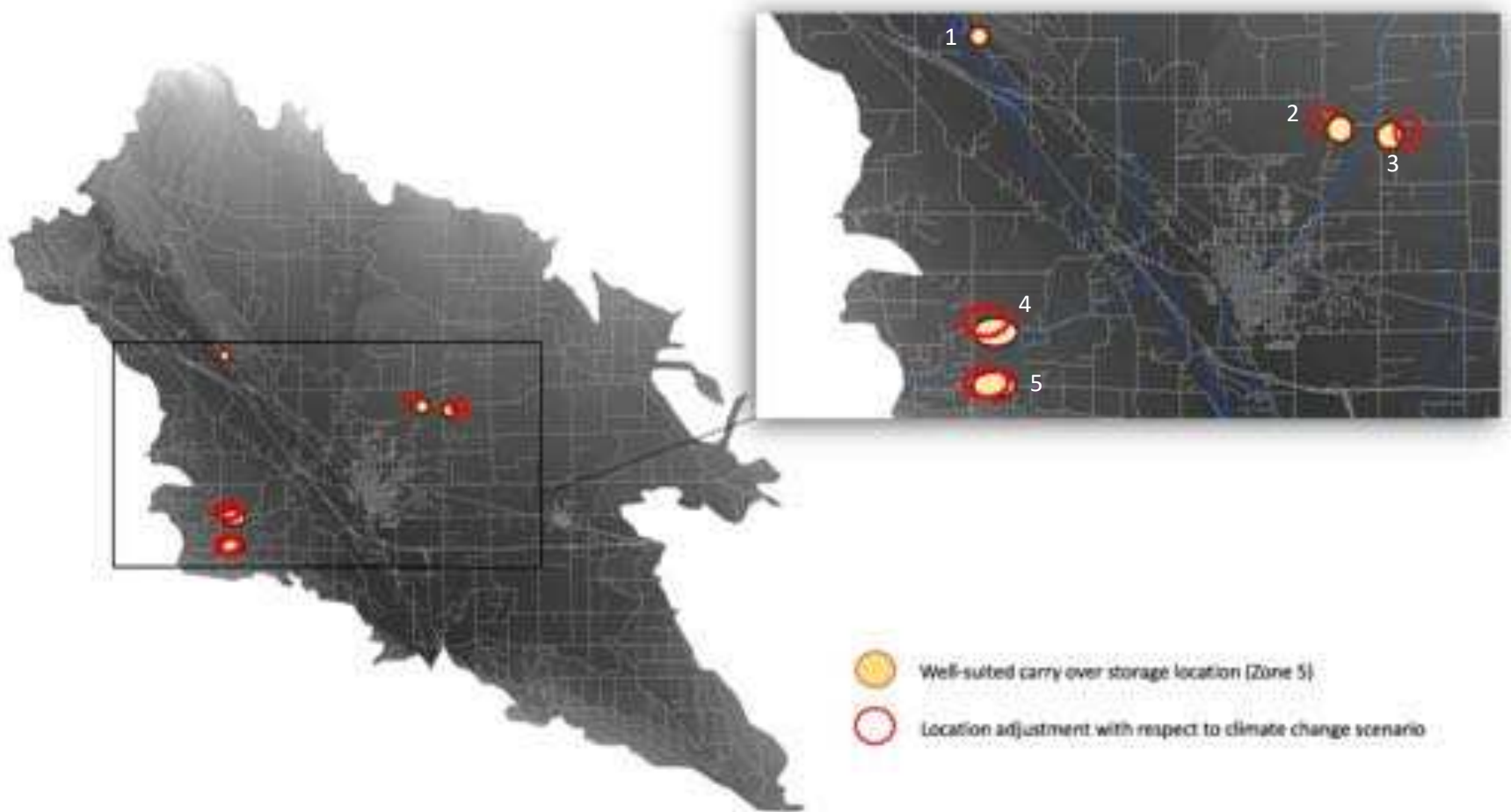
1) Location 1 is in the northern region of the Kittitas Basin. It is located within Quaternary alluvium, adjacent to Thorp Gravel, and is near the spine of the Kittitas Valley Syncline. Wintertime depth to static water level is estimated at 50 ft below the ground surface, and transmissivity is calculated at 6350 ft²/day. It is bounded by the Yakima River, which is less than 0.5 miles to the west, and a north-south trending irrigation canal, which separates the land parcel from the adjoining ridgeline to the east. Land use is considered undeveloped, and it has an SDF of 100 days. This location has an estimated mean rate of recharge of 3 AF per day. Results from STELLA suggest 120 days of surface water capture for recharge is possible downstream of the YUMN gauge. Preliminary estimates suggest during less-than-average precipitation years, 4.0% of the YUMN gauge surface water is available for diversion during winter months. At this location, if recharge ceases by the end of February, streamflow improvements will be observed through May. However, layers of clay have been identified in local well logs, which may reduce rates of infiltration, and standing water was present during wintertime within the vicinity.

2 and 3) Location 2 and 3 is northeast of the city of Ellensburg and is along Wilson Creek near Brick Mill Road. The region is underlain by Quaternary alluvium; however, Thorp Gravel and alpine glacial outwash of the Lakedale Drift are within 2 miles of these locations, likely due to a normal fault cross-cutting this location. Standing water was not apparent in the MNDWI, but ponds dot the local

landscape. Static water level is estimated to range from 80 to 100 feet below ground surface on either side of Wilson Creek and transmissivity is estimated at 6530 ft²/day. Groundwater recharge potential is estimated at 2 AF per day, and the area has an average SDF of 125 days. At these locations, if recharge ceases by the end of February, observed changes to streamflow is estimated to persist until the end of July. As climate alters streamflow patterns and runoff available for recharge is predicted to occur earlier in the year, it is estimated the area of suitability will likely need to be relocated further from Wilson Creek, as SDF is increased to 280 days.

4 and 5) Location 4 and 5 are within 0.5 miles from Manatash Creek. These locations are underlain by Quaternary alluvium with adjacent Quaternary terraced deposits present. Depth to static water level is estimated at 100 ft below ground surface, transmissivity is calculated at 6530 ft²/day, and the SDF is between 77 and 100 days. The groundwater storage recharge rate of 1.25 AF is expected at both locations; therefore, stream improvements to Manatash Creek is estimated to persist until the end of May, assuming recharge ceases at the end of February. However, small areas of standing water are present on the January 2014 MNDWI, but no standing water was observed on March 2018 during a field survey. As the streamflow undergoes changes in climate the locations move slightly upstream to compensate for alterations in runoff, which are expected to occur earlier in the year.

Figure 37. Suitable locations for groundwater storage in the Kittitas Basin.



Selah Basin

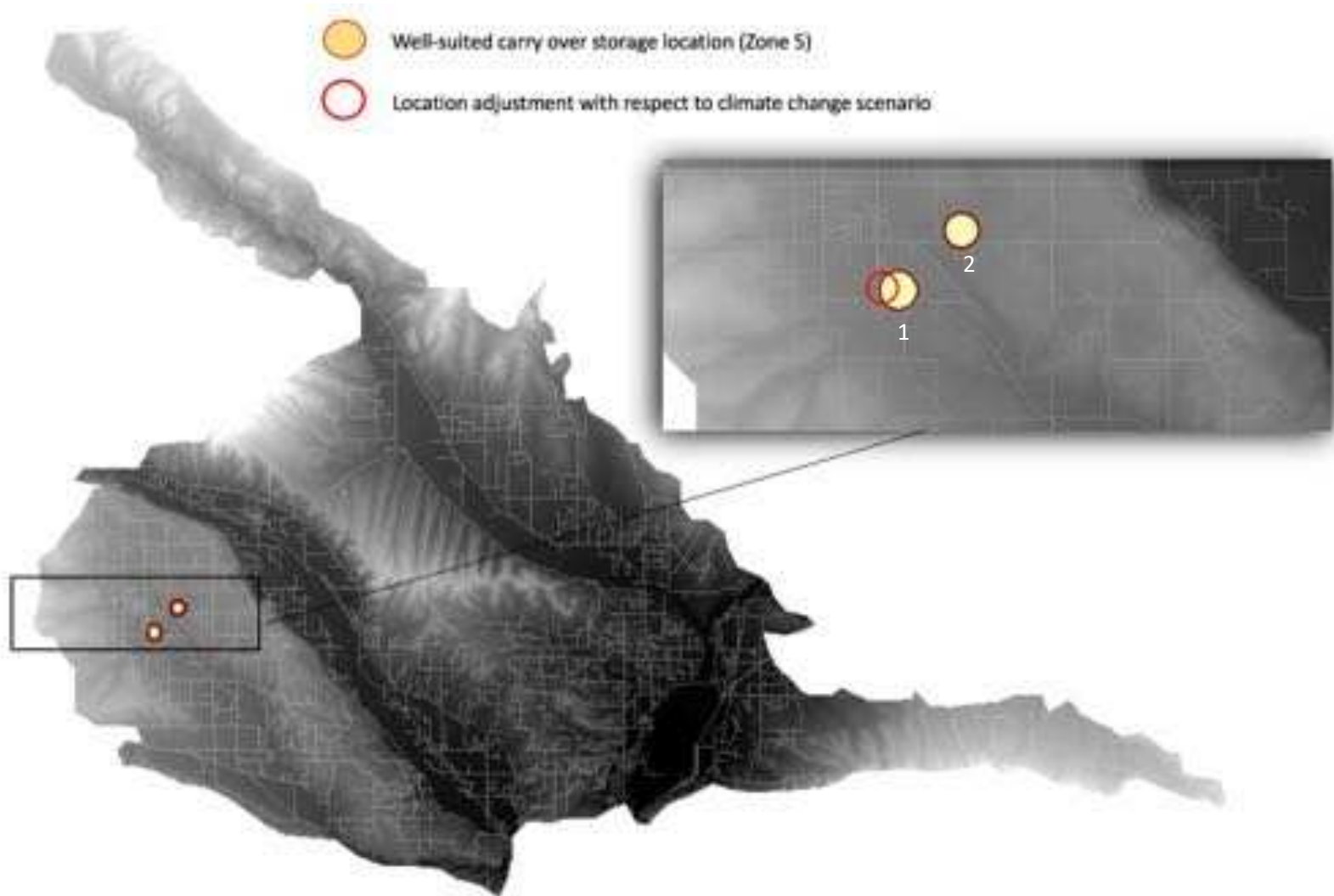
Within the Selah Basin, two locations were considered suitable for groundwater storage based on the weighted overlay method, calculated recharge rates, and stream depletion factors (Figure #). Both locations reside near the town of Tieton.

Locations (Figure 38):

1) This location is less than 0.5 miles from the North Fork of Chowiche Creek. It is underlain by the Ellensburg Formation and possibly Thorp Gravel. Land use in this area is predominantly agriculture. The depth to static water level is estimated at 150 ft below ground surface, with an aquifer transmissivity estimated at 2800 ft² per day. The recharge capacity is around 3.25 AF per day and the SDF is estimated at 122 days. At 3.25 AF per day for a capture period of 120 days, the Cowiche Creek will see streamflow improvements through July, if the recharge period begins in November. To accommodate for changes in streamflow due to climate change, location 1 will require a slight shift to the west.

2) This location is 0.6 miles from the North Fork of Cowiche Creek and agricultural purposes dominate local land use. This area is underlain by the Ellensburg Formation, with Thorp Gravel nearby, and is estimated to have depth to static water level of 250 ft below ground surface. Transmissivity of the aquifer is calculated at 2600 ft² per day. Estimated groundwater recharge is 3.75 AF per day with an SDF of 40 days. At 30 AF per day for a capture period of 40 days, the Cowiche Creek will see streamflow improvements ending at the start of irrigation season, if the recharge period begins in November.

Figure 38. Suitable locations for groundwater storage in the Selah Basin.



Lower Yakima Basin

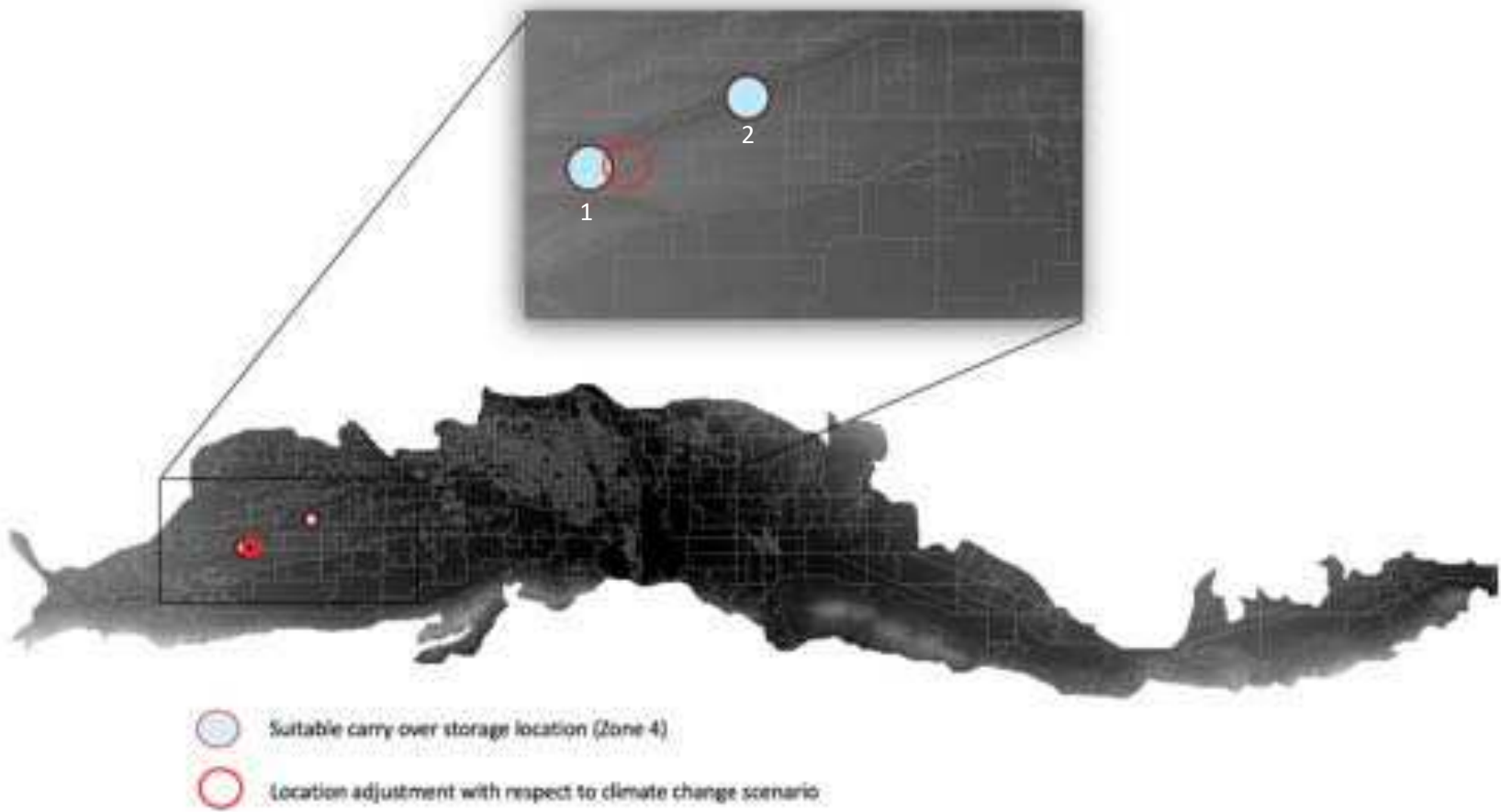
Site-specific recommendations are based on weighted overlay results from Section 1 - where spatial criteria are considered well-suited (Zone 5: met all criteria) for groundwater storage - and a stream depletion factor, which provides an estimate of travel time from the point of groundwater recharge to the local stream. However, in the Lower Yakima Basin, the high uncertainty of the SDF within Zone 5, eliminated these areas from consideration; therefore, the following is based on locations within Zone 4 (met most of the criteria suitable for groundwater storage) with the respective SDF.

Locations (Figure 39):

1. This location is underlain by the Ellensburg Formation and is near Thorp Gravel. The estimated transmissivity is 15,000 ft² per day with a depth to static water level at 70 ft below ground surface. Bachelor Creek is the closest surface water body and land in this area is used for agricultural purposes. Location 1 has an SDF of 37 days, with an estimated recharge rate of 1.5 AF per day. If recharge took place late winter season, Bachelor Creek may see streamflow improvements by April. Climate change is expected to cause an increase in runoff earlier in the season. To accommodate these changes, a slight shift to the east of location 1 is estimated to have an SDF of 110 days, while recharge rates remain the same.

2. This location is underlain by the Ellensburg Formation and is near Thorp Gravel. Transmissivity is estimated at 15,000 ft² per day, with a depth to static water level expected within 150 ft below ground surface. Location 2 has an SDF of 80 days and is predominantly used for agricultural purposes. The estimated recharge rate of 2.5 AF per day. If groundwater recharge ceases by the end of February, streamflow improvements will likely be observed in May.

Figure 39. Suitable locations for groundwater storage in the Lower Yakima Basin.

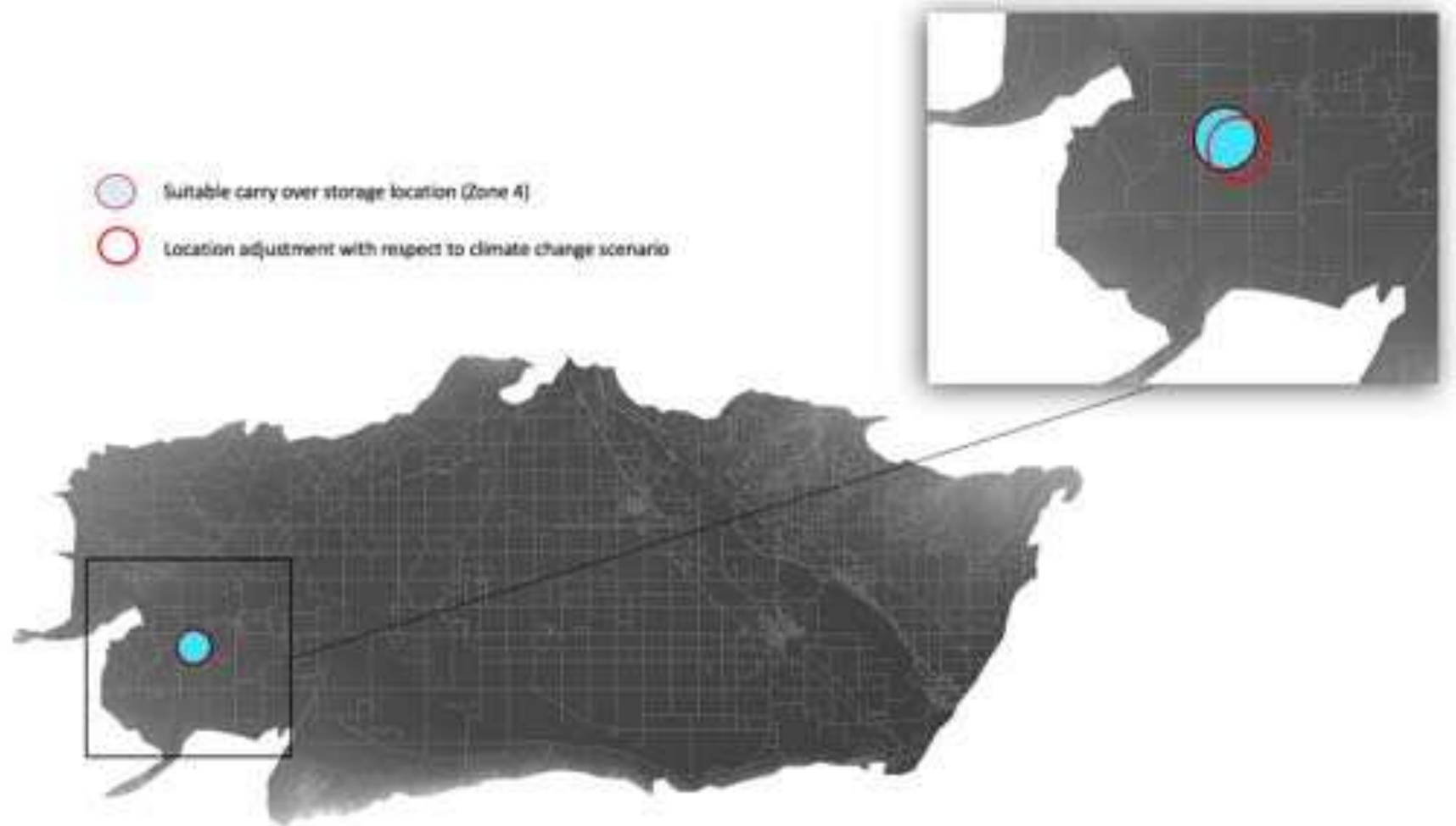


Toppenish Basin

Site-specific recommendations are based on weighted overlay results from Section 1 - where spatial criteria are considered well-suited (Zone 5: met all criteria) for groundwater storage - and a stream depletion factor, which provides an estimate of travel time from the point of groundwater recharge to the local stream. However, in the Toppenish Basin, the high uncertainty of the SDF within Zone 5, eliminated these areas from consideration; therefore, the following is based on locations within Zone 4 (met most of the criteria suitable for groundwater storage) with the respective SDF.

The area most suitable for groundwater storage is located within the southwest section of the watershed and 0.5 miles from Agency Creek (Figure 40). This region is located within Quaternary alluvium and is estimated to have a transmissivity of 8000 ft² per day, with static water level predicted to occur at 100 ft below ground surface. The calculated groundwater storage recharge rate up to 8 AF per day and an SDF of 150 days. Therefore, streamflow improvements may persist into July, if surface water capture and groundwater recharge end in February. Climate change is expected to cause an increase in runoff earlier in the season. To accommodate these changes, a slight shift to the southeast of location 1 is estimated to have an SDF of 110 days, while recharge rates remain the same.

Figure 40. Suitable location for groundwater storage in the Toppenish Basin.



Benton Basin

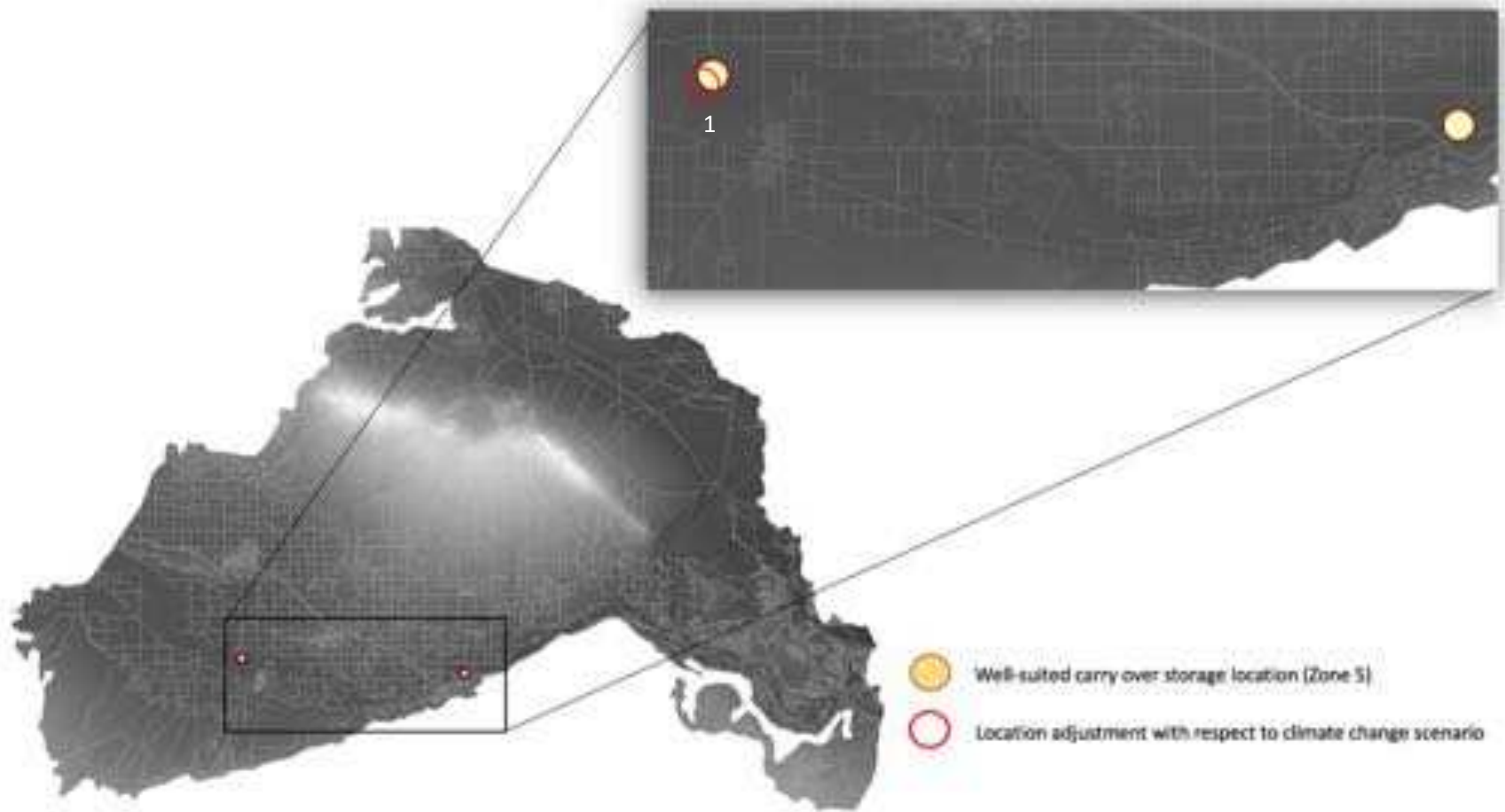
Two locations are considered well-suited for further investigation into the feasibility of groundwater storage in the Benton Basin (Figure 41).

Locations:

1. This location is slightly northwest of Mabton – between Highway 22 and the Yakima River. It is mostly underlain by Quaternary alluvium, near the Touchet Beds, which are outburst flood deposits that contain sand and silt. The depth to static water level is estimated at 30 ft below ground surface, and the transmissivity of the aquifer is calculated at 4300 ft² per day. The area is a mix of agriculture and undeveloped land. The estimated groundwater recharge rate is 2.4 AF per day with an SDF of 100 days. Therefore, if groundwater recharge occurred over a 120-day period during winter, stream improvements is estimated to persist into May. Climate change is expected to cause an increase in runoff earlier in the season. To accommodate these changes, a slight shift to the southwest of location 1 is estimated to have an SDF of 150 days, while recharge rates remain the same.

2. This location is outside the city of Prosser. It is underlain by Quaternary alluvium and Missoula flood glacial lake deposits. It has a transmissivity of 4300 ft² per day and a depth to static water level estimated at 40 ft below ground surface. The anticipated groundwater recharge rate is up to 2.5 AF per day, with an SDF of 130 days. Land use is a mix of industrial, agricultural, and open space. Therefore, if groundwater recharge ceases in February, streamflow will likely increase throughout June.

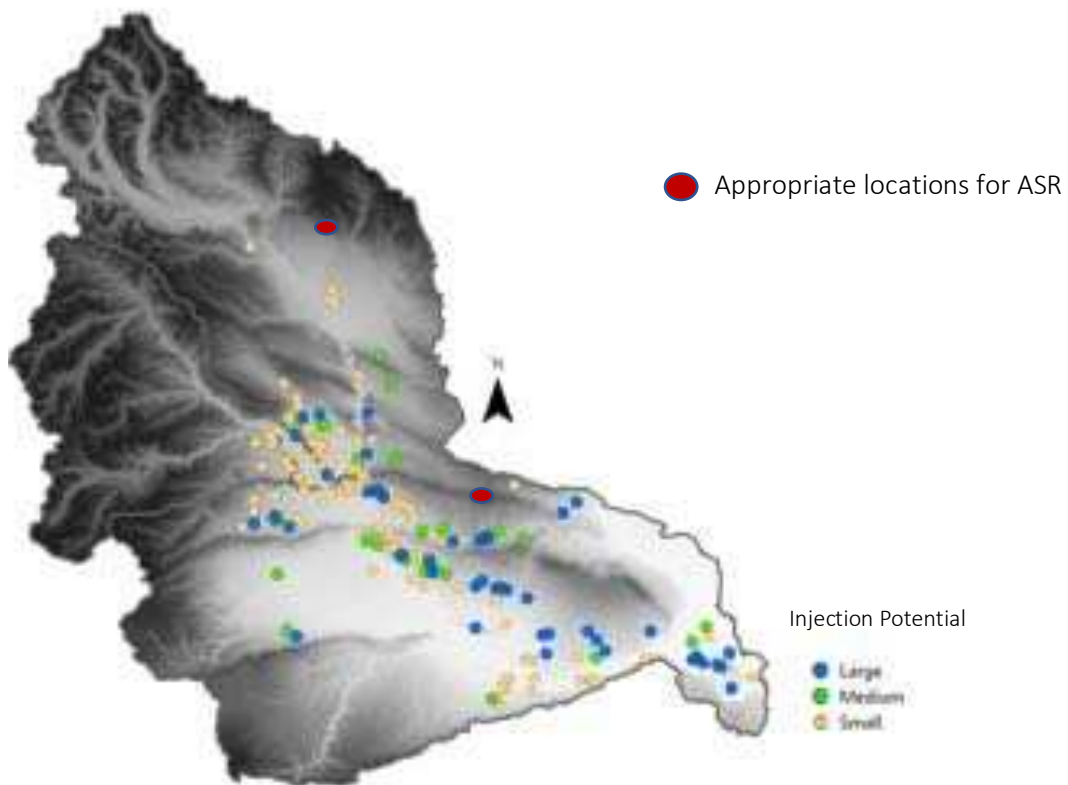
Figure 41. Suitable locations for groundwater storage in the Benton Basin.



ASR Results

Injection rates for ASR are discussed in Section 1. Small scale (< 5 cfs) to large scale (>15 cfs) projects are potentially feasible throughout the Yakima River Basin. Ideally implementing ASR in the Kittitas Basin would likely benefit users downstream as stored water could be 'banked' in the Ellensburg Formation, providing flexibility beyond annual replenishment. Two locations are deemed appropriate for ASR, since federal regulations reduce suitably because of treatment requirements prior to injection (Gibson, 2017). As injected water is not allowed to degrade underground sources of drinking water, it typically requires treating surface water to drinking water standards prior to injection. Within the Yakima River Basin, the city of Yakima and the city of Cle Elem operate treatment facilities. Although no wells were identified as suitable for ASR in the Cle Elem area, further investigation into its feasibility is likely warranted, as it is cost effective to have a treatment facility near ASR wells. Given these restrictions, expansion of the city of Yakima's ASR program should be considered as the proper infrastructure is currently in place to support its use.

Figure 42. Locations for ASR expansion or development



References

- Abatzoglou, J.T. and Brown, T.J., 2012. A comparison of statistical downscaling methods suited for wildfire applications. *International Journal of Climatology*, 32(5), pp.772-780.
- Anderson, R., Pitre, C. & Neir, A., 2009. Technical report on groundwater storage alternatives for the Yakima River Basin Storage Assessment, s.l.: Washington State Department of Ecology.
- Antunes, P., Santos, R. and Videira, N., 2006. Participatory decision making for sustainable development—the use of mediated modelling techniques. *Land use policy*, 23(1), pp.44-52.
- Asano, T. ed., 1985. *Artificial recharge of groundwater*. Butterworth Publishers. Stoneham, MA
- Babiker, I.S., Mohamed, M.A., Hiyama, T. and Kato, K., 2005. A GIS-based DRASTIC model for assessing aquifer vulnerability in Kakamigahara Heights, Gifu Prefecture, central Japan. *Science of the Total Environment*, 345(1-3), pp.127-140.
- Balali, H. and Viaggi, D., 2015. Applying a system dynamics approach for modeling groundwater dynamics to depletion under different economical and climate change scenarios. *Water*, 7(10), pp.5258-5271.
- Blakely, R.J., Sherrod, B.L., Weaver, C.S., Wells, R.E., Rohay, A.C., Barnett, E.A. and Knepprath, N.E., 2011. Connecting the Yakima fold and thrust belt to active faults in the Puget Lowland, Washington. *Journal of Geophysical Research: Solid Earth*, 116(B7).
- Bockermann, A., Meyer, B., Omann, I. and Spangenberg, J.H., 2005. Modelling sustainability: Comparing an econometric (PANTA RHEI) and a systems dynamics model (SuE). *Journal of Policy Modeling*, 27(2), pp.189-210.
- Bonilla Valverde, J.P., Blank, C., Roidt, M., Schneider, L. and Stefan, C., 2016. Application of a GIS multi-criteria decision analysis for the identification of intrinsic suitable sites in Costa Rica for the application of managed aquifer recharge (MAR) through spreading methods. *Water*, 8(9), p.391.
- Bouwer, H., 2002. Artificial recharge of groundwater: hydrogeology and engineering. *Hydrogeology Journal*, 10(1), pp.121-142.
- Brown, C.J., 2005. *Planning decision framework for brackish water aquifer, storage and recovery (ASR) projects*. University of Florida.
- Brunelli, M., 2014. *Introduction to the analytic hierarchy process*. Springer.
- Campbell, N.P. and Bentley, R.D., 1981. Late Quaternary deformation of the Toppenish Ridge uplift in south-central Washington. *Geology*, 9(11), pp.519-524.
- Cassell, E.A., Dorioz, J.M., Kort, R.L., Hoffmann, J.P., Meals, D.W., Kirschtel, D. and Braun, D.C., 1998. Modeling phosphorus dynamics in ecosystems: mass balance and dynamic simulation approaches. *Journal of environmental quality*, 27(2), pp.293-298.
- Chi, K.C., Nuttall, W.J. and Reiner, D.M., 2009. Dynamics of the UK natural gas industry: System dynamics modelling and long-term energy policy analysis. *Technological Forecasting and Social Change*, 76(3), pp.339-357.

- Chipongo, K. and Khiadani, M., 2015. Comparison of simulation methods for recharge mounds under rectangular basins. *Water Resources Management*, 29(8), pp.2855-2874
- Cooper, H.H. and Jacob, C.E., 1946. A generalized graphical method for evaluating formation constants and summarizing well-field history. *Eos, Transactions American Geophysical Union*, 27(4), pp.526-534.
- Dhungle, R. and Fiedler, F., 2016. Water Balance to Recharge Calculation: Implications for Watershed Management Using Systems Dynamics Approach. *Hydrology*, 3(1), p.13.
- Dillon, P., Stuyfzand, P., Grischek, T., Lluria, M., Pyne, R.D.G., Jain, R.C., Bear, J., Schwarz, J., Wang, W., Fernandez, E. and Stefan, C., 2018. Sixty years of global progress in managed aquifer recharge. *Hydrogeology Journal*, pp.1-30.
- El-Baz, F., Himida, I. 1995. Groundwater potential of the Sinai Peninsula, Egypt. Cairo, Egypt. Center for Remote Sensing. Research project.
<http://www.bu.edu/remotesensing/research/completed/egypt-groundwater/>. Accessed September 2017.
- Elshorbagy, A., Teegavarapu, R.S. and Ormsbee, L., 2006. Assessment of pathogen pollution in watersheds using object-oriented modeling and probabilistic analysis. *Journal of Hydroinformatics*, 8(1), pp.51-63.
- Ely, D.M., Bachmann, M.P. and Vaccaro, J.J., 2011. *Numerical simulation of groundwater flow for the Yakima River basin aquifer system, Washington*. U. S. Geological Survey.
- Forrester, J. 1961. *Industrial dynamics*. MIT Press, Cambridge, MA
- Forrester, J. 1969. *Urban dynamics*. MIT Press, Cambridge, MA
- Forrester, J.W., 1987. Lessons from system dynamics modeling. *System Dynamics Review*, 3(2), pp.136-149.
- Gibson, M. 2017. The Regulatory Environment of Managed Aquifer Recharge in the United States and its Spatial Shortcomings. *IMPACT*. 19:5. p 11-14.
- Gdoura, K., Anane, M. and Jellali, S., 2015. Geospatial and AHP-multicriteria analyses to locate and rank suitable sites for groundwater recharge with reclaimed water. *Resources, Conservation and Recycling*, 104, pp.19-30.
- Glover, R.E., 1960. Mathematical derivations as pertain to groundwater recharge, report. *Agric. Res. Serv., US Dep. of Agric., Fort Collins, Colo.*
- Golder Associates & HDR Engineering, 2011. *Yakima River Basin Study: Groundwater infiltration appraisal-level study technical memorandum*. 179 p., s.l.: s.n.
- Golder Associates, 2002. *Naches (WRIA 38) Storage Assessment*. Yakima Basin Watershed Planning., s.l.: s.n.
- Golder Associates, 2013. *Yakima River Basin Integrated Water Resource Management Plan Technical Memorandum: Field investigation of shallow groundwater recharge - Eastern Kittitas Valley, WA.*, s.l.: Prepared for the U.S. Bureau of Reclamation and Washington State Department of Ecology.
- Gomberg, J., Sherrod, B., Trautman, M., Burns, E. and Snyder, D., 2012. Contemporary seismicity in and around the Yakima fold-and-thrust belt in eastern Washington. *Bulletin of the Seismological Society of America*, 102(1), pp.309-320.

- Hantush, M.S., 1967. Growth and decay of groundwater-mounds in response to uniform percolation. *Water Resources Research*, 3(1), pp.227-234.
- HDR Engineering. 2014. Yakima River Basin integrated water recourse management plan. *Technical memorandum: hydrologic modeling of system improvements, U.S. Bureau of Reclamation*, 438 p.
- Huntoon, P.W., 1980. Computationally efficient polynomial approximations used to program the Theis equation. *Groundwater*, 18(2), pp.134-136.
- Ilias, T.S., Thomas, Z.S. and Andreas, P.C., 2008. Water table fluctuation in aquifers overlying a semi-impervious layer due to transient recharge from a circular basin. *Journal of hydrology*, 348(1), pp.215-223.
- International Groundwater Resources Assessment Centre (IGRAC). 2018. Managed Aquifer Recharge Portal. <https://apps.geodan.nl/igrac/ggisviewer/viewer/globalmar/public/default>
- Jamali, I.A., Mörtberg, U., Olofsson, B. and Shafique, M., 2014. A spatial multi-criteria analysis approach for locating suitable sites for construction of subsurface dams in Northern Pakistan. *Water resources management*, 28(14), pp.5157-5174.
- Jenkins, C.T., 1968. Techniques for Computing Rate and Volume of Stream Depletion by Wells a. *Groundwater*, 6(2), pp.37-46.
- Jiao, W. and Xu, Z., 2013. A distributed runoff model for the mountainous region of the Heihe River Basin (China) based on the spatial modeling environment (SME) II: model calibration and validation. *Environmental earth sciences*, 69(7), pp.2189-2197.
- Jones, M.A. and Vaccaro, J.J., 2008. *Extent and Depth to Top of Basalt and Interbed Hydrogeologic Units, Yakima River Basin Aquifer System, Washington*. US Department of the Interior, US Geological Survey.
- Jones, M.A., Vaccaro, J.J. and Watkins, A.M., 2006. *Hydrogeologic framework of sedimentary deposits in six structural basins, Yakima River basin, Washington*. US Department of the Interior, US Geological Survey.
- Kazakis, N., 2018. Delineation of Suitable Zones for the Application of Managed Aquifer Recharge (MAR) in Coastal Aquifers Using Quantitative Parameters and the Analytical Hierarchy Process. *Water (20734441)*, 10(6).
- Korkmaz, S., 2013. Transient solutions to groundwater mounding in bounded and unbounded aquifers. *Groundwater*, 51(3), pp.432-441.
- Kotir, J.H., Smith, C., Brown, G., Marshall, N. and Johnstone, R., 2016. A system dynamics simulation model for sustainable water resources management and agricultural development in the Volta River Basin, Ghana. *Science of the Total Environment*, 573, pp.444-457.
- Li, Z., Li, C., Wang, X., Peng, C., Cai, Y. and Huang, W., 2018. A hybrid system dynamics and optimization approach for supporting sustainable water resources planning in Zhengzhou City, China. *Journal of Hydrology*, 556, pp.50-60.
- Lodwick, W.A., Monson, W. and Svoboda, L., 1990. Attribute error and sensitivity analysis of map operations in geographical informations systems: suitability analysis. *International Journal of Geographical Information System*, 4(4), pp.413-428.

- Magesh, N.S., Chandrasekar, N. and Soundranayagam, J.P., 2012. Delineation of groundwater potential zones in Theni district, Tamil Nadu, using remote sensing, GIS and MIF techniques. *Geoscience Frontiers*, 3(2), pp.189-196.
- Mankad, A., Walton, A. and Alexander, K., 2015. Key dimensions of public acceptance for managed aquifer recharge of urban stormwater. *Journal of Cleaner Production*, 89, pp.214-223.
- Marino, M.A., 1974. Growth and decay of groundwater mounds induced by percolation. *Journal of Hydrology*, 22(3-4), pp.295-301.
- McCaffrey, R., King, R.W., Wells, R.E., Lancaster, M. and Miller, M.M., 2016. Contemporary deformation in the Yakima fold and thrust belt estimated with GPS. *Geophysical Journal International*, 207(1), pp.1-11.
- McWhorter, D., and Sunaka, D. 1977. Groundwater hydrology and hydraulics. *Water Resources Publications*, Ft. Collins, Colorado, 290 pp.
- Moffatt, I. and Hanley, N., 2001. Modelling sustainable development: systems dynamic and input-output approaches. *Environmental modelling & software*, 16(6), pp.545-557.
- Molden, D.J. 1982. Mathematical modeling of artificial recharge. Thesis, Colorado State University, Ft. Collins, Colorado. 164 pp.
- Morel-Seytoux, H.J., Miracapillo, C. and Abdulrazzak, M., 1989. Distribution of aquifer recharge from a circular spreading basin under transient operations. In *Proc., Symp. on Groundwater Management Quantity and Quality, International Association of Hydrological Sciences (IAHS), UK*.
- National Ocean and Atmospheric Administration (NOAA). 2018. NOW Data. <https://w2.weather.gov/climate/xmacis.php?wfo=pdf>
- Niazi, A., Prasher, S.O., Adamowski, J. and Gleeson, T., 2014. A system dynamics model to conserve arid region water resources through aquifer storage and recovery in conjunction with a dam. *Water*, 6(8), pp.2300-2321.
- Ohab-Yazdi, S.A. and Ahmadi, A., 2018. Using the agent-based model to simulate and evaluate the interaction effects of agent behaviors on groundwater resources, a case study of a sub-basin in the Zayandehroud River basin. *Simulation Modelling Practice and Theory*, 87, pp.274-292.
- Oni, S.K., Dillon, P.J., Metcalfe, R.A. and Futter, M.N., 2012. Dynamic modelling of the impact of climate change and power flow management options using STELLA: application to the Steephill Falls Reservoir, Ontario, Canada. *Canadian Water Resources Journal*, 37(2), pp.125-148.
- Pachauri, R.K., Allen, M.R., Barros, V.R., Broome, J., Cramer, W., Christ, R., Church, J.A., Clarke, L., Dahe, Q., Dasgupta, P. and Dubash, N.K., 2014. *Climate change 2014: synthesis report. Contribution of Working Groups I, II and III to the fifth assessment report of the Intergovernmental Panel on Climate Change* (p. 151). IPCC.
- Pandey, R., 2002. Energy policy modelling: agenda for developing countries. *Energy Policy*, 30(2), pp.97-106.
- Pedrero, F., Albuquerque, A., do Monte, H.M., Cavaleiro, V. and Alarcón, J.J., 2011. Application of GIS-based multi-criteria analysis for site selection of aquifer recharge with reclaimed water. *Resources, Conservation and Recycling*, 56(1), pp.105-116.

- Pluchinotta, I., Pagano, A., Giordano, R. and Tsoukiàs, A., 2018. A system dynamics model for supporting decision-makers in irrigation water management. *Journal of environmental management*, 223, pp.815-824.
- Qureshi, M.E., Harrison, S.R. and Wegener, M.K., 1999. Validation of multicriteria analysis models. *Agricultural Systems*, 62(2), pp.105-116.
- Rahman, M.A., Rusteberg, B., Gogu, R.C., Ferreira, J.L. and Sauter, M., 2012. A new spatial multi-criteria decision support tool for site selection for implementation of managed aquifer recharge. *Journal of environmental management*, 99, pp.61-75.
- Rai, S.N., Ramana, D.V. and Singh, R.N., 1998. On the prediction of ground-water mound formation in response to transient recharge from a circular basin. *Water resources management*, 12(4), pp.271-284.
- Rehman, S.A.U., Cai, Y., Mirjat, N.H., Walasai, G.D., Shah, I.A. and Ali, S., 2017. The Future of Sustainable Energy Production in Pakistan: A System Dynamics-Based Approach for Estimating Hubbert
- Reidel, S.P., Martin, B.S. and Petcovic, H.L., 2003. The Columbia River flood basalts and the Yakima fold belt. *Western Cordillera and adjacent areas. Edited by TW Swanson. Geological Society of America Field Guide*, 4, pp.87-105.
- Rivera, E.C., de Queiroz, J.F., Ferraz, J.M. and Ortega, E., 2007. Systems models to evaluate eutrophication in the Broa Reservoir, São Carlos, Brazil. *Ecological Modelling*, 202(3-4), pp.518-526.
- Ryu, J.H., Contor, B., Johnson, G., Allen, R. and Tracy, J., 2012. System Dynamics to Sustainable Water Resources Management in the Eastern Snake Plain Aquifer Under Water Supply Uncertainty 1. *JAWRA Journal of the American Water Resources Association*, 48(6), pp.1204-1220.
- Saaty, T.L., 1980. The Analytical Hierarchy Process, Planning, Priority. *Resource Allocation. RWS Publications, USA.*
- Saraf, A.K. and Choudhury, P.R., 1998. Integrated remote sensing and GIS for groundwater exploration and identification of artificial recharge sites. *International journal of Remote sensing*, 19(10), pp.1825-1841.
- Seerley, D., 2003. *An analysis of the evolution of public policy for aquifer storage and recovery: experiences in three Southeastern states* (Doctoral dissertation, University of Georgia).
- Selvam, S., Magesh, N.S., Sivasubramanian, P., Soundranayagam, J.P., Manimaran, G. and Seshunarayana, T., 2014. Deciphering of groundwater potential zones in Tuticorin, Tamil Nadu, using remote sensing and GIS techniques. *Journal of the Geological Society of India*, 84(5), pp.597-608.
- Sener, E. and Davraz, A., 2013. Assessment of groundwater vulnerability based on a modified DRASTIC model, GIS and an analytic hierarchy process (AHP) method: the case of Egirdir Lake basin (Isparta, Turkey). *Hydrogeology Journal*, 21(3), pp.701-714.
- Shaban, A., Khawlie, M. and Abdallah, C., 2006. Use of remote sensing and GIS to determine recharge potential zones: the case of Occidental Lebanon. *Hydrogeology Journal*, 14(4), pp.433-443.

- Singh, A., Panda, S.N., Kumar, K.S. and Sharma, C.S., 2013. Artificial groundwater recharge zones mapping using remote sensing and GIS: a case study in Indian Punjab. *Environmental management*, 52(1), pp.61-71.
- Singh, R., 1976. Prediction of mound geometry under recharge basins. *Water Resources Research*, 12(4), pp.775-780.
- Slootweg, J.G. and Kling, W.L., 2003, June. Aggregated modelling of wind parks in power system dynamics simulations. In *Power Tech Conference Proceedings, 2003 IEEE Bologna* (Vol. 3, pp. 6-pp). IEEE.
- Smith, A.J. and Pollock, D.W., 2012. Assessment of managed aquifer recharge potential using ensembles of local models. *Groundwater*, 50(1), pp.133-143.
- Solomon, S. and Quiel, F., 2006. Groundwater study using remote sensing and geographic information systems (GIS) in the central highlands of Eritrea. *Hydrogeology Journal*, 14(5), pp.729-741.
- Sprenger, C., Hartog, N., Hernández, M., Vilanova, E., Grützmacher, G., Scheibler, F. and Hannappel, S., 2017. Inventory of managed aquifer recharge sites in Europe: historical development, current situation and perspectives. *Hydrogeology Journal*, 25(6), pp.1909-1922
- Stave, K.A., 2002. Using system dynamics to improve public participation in environmental decisions. *System Dynamics Review: The Journal of the System Dynamics Society*, 18(2), pp.139-167.
- Susnik, J., Molina, J.L., Vamvakieridou-Lyroudia, L.S., Savić, D.A. and Kapelan, Z., 2013. Comparative analysis of system dynamics and object-oriented bayesian networks modelling for water systems management. *Water resources management*, 27(3), pp.819-841.
- Theis, C.V., 1935. The relation between the lowering of the piezometric surface and the rate and duration of discharge of a well using ground-water storage. *Eos, Transactions American Geophysical Union*, 16(2), pp.519-524.
- United States Bureau of Reclamation, and Washington State Department of Ecology, 2012. Yakima River Basin Integrated Water Resource Management Plan Final Programmatic Environmental Impact Statement. <http://www.usbr.gov/pn/programs/yrbwep/reports/FPEIS/fpeis.pdf>. Accessed January 2017.
- United States Geological Survey. 2015. National Elevation Dataset. <https://ita.cr.usgs.gov/NED>. Accessed June, 2017. US Department of the Interior, US Geological Survey. 120 p.
- United States Geological Society (USGS). 2017. Earth Explorer. <https://earthexplorer.usgs.gov>
- United States Geological Survey. 2018. The National Map. <https://viewer.nationalmap.gov/advanced-viewer/>. Accessed 2017.
- United States. Bureau of Reclamation. Yakima Project Hydromet System. Accessed May 2018. <https://www.usbr.gov/pn/hydromet/yakima/index.html>
- University of Washington Hydro. 2018. Columbia River climate change. Accessed 2018. <http://www.hydro.washington.edu/CRCC/>

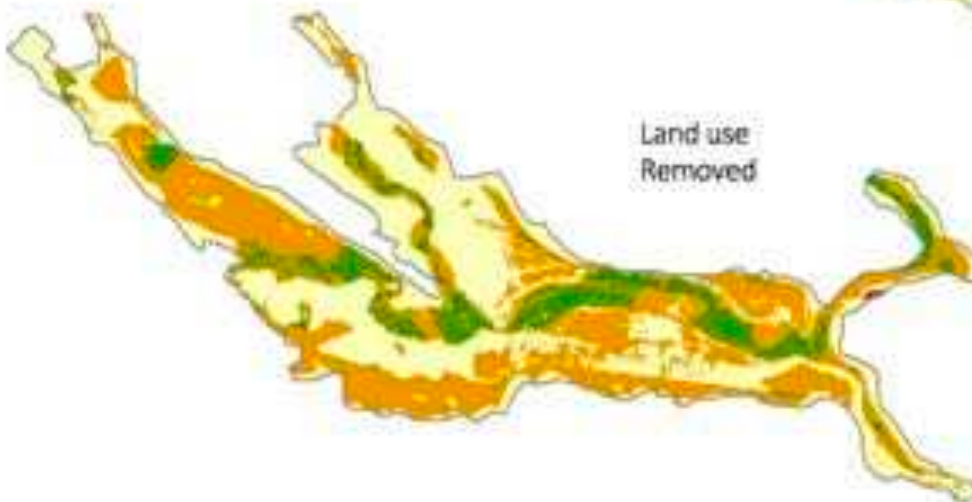
- Vaccaro, J.J. and Sumioka, S.S., 2006. *Estimates of Ground-Water Pumpage from the Yakima River Basin Aquifer System, Washington, 1960-2000*. US Department of the Interior, US Geological Survey.
- Vaccaro, J.J., Jones, M.A., Ely, D.M., Keys, M.E., Olsen, T.D., Welch, W.B., 2009. *Hydrogeologic Framework of the Yakima River Basin Aquifer System, Washington*.
- Vano, J.A., Scott, M.J., Voisin, N., Stöckle, C.O., Hamlet, A.F., Mickelson, K.E., Elsner, M.M. and Lettenmaier, D.P., 2010. Climate change impacts on water management and irrigated agriculture in the Yakima River Basin, Washington, USA. *Climatic Change*, 102(1-2), pp.287-317.
- Wang, J.J., Jing, Y.Y., Zhang, C.F. and Zhao, J.H., 2009. Review on multi-criteria decision analysis aid in sustainable energy decision-making. *Renewable and Sustainable Energy Reviews*, 13(9), pp.2263-2278.
- Warner, J.W., Molden, D., Chahata, M. and Sunada, D.K., 1989. Mathematical analysis of artificial recharge from basins. *JAWRA Journal of the American Water Resources Association*, 25(2), pp.401-411
- Washington Department of Natural Resources. 2016. 1:100,000-scale geologic mapping database of Washington State Digital Data Series 18. Accessed Dec 2016.
https://www.dnr.wa.gov/publications/ger_readme_surface_geology_100k.htm
- Washington State Department of Ecology. 2010. Land use GIS Data Layer
<https://ecology.wa.gov/Research-Data/Data-resources/Geographic-Information-Systems-GIS/Data#l>. Accessed 8/15/2017
- Washington State Department of Ecology. 2012. Water Resources Explorer. Available online:
<https://fortress.wa.gov/ecy/waterresources/map/WaterResourcesExplorer.aspx>.
- Washington State Department of Ecology. 2018. Water well reports.
<https://ecology.wa.gov/Research-Data/Data-resources/Geographic-Information-Systems-GIS/Data>. Accessed June, 2017.
- Waters, A.C., 1955. Volcanic rocks and the tectonic cycle. *Geological Society of America Special Papers*, 62, pp.703-722.
- Winz, I., Brierley, G. and Trowsdale, S., 2009. The use of system dynamics simulation in water resources management. *Water resources management*, 23(7), pp.1301-1323.
- Yang, J., Lei, K., Khu, S., Meng, W. and Qiao, F., 2015. Assessment of water environmental carrying capacity for sustainable development using a coupled system dynamics approach applied to the Tieling of the Liao River Basin, China. *Environmental Earth Sciences*, 73(9), pp.5173-5183.
- Xu, H., 2006. Modification of normalised difference water index (NDWI) to enhance open water features in remotely sensed imagery. *International journal of remote sensing*, 27(14), pp.3025-3033.
- Yeh, H.F., Cheng, Y.S., Lin, H.I. and Lee, C.H., 2016. Mapping groundwater recharge potential zone using a GIS approach in Hualian River, Taiwan. *Sustainable Environment Research*, 26(1), pp.33-43.

- Zomorodi, K., 2009. Simplified solution for groundwater mounding under round stormwater infiltration facilities. In *World Environmental and Water Resources Congress 2009: Great Rivers* (pp. 1-17).
- Zomorodian, M., Lai, S.H., Homayounfar, M., Ibrahim, S. and Pender, G., 2017. Development and application of coupled system dynamics and game theory: A dynamic water conflict resolution method. *PloS one*, 12(12)

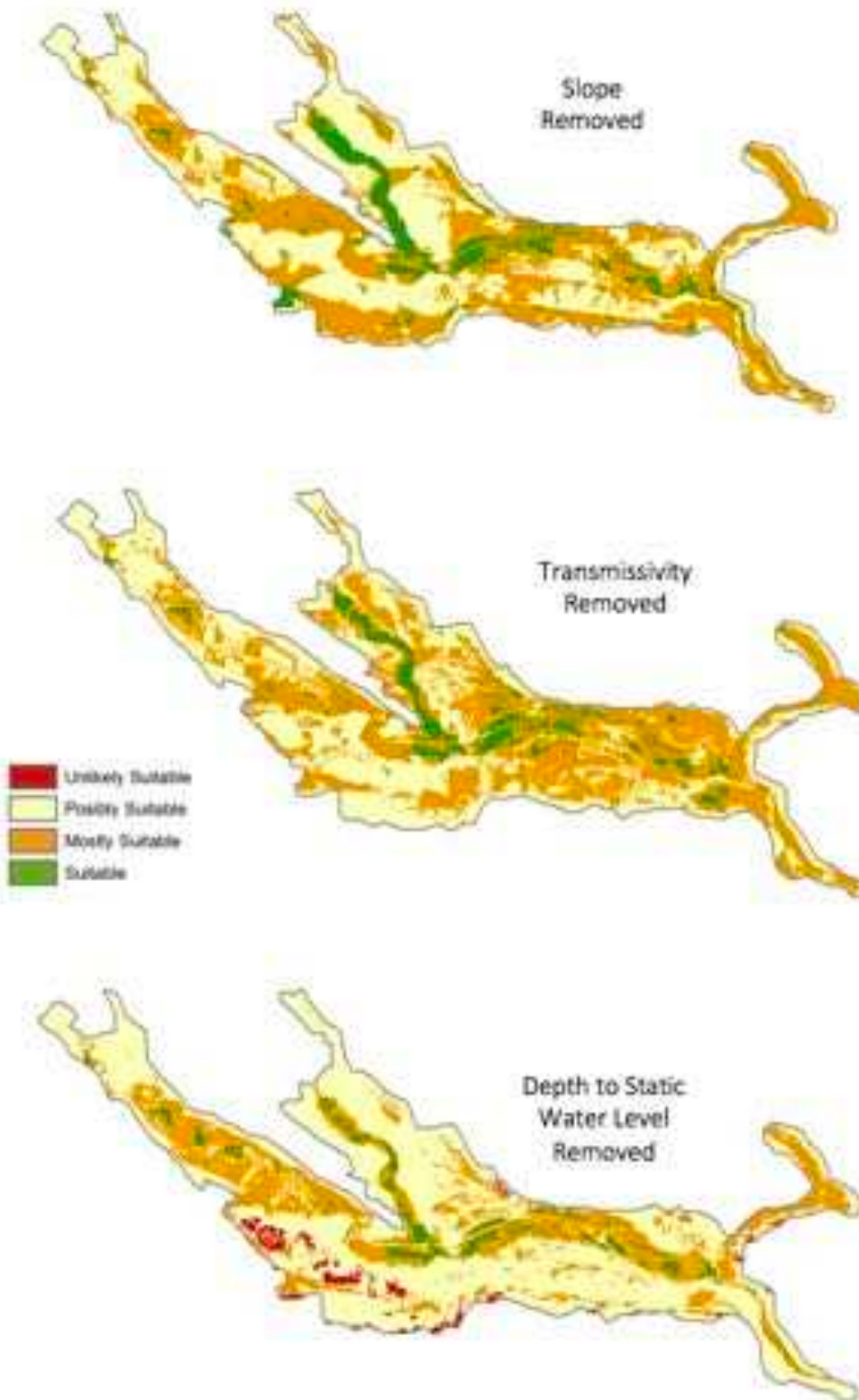
Appendices

Appendix A: Sensitivity Results

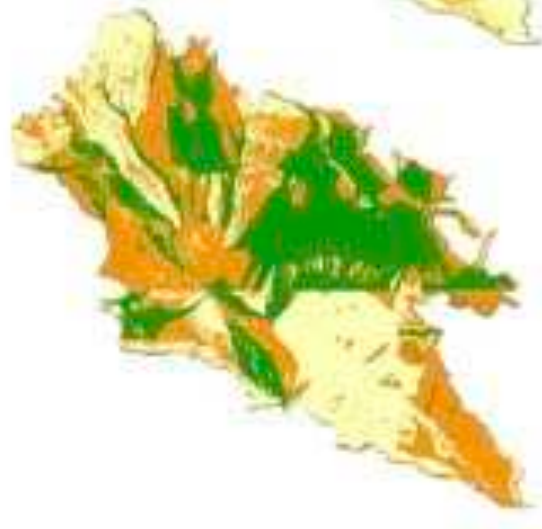
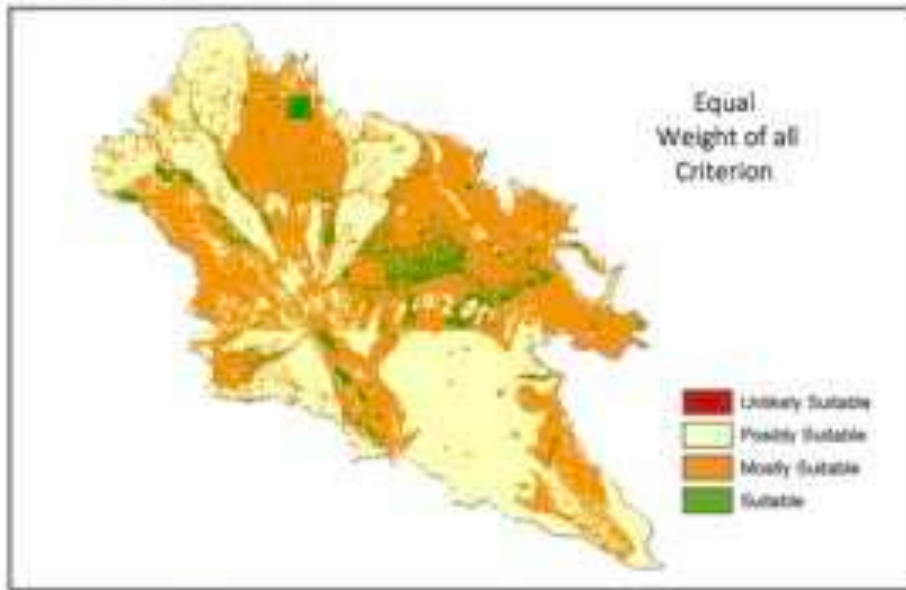
Roslyn Basin



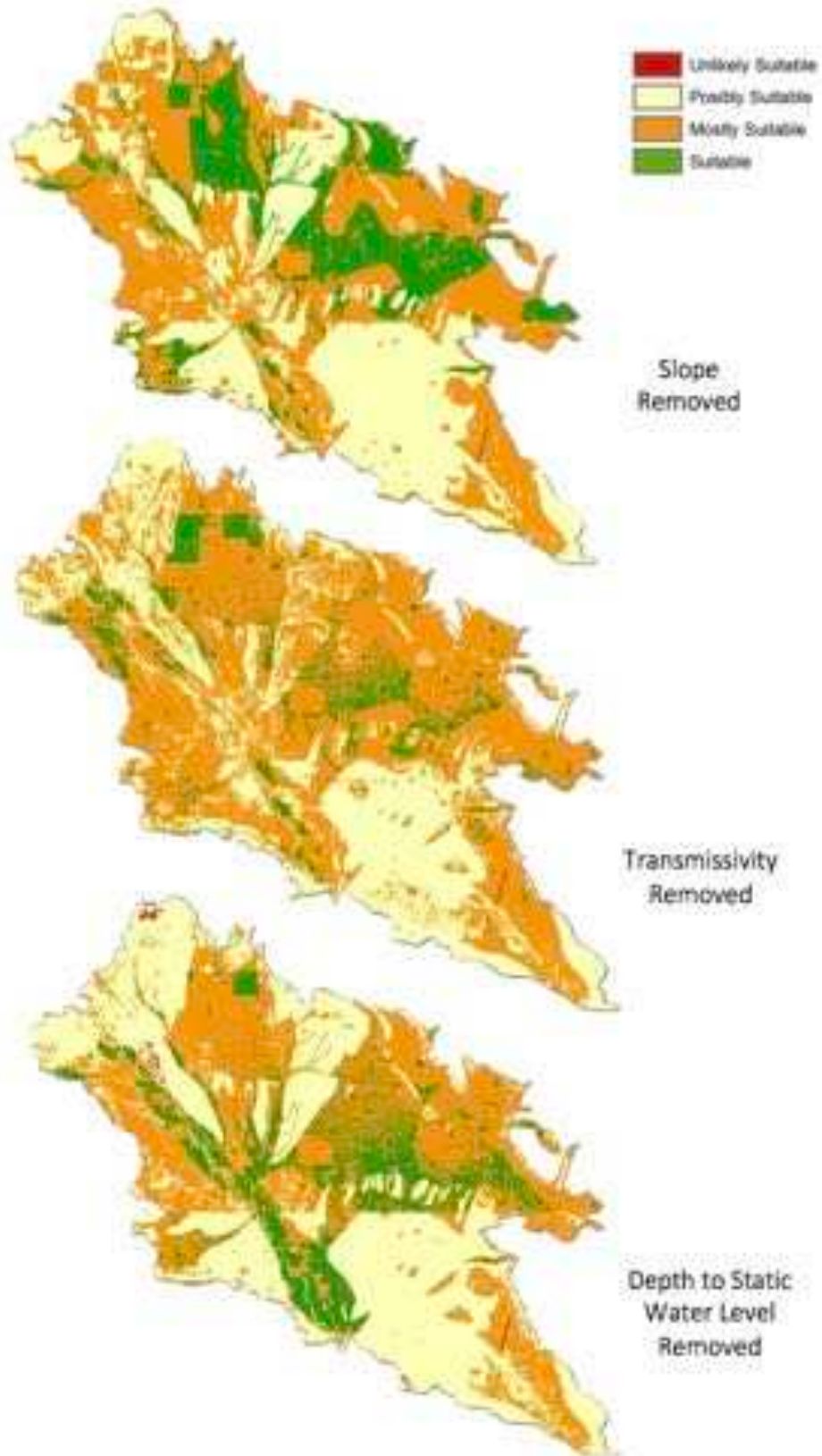
Roslyn Basin Continued



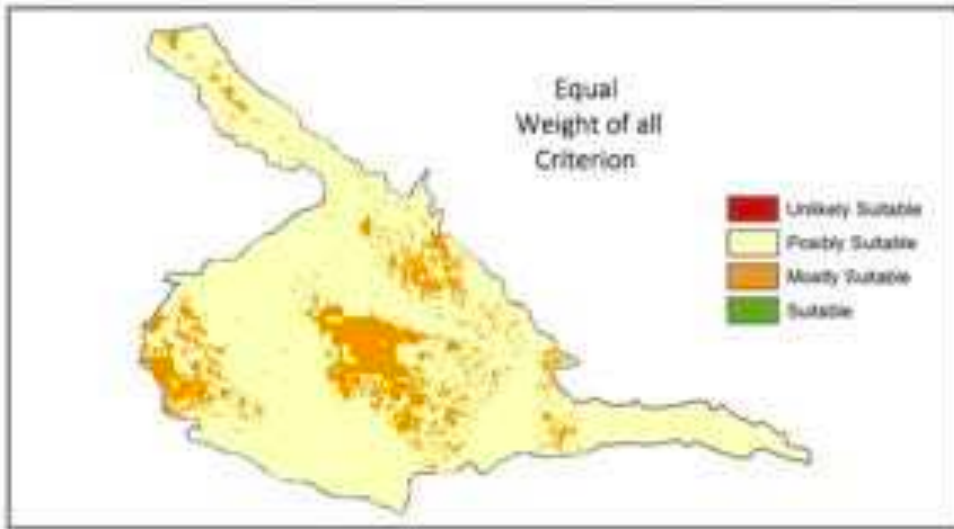
Kittitas Basin



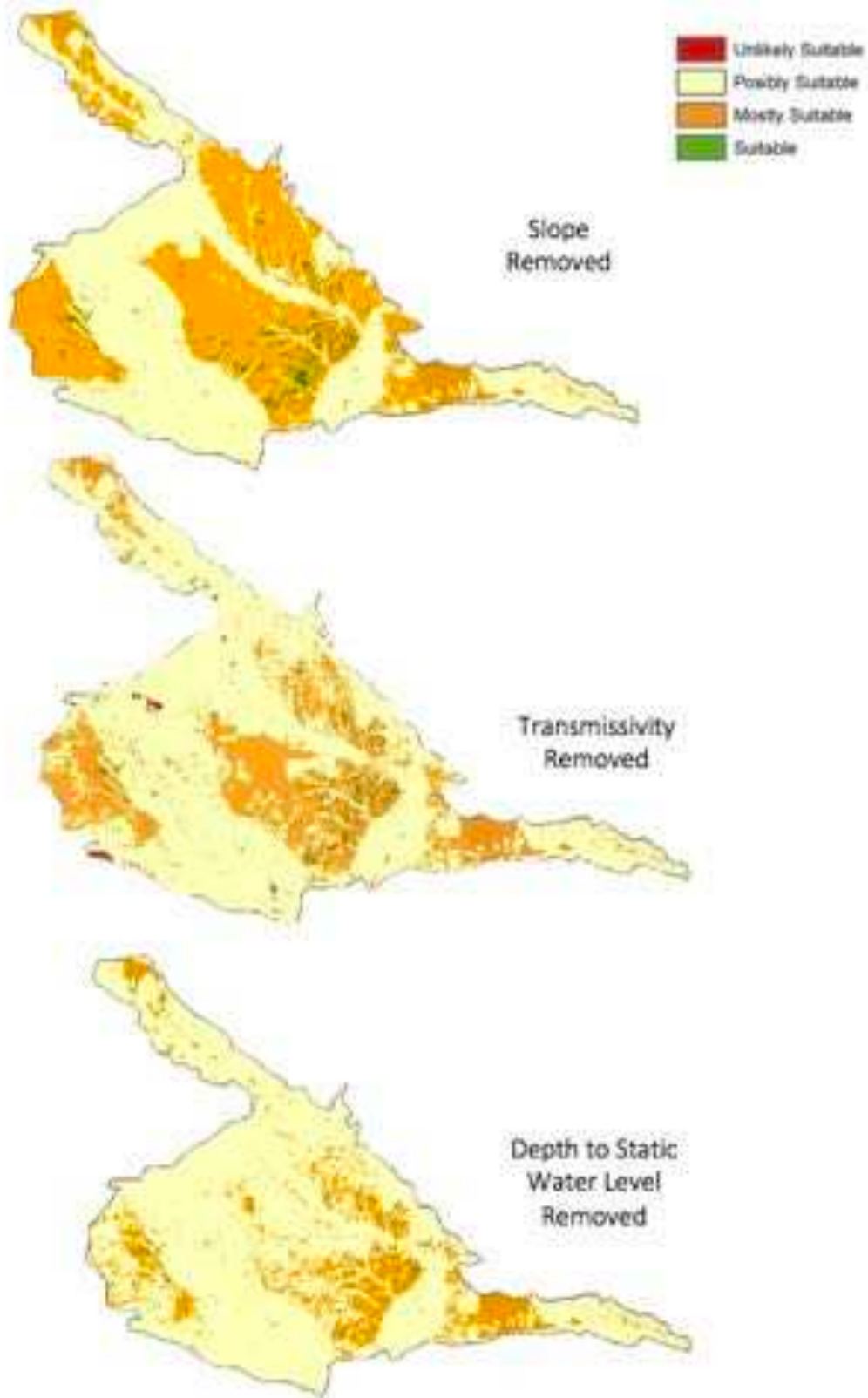
Kittitas Basin Continued



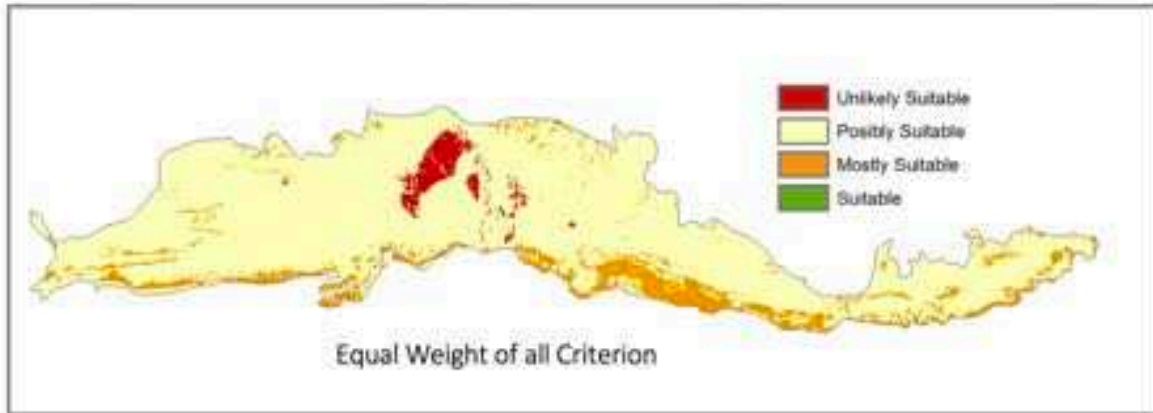
Selah Basin



Selah Basin Continued



Lower Yakima Basin



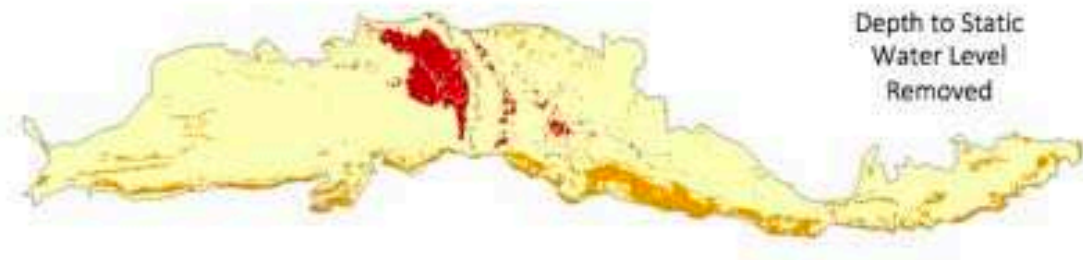
Lithology
Removed



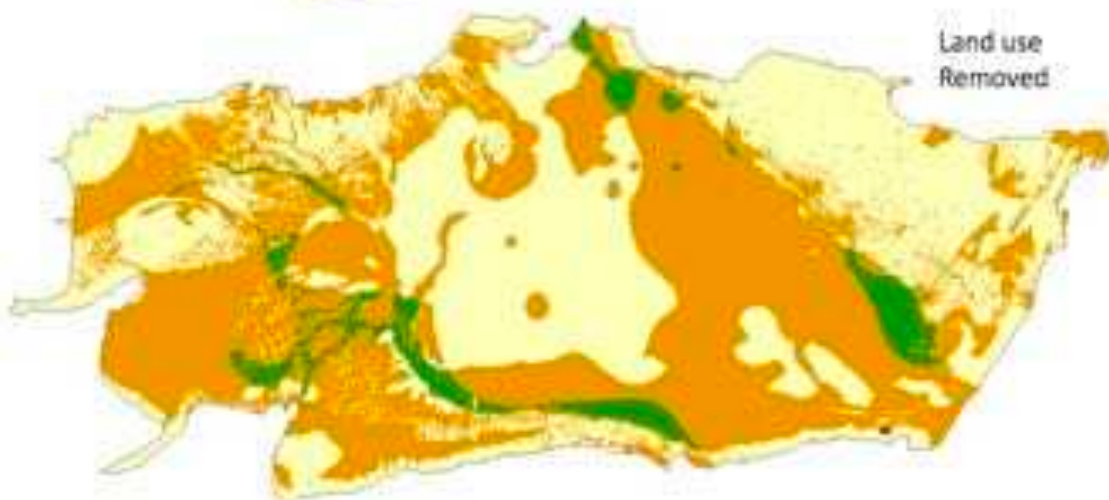
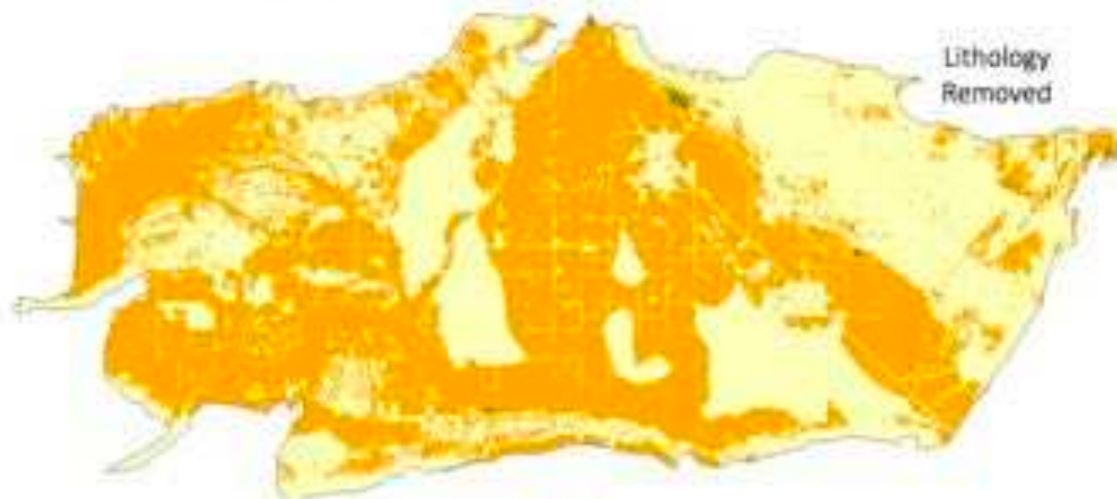
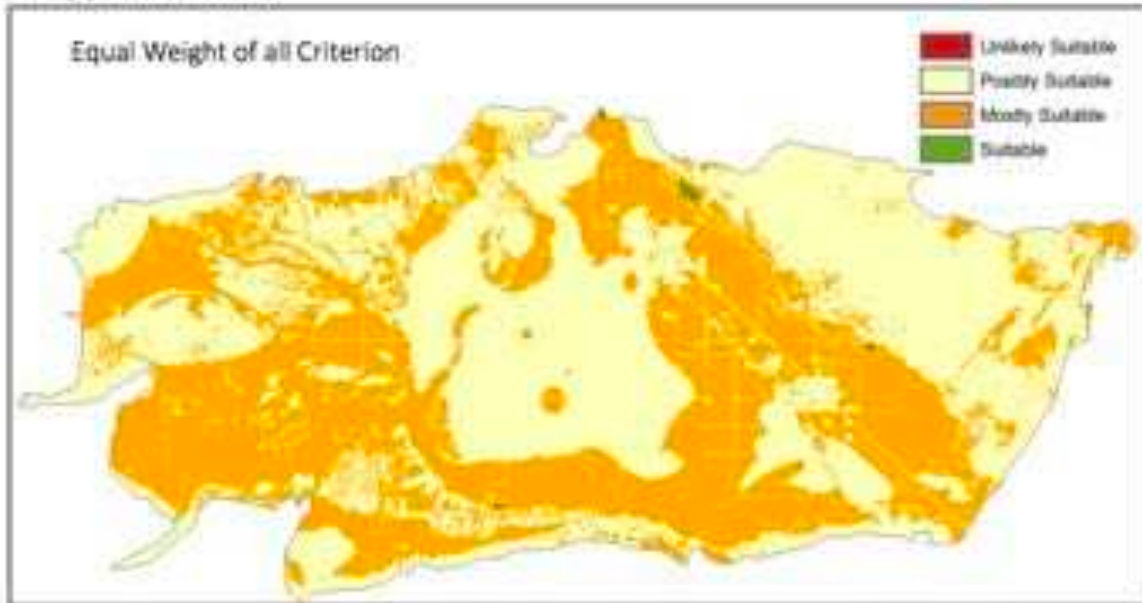
Land use
Removed



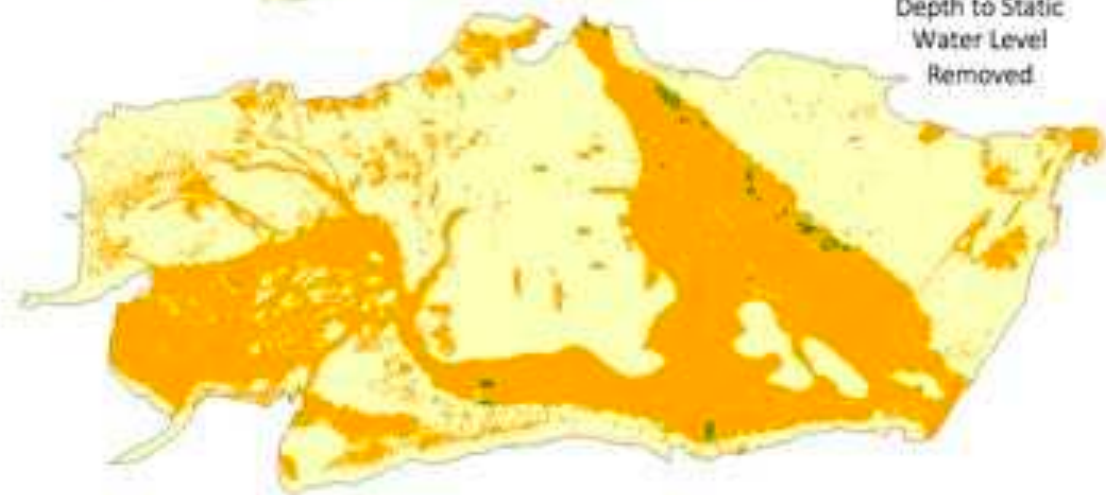
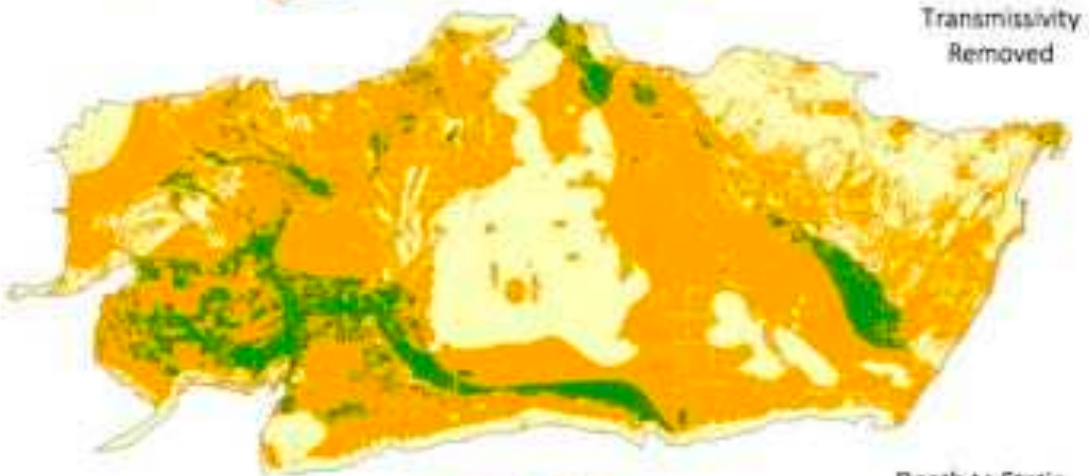
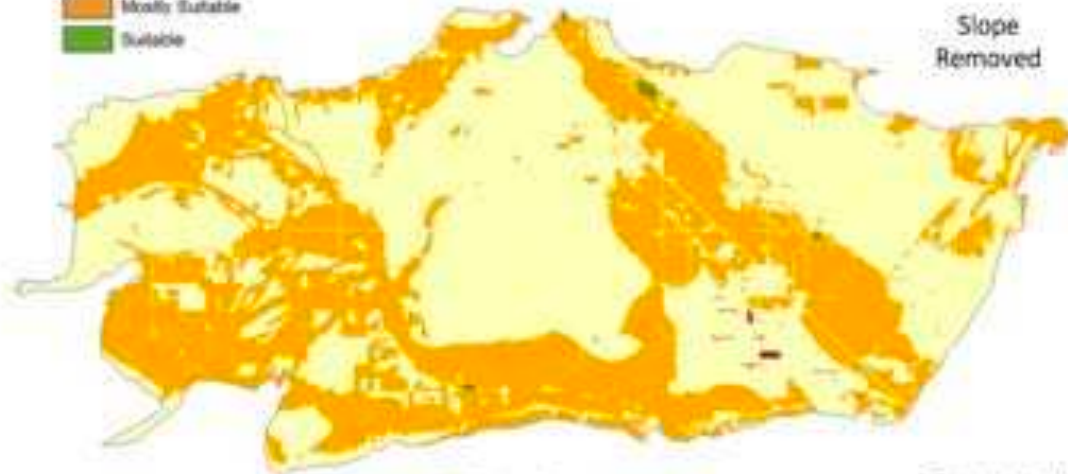
Lower Yakima Basin Continued



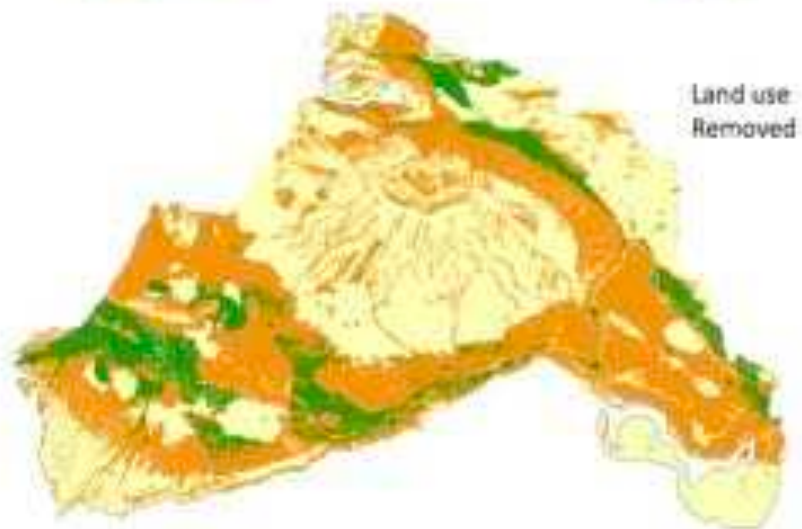
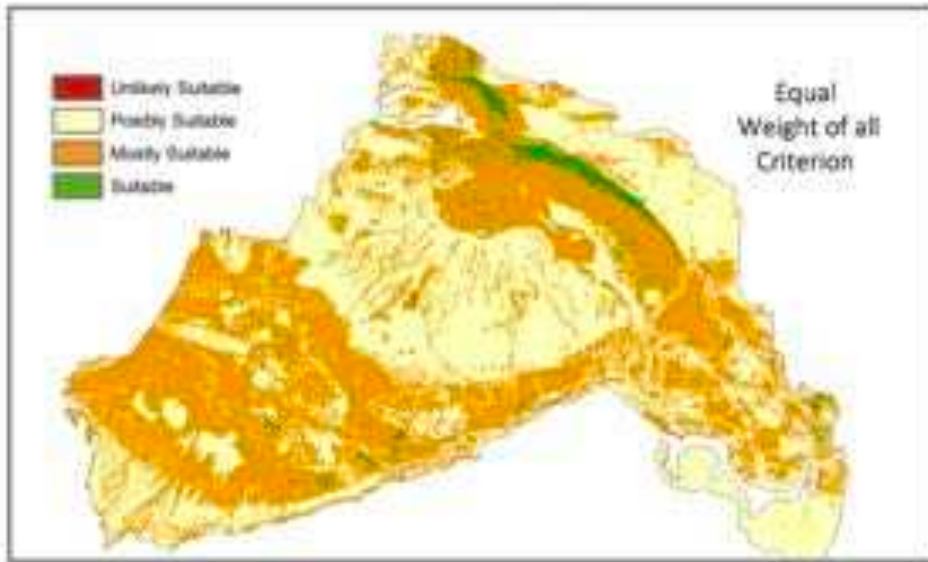
Toppenish Basin



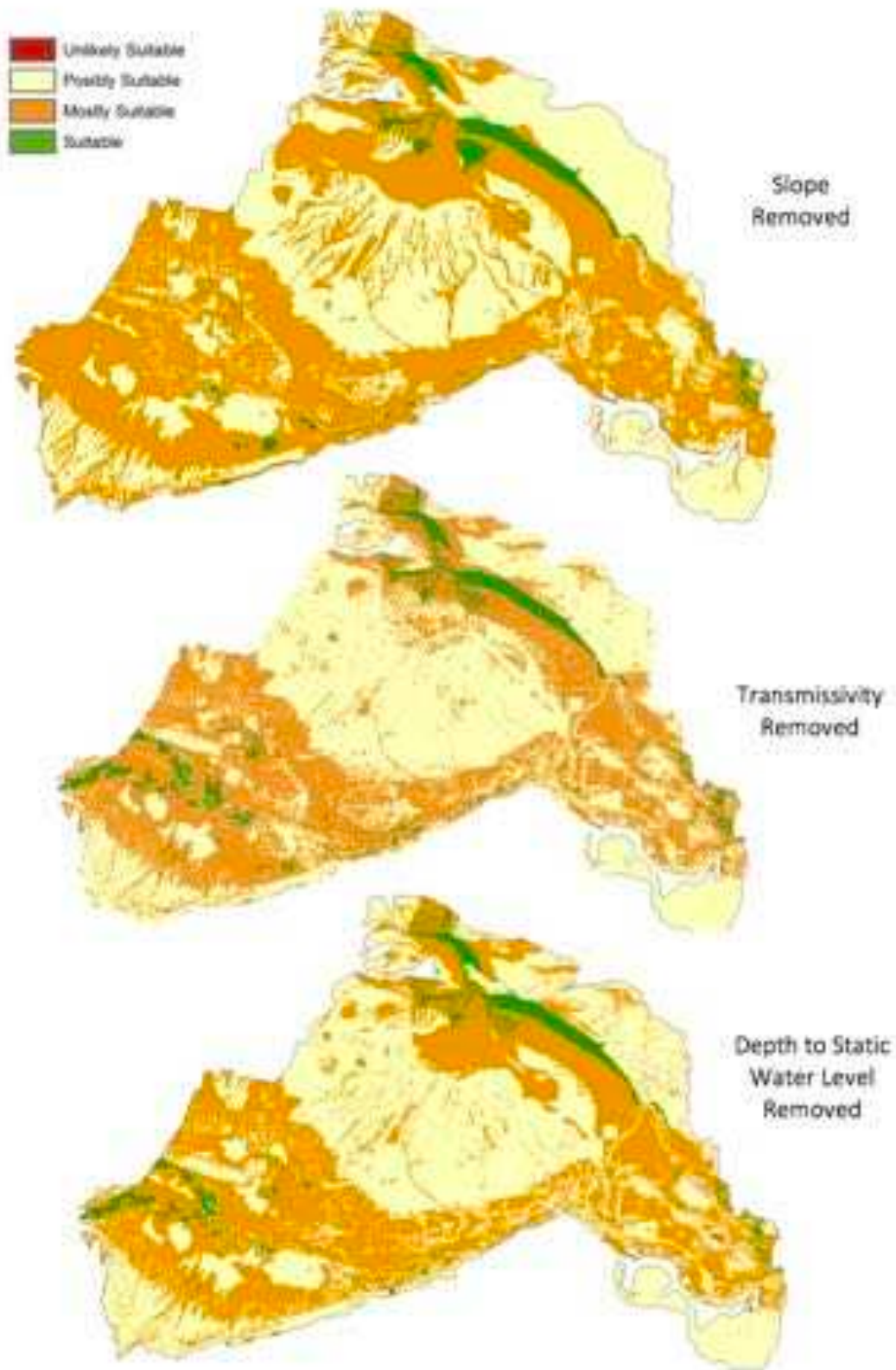
Toppenish Basin Continued



Benton Basin



Benton Basin Continued



Appendix B: Raster Datasets Reclassified



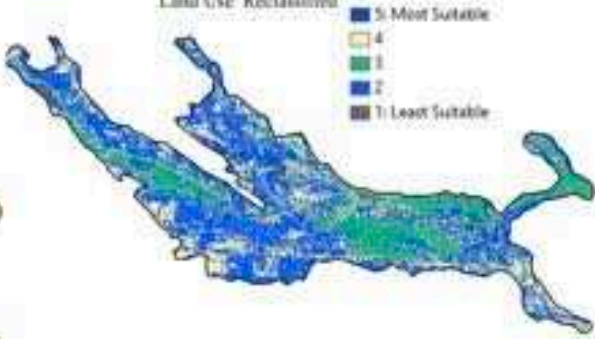
Depth to Static Water Level: Winter Months (Reclassified)



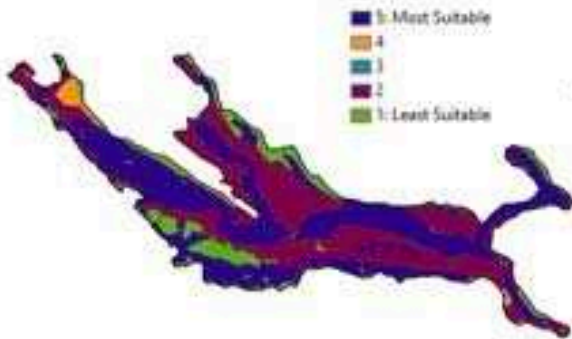
Slope Reclassified



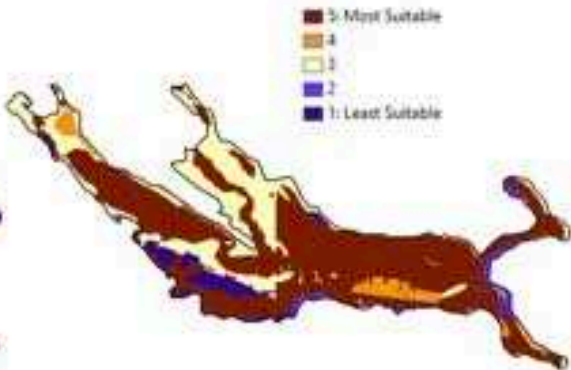
Land Use Reclassified



Transmissivity Reclassified



Lithology Reclassified



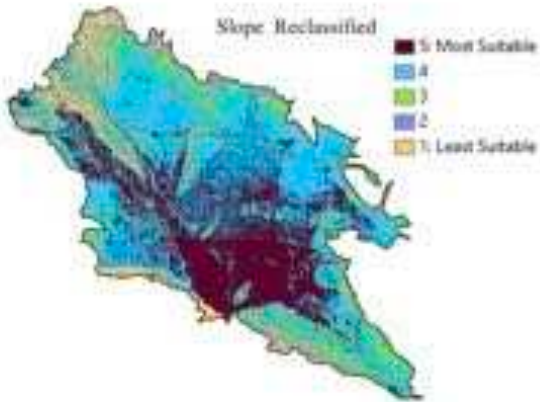
Kittitas Basin



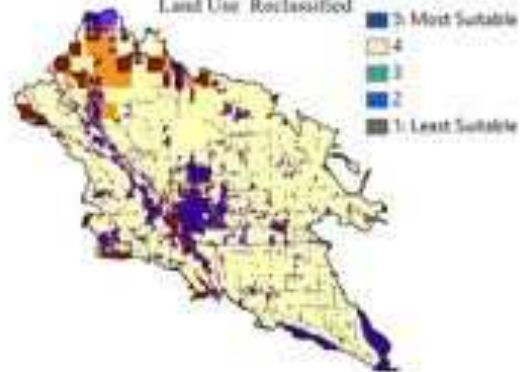
Depth to Static Water Level: Winter Months (Reclassified)



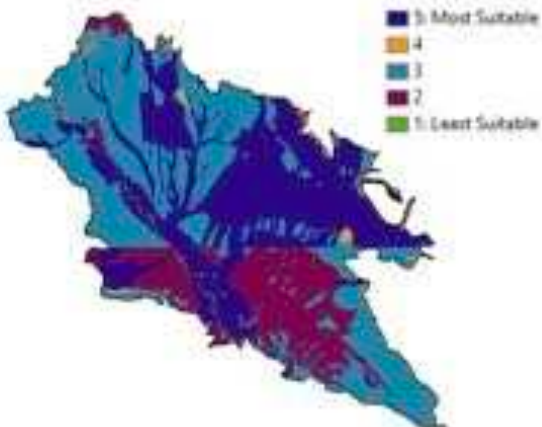
Slope Reclassified



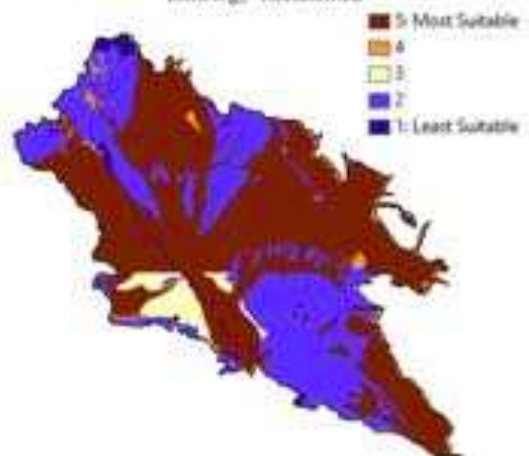
Land Use Reclassified



Transmissivity Reclassified



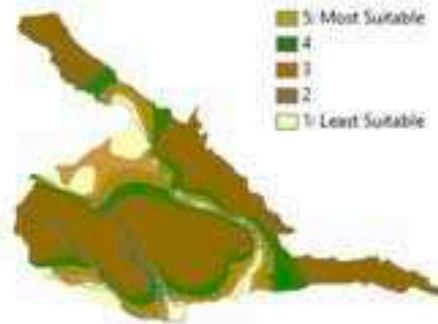
Lithology Reclassified



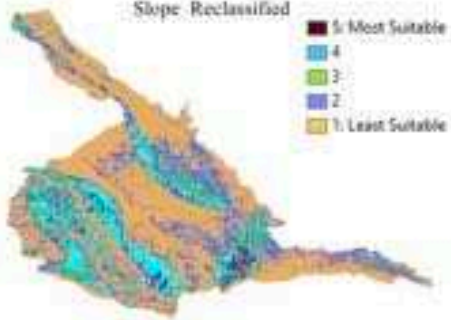
Selah Basin



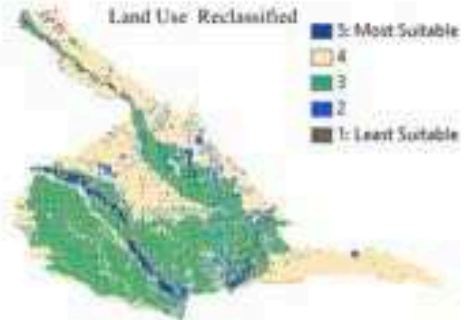
Depth to Static Water Level: Winter Months (Reclassified)



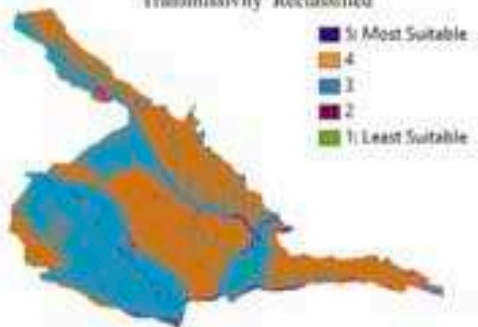
Slope - Reclassified



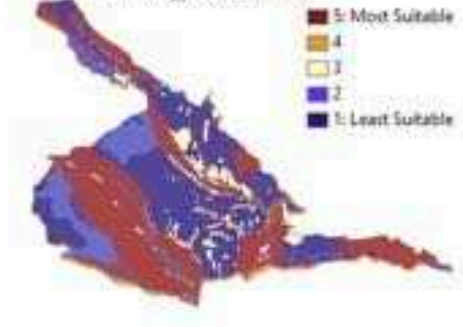
Land Use - Reclassified



Transmissivity Reclassified



Lithology Reclassified



Lower Yakima Basin



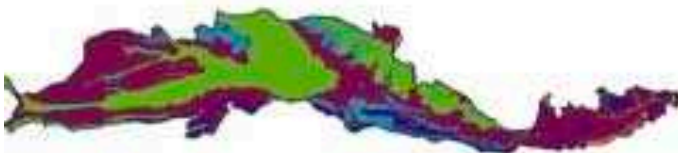
Slope Reclassified



Depth to Static Water Level: Winter Months (Reclassified)



Transmissivity Reclassified



Land Use Reclassified



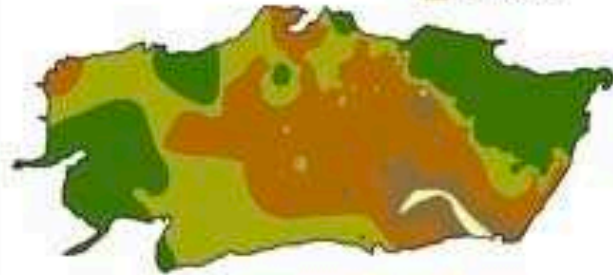
Lithology Reclassified



Toppenish Basin



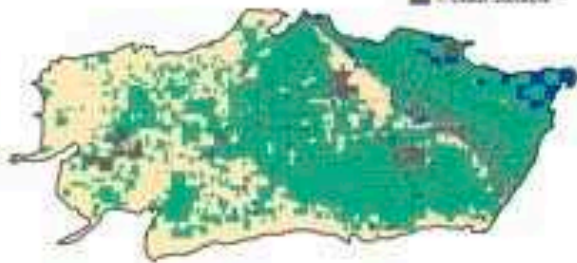
Depth to Static Water Level, Winter Months (Reclassified)



Slope Reclassified



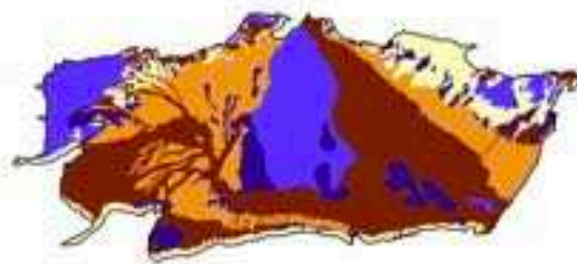
Land Use Reclassified



Transmissivity Reclassified



Lithology Reclassified



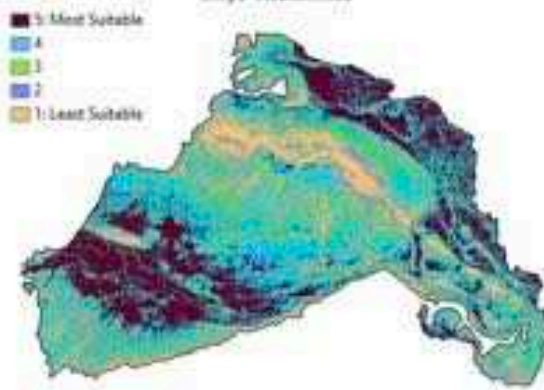
Benton Basin



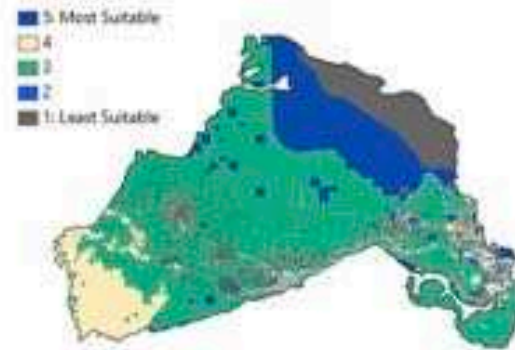
Depth to Static Water Level: Winter Months (Reclassified)



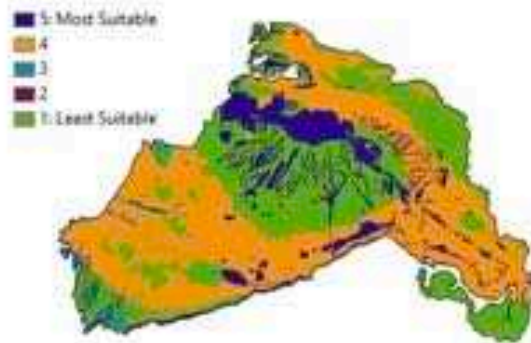
Slope Reclassified



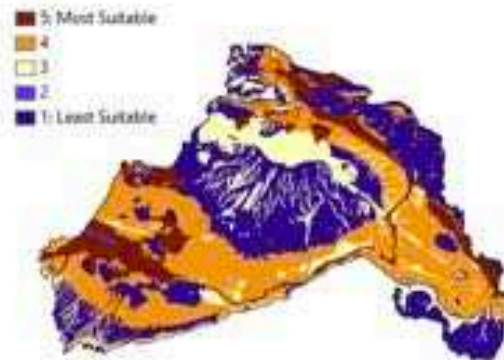
Land Use Reclassified



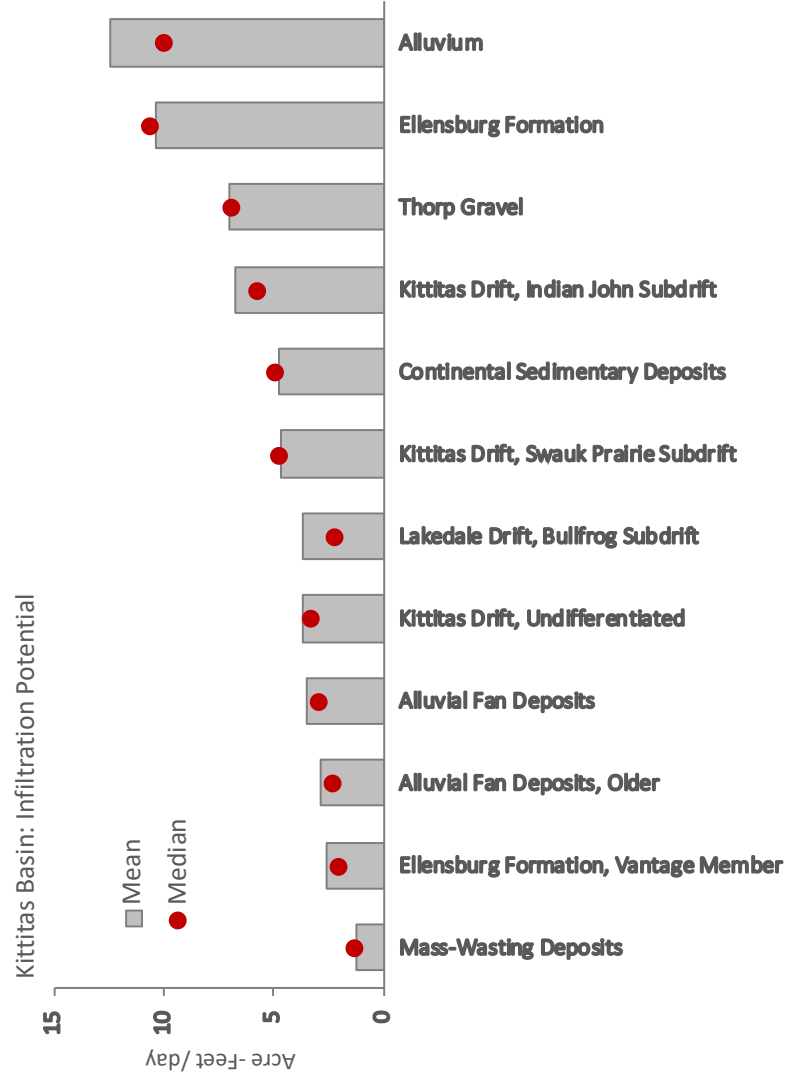
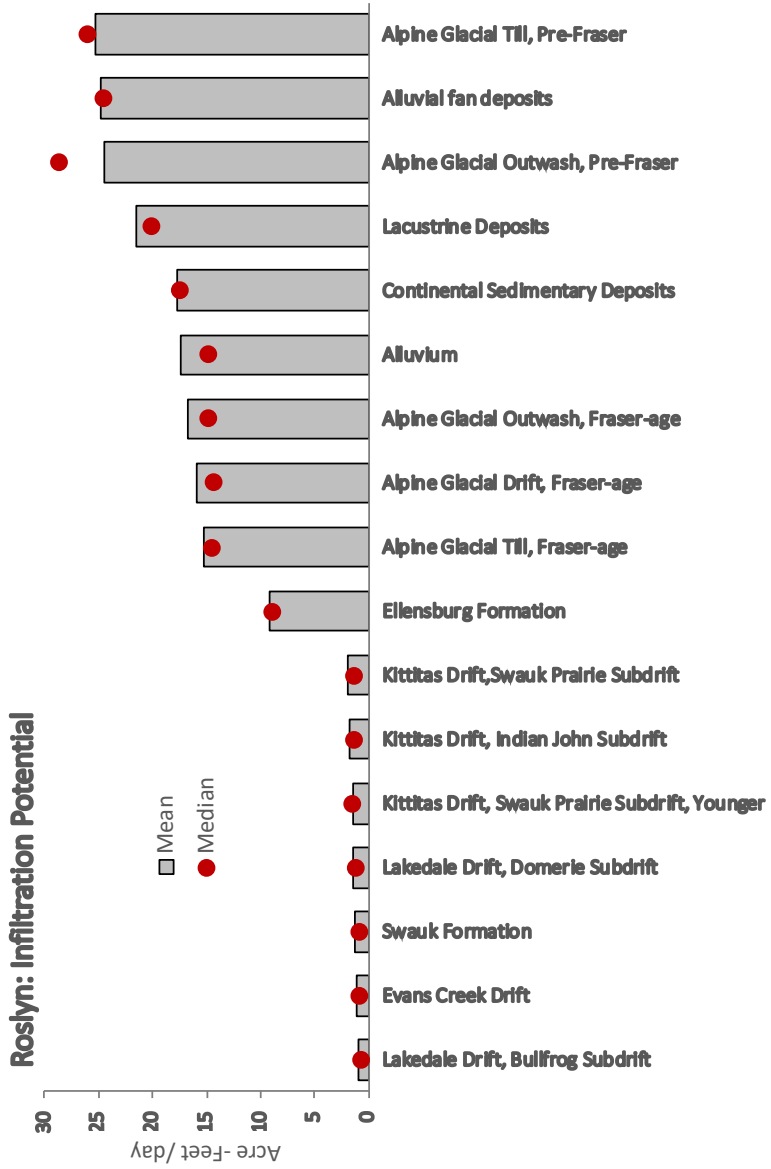
Transmissivity Reclassified



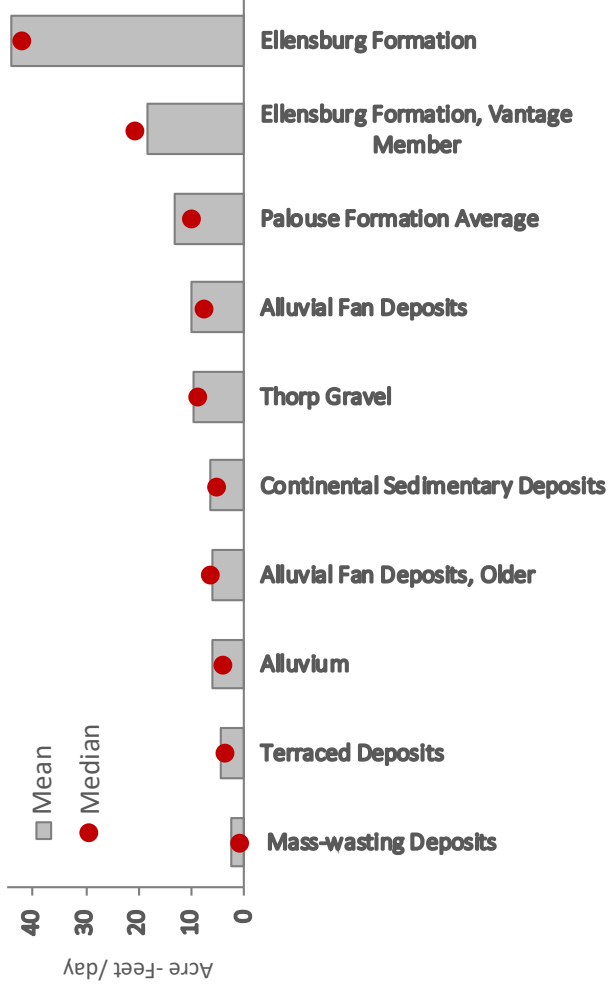
Lithology Reclassified



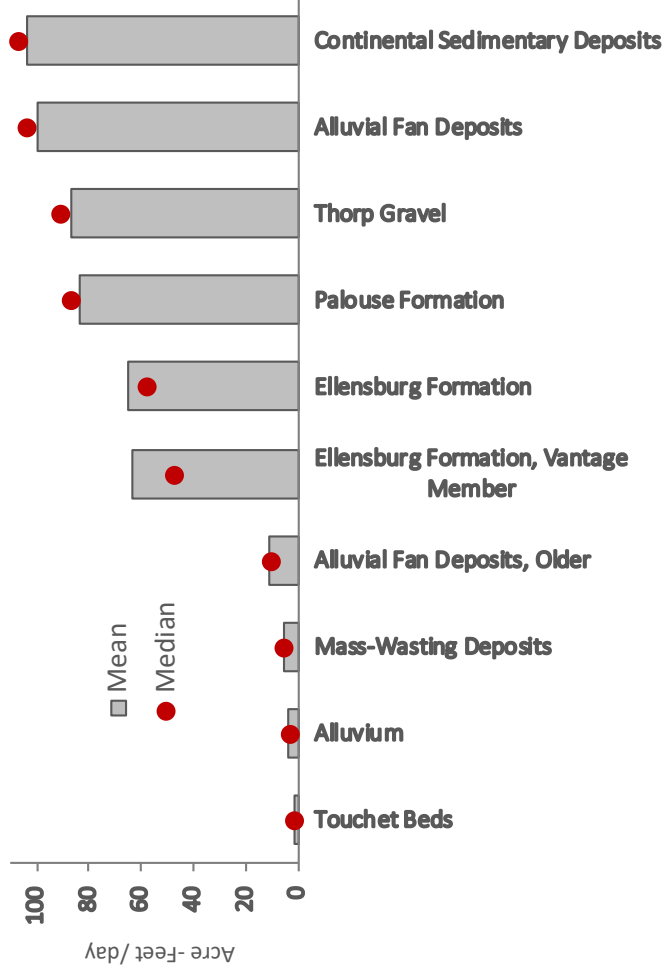
Appendix C: Mean and Median Infiltration Rates of Select Geologic and Lithologic Units

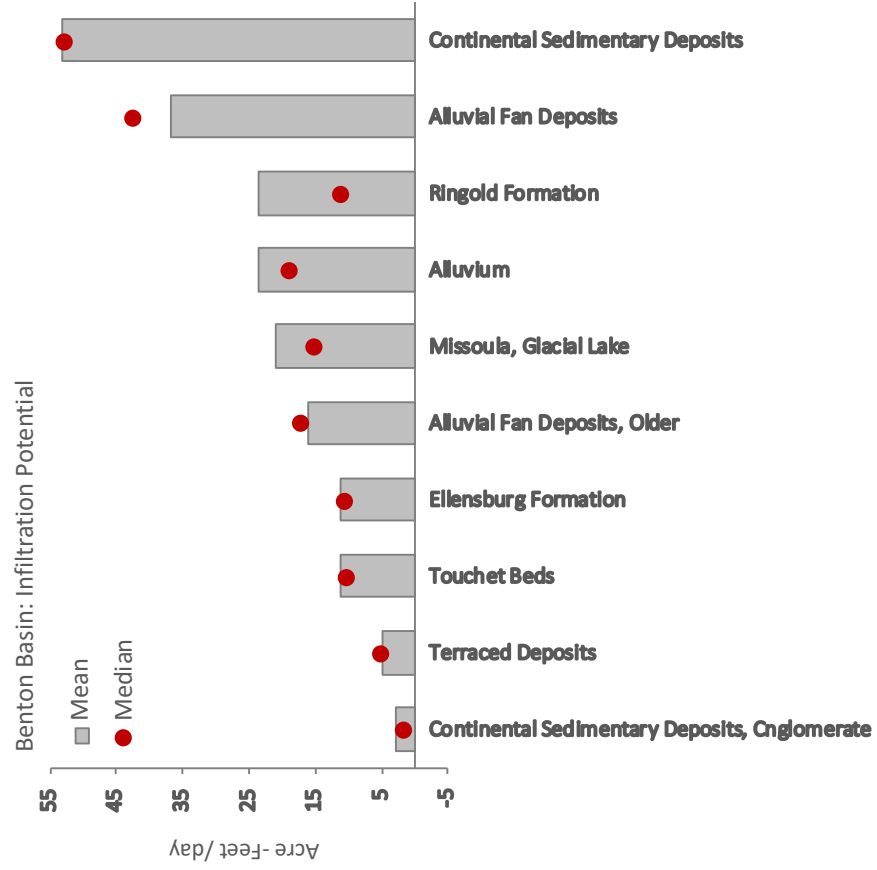
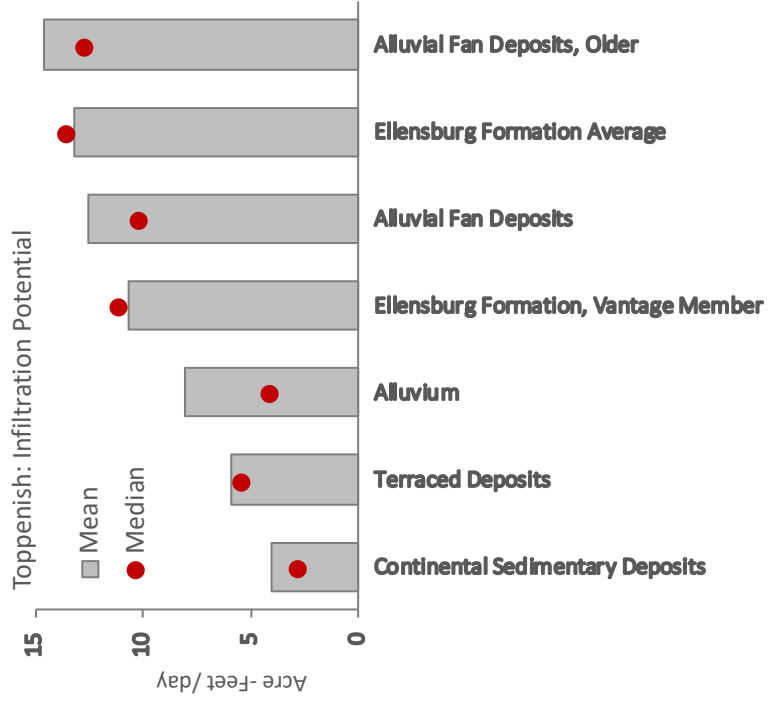


Selah Basin: Infiltration Potential



Lower Yakima Basin: Infiltration Potential





Appendix D: Stream Depletion Factor Maps

